الجمهورية الجزائرية الديمقراطية الشعبية

**République Algérienne Démocratique et Populaire**

**Ministère de l'Enseignement Supérieur et de la Recherche Scientifique.**
**Ecole Supérieure des Sciences Appliquées d'Alger**

وزارة التعليم العالي و البحث العلمي
المدرسة العليا في العلوم التطبيقية في الجزائر

**Département de second cycle**

# Mémoire de Fin d'Etudes

**En vue de l'obtention du diplôme d'ingéniorat d'état**

Filière : **Electrotechnique**

Spécialité : **Traction électrique**

## Thème :

# Study and Conception of a Variable Speed Drive for Induction Machine

Présenté par : GHERSI Tarak
et par : ZEROUALI Nabil

Encadré (e) par : BEN ACHOUR Ali
Co-encadré(e) par : BOUTOUCEHE Hicham

Soutenu publiquement, le :02/09/2020, Devant le Jury composé de :

| | | |
|---|---|---|
| M | HAMACHE Amar | Président (e) |
| M | BENACHOUR Ali | Encadreur |
| M | BOUTOUCHE Hicham | Co-encadreur |
| M | DEBOUCHA Abdelhakim | Examinateur |

Binôme N° : 13/PFE. / 2020

الجمهورية الجزائرية الديمقراطية الشعبية

**République Algérienne Démocratique et Populaire**

**Ministère de l'Enseignement Supérieur et de la Recherche Scientifique.**
**Ecole Supérieure des Sciences Appliquées d'Alger**

وزارة التعليم العالي و البحث العلمي
المدرسة العليا في العلوم التطبيقية في الجزائر

**Département de second cycle**

# Mémoire de Fin d'Etudes

**En vue de l'obtention du diplôme d'ingéniorat d'état**

Filière : **Electrotechnique**

Spécialité : **Traction électrique**

## Thème :

# Study and Conception of a Variable Speed Drive for Induction Machine

Présenté par : GHERSI Tarak
et par : ZEROUALI Nabil

Encadré (e) par : BEN ACHOUR Ali
Co-encadré(e) par : BOUTOUCEHE Hicham

Soutenu publiquement, le : 02/09/2020, Devant le Jury composé de :

| | | |
|---|---|---|
| M | HAMACHE Amar | Président (e) |
| M | BENACHOUR Ali | Encadreur |
| M | BOUTOUCHE Hicham | Co-encadreur |
| M | DEBOUCHA Abdelhakim | Examinateur |

Binôme N° : 13/PFE. / 2020

**ملخص**

الهدف الرئيسي من هذا العمل هو دراسة محاكاة وتحقيق محرك متغير السرعة (VSD) لآلة غير متزامنة ثلاثية الطور .نبدأ دراستنا بأحدث ما توصلت إليه التقنية حول المحولات AC-AC حيث تم تقديم هياكل مختلفة .بعد ذلك ، يتم تقديم دراسة حول أسواق VSD مع اتجاهاتها .تم تقديم دراسة مفصلة لكل جزء من VSD بعد ذلك قبل اختيار كل مكون من مختلف الشركات المصنعة .تم اختيار برنامج Matlab / Simulink للمحاكاة بسبب أدائه الخاص وبساطته ، تم تطبيق نظام تحكم ثابت V / f. أما بالنسبة لتخطيط لوحة الدارات المطبوعة ، فقد تم اختيار ORCAD لمكتبته الواسعة .تم تقديم ثلاث محاكات، في حالة مصدر ثلاثي الطور ، ثنائي الطور و مصدر أحادي الطور. و في الأخير، تم تقديم حلين، مع لتخطيط لوحة الدارات المطبوعة الخاصة بكل منهما، أحدهما يستخدم IPM والآخر يستخدم IGBTs منفصلة.

**الكلمات المفتاحية** : VSD ، محولات AC-AC ، تخطيط لوحة الدارات المطبوعة ، نظام التحكم الثابتV/f،IPM،IGBTS.

**Abstract………………………………………………………………………………………**

The main objective of this work is to study, simulate and realize a variable speed drive (VSD) for a three-phase asynchronous machine. We begin our study by a state of the art on the AC-AC converters where various topologies are presented. Then, a study on the VSD markets is presented with its trends. A detailed study of each part of the VSD is presented afterwards before selecting each component from different manufacturers. Matlab/Simulink is utilized for simulation because of its particular performances and its simplicity. A V/f constant control system is applied. As for the PCB layout ORCAD is selected for is vast library. Three simulations are presented in case of three phase source, two phases and single-phase source. Finally, two solutions are presented, with their PCB layers one using IPM and the other using discrete IGBTs. After a comparison between the two solution , The IPM is seen as a better choice.

**Key words:** VSD, AC-AC Converters, PCB layout, V/f constant control system, IPM, IGBTs.

**Résumé: ………………………………………………………………………………………**

L'objectif principal de ce travail est d'étudier, simuler et réaliser un variateur de vitesse (VSD) pour une machine asynchrone triphasée. Nous commençons notre étude par un état de l'art sur les convertisseurs AC-AC où différentes topologies ont été présentées. Ensuite, une étude sur les marchés VSD est présentée avec ses tendances. Une étude détaillée de chaque partie du VSD a été présentée par la suite avant de sélectionner chaque composant de différents fabricants. Le logiciel Matlab / Simulink est sélectionné pour la simulation en raison de ses performances particulières et de sa simplicité. Un système de commande V / f constant a été appliqué. En ce qui concerne la disposition du PCB, ORCAD a été sélectionné pour sa vaste bibliothèque. Trois simulations ont été présentées dans le cas d'une source triphasée source biphasé et monophasée. Enfin, deux solutions ont été présentées, avec leurs couches de PCB l'une utilisant l'IPM et l'autre utilisant des IGBTs discrets.

**Mots clés** : VSD, convertisseurs AC-AC, configuration PCB, commande V / f constant, IPM, IGBT

# ***Acknowledgment***

First of all, all thanks are to allah the most powerful and most merciful. We thank allah for giving us the strength and the will to do this project and finish it.

A huge thanks to our beloved teacher M.BEN ACHOUR Ali, one of the most beloved teachers to our hearts, we can’t thank him enough for being patient with us, for staying in our side no matter what and even when things got hard.

We thank as well BOUTOUCHE Hicham for staying with us and helping us even after that happened because of the pandemic, we really do appreciate his position.

We thank GA-tech company as well for accepting us between them and helping us, we wish you the best

We thank as well all the teachers in ESSA-ALGER for all the valuable lessons and pieces of advice throw those whole three years.

We thank our families, our aid and everything for us for helping and encouraging us all the way long and for believing in us.

And last but not least a special thanks to everyone that helped us in this project.

# *Dedications*

*I dedicate this work:*

*Firstly, to my teacher Ali BEN ACHOUR, to thank him for standing by our side till the last minute.*

*To my parents, my light in those nights where I thought that there is no hope left, my road to the right. My candle that kept shining when the darkness left my heart whining.*

*To my six brother and sister and all my family that has been with me in the good and the bad*

*Special dedication to my other two brothers MEKHILEF Aymen Abd Elmonim and Kaced Abd Elrahman my friends and brothers and a lifelong company.*

*To the two other brothers BAHIDJ Ryad and ZEROUALI Nabil, it has been a pleasure working with you.*

*To GATECH workers specially Hicham BOUTOUCHE for his help and advice in this project day and night till the end.*

*And finally, to my other sister that without whom I wound not be here. My sister that was an aid and a life savior for me throw 5 years. My sister that never turned me down.*

*To you MECHAB Nessrine.*

***GHERSI Tarak***

*I dedicate this work:*

*Firstly, to my teacher Ali BEN ACHOUR, to thank him for standing by our side and bear with us till the end.*

*To my parents, my support for all those years of hardship where I though there will be no end to them, my light in the darkest nights, my hope for a success that wouldn't be without them and there cheering visible or hidden to me.*

*To my three brothers that has been with me in the good and the bad.*

*My special dedication to the two persons that took care of me when I was far away from home, Mr.Saker Lamine & his wife Saliha .*

*To my family friends, Balamane Tamime-Dar and Radia Fenni for their help and support.*

*To my friends that I made in my promotion at ESSAA, a friend that we passed both Good and Bad moments, Special dedications to ALI MOUHERI Mawloud, MEKHILEF Aymen Abdelmounaim, KACED Abderrahmane and LABADI Saida.*

*To the two other brothers that I made GHERSI Tarak and BAHIDJ Ryad, it has been a pleasure working with you both in this project.*

*To GATECH workers specially Hicham BOUTOUCHE for his help and advice in this project day and night till the end.*

***ZEROUALI Nabil***

## TABLE OF CONTENT

# SYMBOLS LIST

**$V_{DC}$ :** DC bus voltage

**i :** phase current.

**R :** resistance .

**Φ :** phase flux.

**L1, 2,3** : phases inductances

**Ω :** machine’s speed

**P :** poles number.

**$T_C$ :** torque,

**$T_{em}$ :** electromagnetic torque.

**J :** machines inertia .

**$I_{dc}$ :** DC bus current.

**THD% :** distortion factor.

**PWM :** Pulse Width Modulation.

**IGBT:** Insulated Gate Bipolar Transistor.

# FIGURES LIST

# TABLES LIST

# GENERAL INTRODUCTION

Electric motors have long been and will continue to be the general workhorse of industry providing an efficient and reliable transfer of power for industrial and commercial applications. In relation to the benefits of transferring electrical energy to mechanical energy the squirrel-cage induction motor is rugged and reliable requiring minimum maintenance at a very reasonable cost.[1]

Over the years many different ways were applied to change the speed of the motor through either mechanical or electrical. Until the advent of the AC variable frequency drive in the late 1950's.[1]

Technology has made great strides in improving the AC variable frequency drive to present day standards. Variable speed drives (VSDs) together with motors have emerged throughout industry as the popular approach to improve process control, product quality, reduce energy consumption.[1]

In the market, many famous companies have their own VSDs, which are commercialized with international standards such as: Danfoss, ABB, Schneider Electric, Siemens, Yaskawa… etc. These VSDs were studied and produced for many industrial applications, in different ranges in power.

The variety in the market and the high expectations of its grow gives hope to a lot of new companies and engineers to enter this field, by building their own VSDs, which is the purpose of this project.

At the beginning a state of the art about AC-AC converters will be presented, where a lot of topologies will be briefly studied and compared. in order to choose one topology. Another short and fast study of the market is going to be presented while highlighting the trends and the prediction of VSDs market in the next years.

In the second chapter, and after choosing one topology, a presentation of its components will be done, as well as presenting some other essential circuits and elements. After that, we move to components selection and choice, depending on some criteria that were either defined in the specifications, or were calculated in the sizing process. At the end of this part a better view on the main topology is resulted.

As for the third part, the full circuits will be presented, plus some circuits that serve the protection of the VSD, measurement circuits, supply circuits …etc. Another comparative study of the component market is done as well in order to choose the appropriate component from the many that exists, with better performances and reasonable price. AT the end of this part the full circuit is almost presented and an estimated price for the VSD is given.

As for the last part, we will perform simulations on a model using MATLAB/SIMULINK, where the V/f control system will be applied. The simulation will take into consideration three cases (three-phase, bi-phase and mono-phase supply). After that the rest of the chapter is devoted to the design of the electronic board circuit. OrCAD will be presented with its tools and the steps needed in order to create the PCB.

# Chapter

# I

# CHAPTER I: STATE OF THE ART ON AC-AC CONVERTERS

## Introduction

From the beginning of VSDs appearance, they have been used to control the speed of electric motors, which consume approximately 25% of the world's electrical energy in industrial and commercial applications [2]. By definition, VSDs enable users to operate a motor at any commanded speed, as opposed to running across-the-line at a fixed speed. This variable speed control improves energy efficiency and lessens the wear and tear on mechanical couplings, such as gears, belts, and pulleys.

Modern electrical VSDs can be used to accurately maintain the speed of a driven machine to within ±0.1%, independent of load, compared to the speed regulation possible with a conventional fixed speed squirrel cage induction motor, where the speed can vary by as much as 3% from no load to full load, these devices have the benefits of energy and cost saving in many applications.[3]

In this chapter, a stat of the art on the ac-ac topologies is done. Another brief state of the art on the control techniques is presented, in the end a study on the VSD's market is presented, as well as some trends and prediction for this market as well.

## I.1 STATE OF THE ART ON AC-AC TOPOLOGIES:

In this section we will talk about the proposed topologies of the VSDs. The following figure (figure I.1) represents a global schematic of the basic families of AC-AC converters (both frequency and amplitude converters):

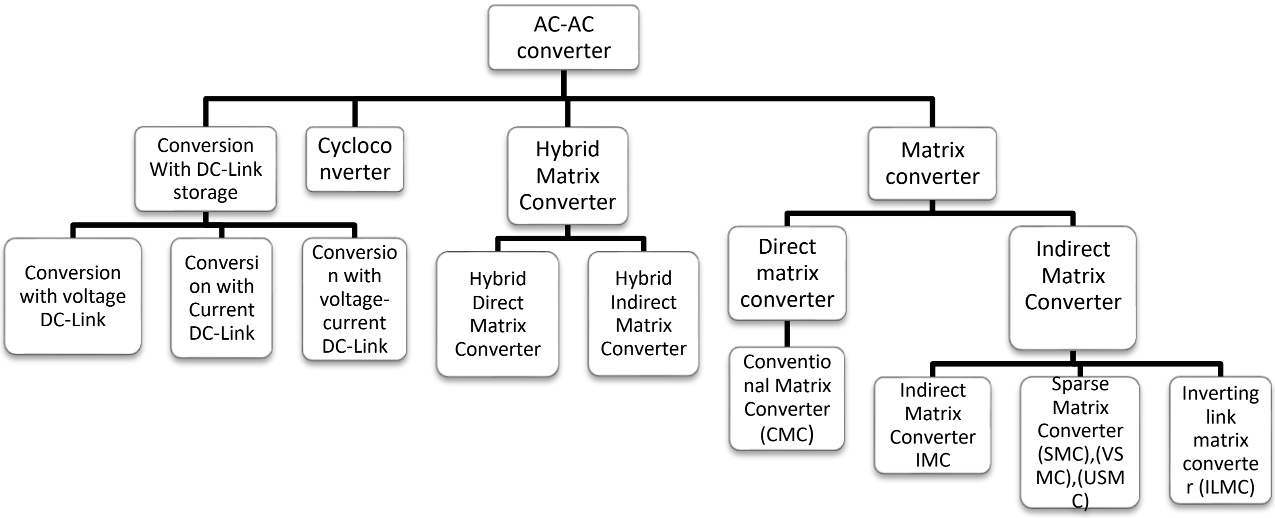


**Figure I-1 global schematic of the basic families of AC-AC converters**

As shown in figure I.1, AC-AC converters can mainly be classified to deferent families according to the type of the AC-AC conversion. The classification of AC–AC frequency converters in the technical literature is varied, because its development is still in progress [4],[5] .So basically AC-AC converters are classified into indirect topologies that contains a main DC energy storage element, direct topologies (without a DC energy storage element) and hybrid structures with small local DC energy storage elements.

### I.1.1 Indirect Topologies:

This family is basically the family of converters with DC-link .It includes the most popular and widely used in industry and households voltage source inverter (VSI) and current source (CSI) inverter.[6]

Figure I.2 (a) Represents the most standard topology of an AC-AC converter which is a voltage source inverter (VSI) with a front-end diode rectifier and a DC link capacitor [7]. It consists of two converter stages and an energy storage element. The first stage (rectifier) converts the supply's AC voltage to DC and then the inverter stage reconverts it back into output AC voltage with variable amplitude and frequency. One of the major disadvantages of this topology is the high distortion of the input current due to the high amount of low-order harmonics such as the 5$^{th}$ and 7$^{th}$ [8].

Figure I.2 (b) represent another topology where the bidirectional flow of energy is insured by coupling the DC-link with fully controlled rectifier bridge based on IGBTs with the VSI inverter. It's called Back to Back VSI (B2B-VSI),[9]. The dc-link quantity is then impressed by an energy storage element that is common to both stages which makes it possible to command them separately [5],[6].The main disadvantage of this topology lays in the medium power converters where the required input filter inductors are bulkier and heavier than the DC link capacitor [6].

Another topology other than the B2B-VSI is presented in Figure I.2 (c) using a Current Source Inverter (B2B –CSI) presented in [10]. It generates an input current waveform similar to the B2B-VSI while using a DC link inductor which is generally larger than DC link capacitor in the VSI. The B2B –CSI also requires an input filter usually smaller than the one used in the VSI (a low pass LC filter)[6].

For Figure I.2 (a) beside the harmonics and the distortion problem there is another problem in the non-reversibility of the rectifier current due to the functionality of diodes which may cause a problem to handle an eventual energy flow reversal, such as during an electromagnetic braking, thus the possibility of the DC bus voltage reaching destructive levels. So the use of dissipation load (resistor) is required (can only be dissipated) which makes it effective only in low energy dissipation applications.[11] The solution was to use the B2B-VSI with IGBTs bridge rectifier Figure I.2.b .With this solution the braking energy can be fed back to the power grid [9].

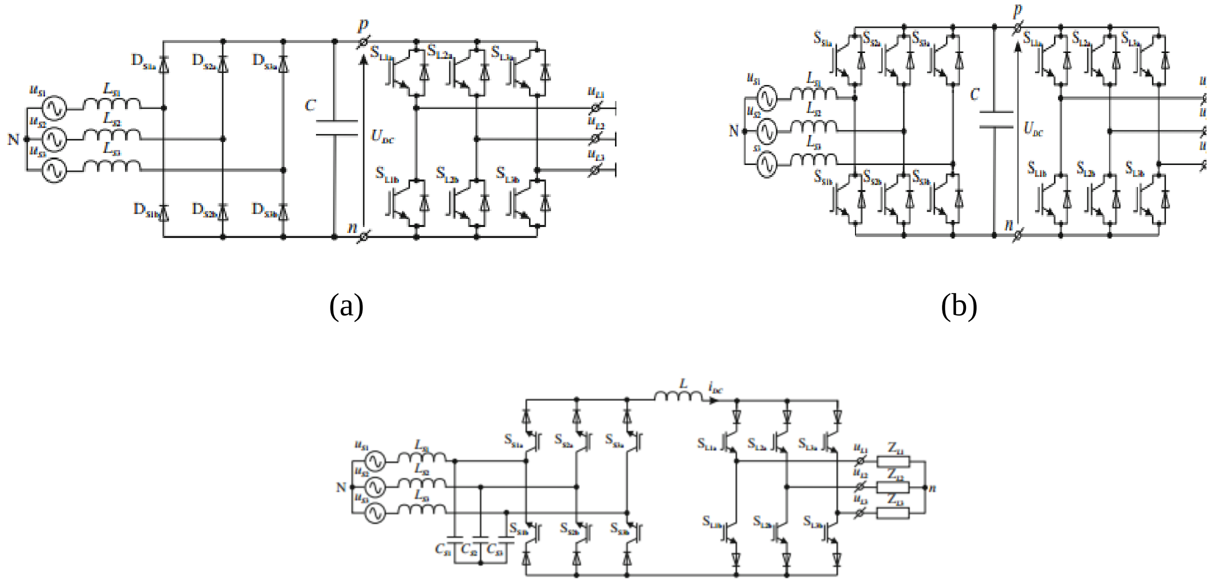

(a) (b)

(c)

**Figure I-2 main topologies for indirect topologies with DC link: (a) VSI using a diode rectifier bridge, (b) BBC-VSI and (c) BBC-CSI.**

Peng et al.[12] proposed a new topology by putting a Z source DC link between the front-end diode rectifier and the controlled inverter, as descripted in [13] the Z-source inverter allows the system output voltage to be stepped down or up as desired by inserting an X-shaped LC impedance. This impedance contains two inductors and two capacitors figure I.3.

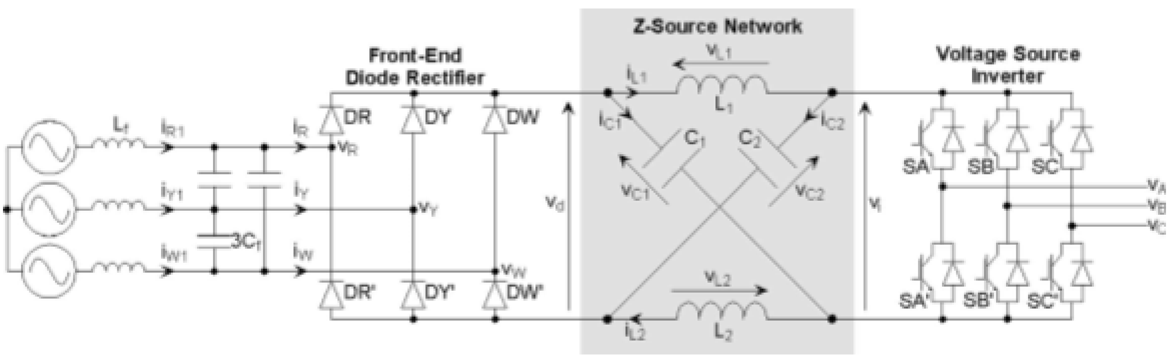


**Figure I-3 AC-DC-AC Converter with Z source**

### I.1.2 Direct Topologies:

**a) Matrix converter:**

The matrix converter (MC) is a direct AC-AC converter. It was proposed in 1976 by Guygyi –Pelly [14],[15]. , it uses a matrix (n x m) of bidirectional power switches, this bidirectionality in both current and voltage allows the MC to generate m output voltages with a variable frequency (theoretically unlimited) from n phases of voltage [16].

This type of converter has been the subject of research and development for around thirty years because of its possibility of replacing conventional indirect converters (AC-DC-AC) with a capacitive DC bus, in particular for embedded systems[14],[15]. The absence of the DC link (capacitors or inductors) make it less bulky compared to the indirect topologies therefore it can be encapsulated in a semiconductor module [14],[15].

The following topology (figure I.4) is the first Direct MC topology which was proposed by Venturini and Alesena in 1980, they described it as a matrix of bidirectional switches and named it “Matrix Converter” [17]. This structure alternates a voltage source with a current source. Another topology (figure I.5) alternates between current and voltage source. The main objective of this topology is to control the output’s amplitude and frequency in order to have voltage ratios greater than 1 [5].

**b) Double stage Matrix Converter:**

The double-stage matrix converter is a new topology of the matrix converter .As the name refers, this type of Matrix converter has two converters[18]. Hence, two stages, a fully controlled rectifier connected directly to a controlled inverter stage.

The Indirect MC is shown in Figure I.6 (a) , The power transistor and diode combinations between the input phases and the positive and negative buses form separately controllable four-quadrant switches, which could also be implemented by an anti-parallel connection of RB-IGBTs [5].The IMC is developed from the V-BBC topology by taking off the DC-link capacitor respectively, becomes the input filter capacitors. This topology was proposed in [19]

As shown in figure I.6 the main deference between the following topologies is in the rectifier bridge where many structures have been used in order to reduce the number of IGBTs used.

The first step to that was accomplished in 2001 when many new topologies appeared other than the Sparse IMC by Kolar at all [14],[20]. (Figure I.6.b).In this topology (Sparse IMC) the number of the used IGBTs has been reduced by a total of three. A connection between the upper cell and the lower cell has been made by the main of one IGBT which can be controlled for both cells[21].with this topology a unit power factor in the input is accomplished with a sinusoidal current and voltage in the output very similar to the Conventional IMC[22].

However, depending on the direction of power transit, three transistors and three diodes (power transmitted to the load) or two transistors and two diodes (power fed back into the input network) are conductive. The conduction losses of this topology will therefore be greater than those generated by the rectifier of the IMC[21].

(Figure I.6.c) represent another topology called Very Sparse IMC (VSIMC). In this topology that was also proposed by Kolar [20], another three IGBTs were deleted and were replaced by diodes to insure the bidirectional power flow. So, in general this topology uses in the rectifier stage a total of six IGBTs and twenty-four diodes. The conduction losses for this topology is higher than the last one cause in functioning more the rectifier needs two IGBTs and four diodes to be active in the same time.

If the DC bus operation is in a single quadrant (that means the current flow is in one direction), the number of IGBTs can be reduced to 12 with 12 diodes as well (unidirectional very sparse MC) (Figure I.6.d). Or to 9 IGBTs and 18 diodes for the “Ultra Sparse IMC” (Figure I.6.e) But the main inconvenient of these two topologies is that they do not allow the regeneration and braking[22],[23].

Figure I.6.f represents another topology of the matrix converter called ‘‘with Inverter Stage’’. In this topology an intermediate stage between the rectifier and the inverter is added, this topology allows the energy recovering thanks to the added inverter stage.

A.Benachour [21] made a comparison between these topologies in term of number of IGBTs and diodes needed, number of conductive components at a time number of isolated drives supplies needed and the bi-directionality of each topology ( table I.1)

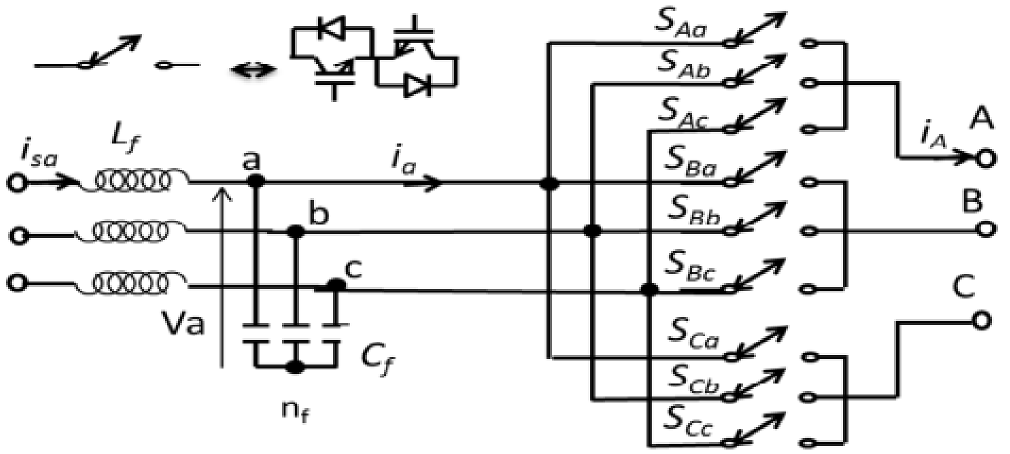


**Figure I-4 Direct MC**

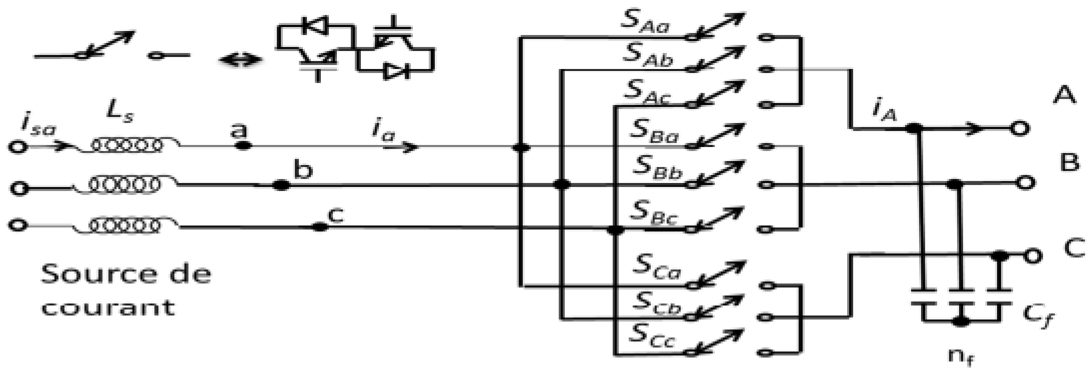


**Figure I-5 Current Direct MC**

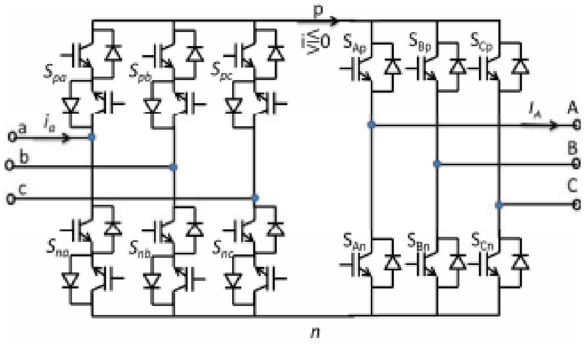


(a) Indirect MC

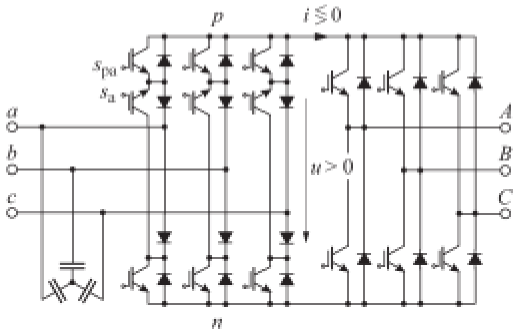


(b) Sparse IMC

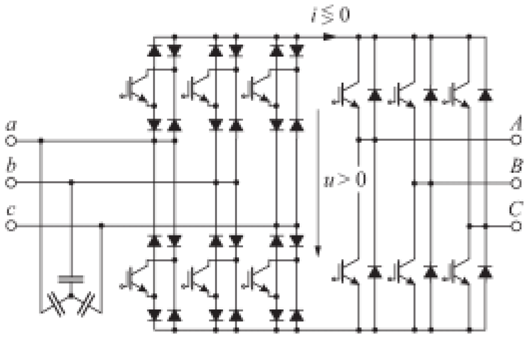


(c) Bidirectional Very Sparse IMC

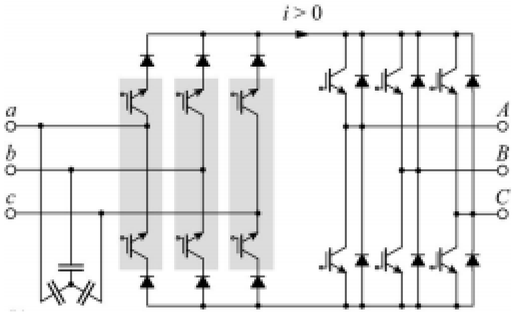


(d) Unidirectional Very Sparse IMC

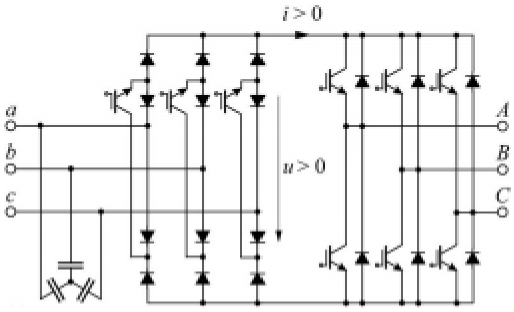


(e) Ultra Sparse IMC

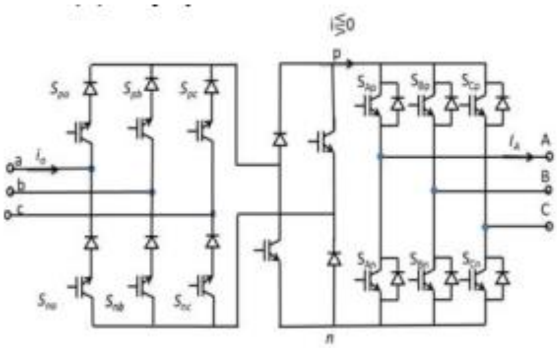


(f) Inverter Stage IMC

**Figure I-6 Double stage MC topologies**

**Table I-1 Comparison between MC topologies**

| topology | Number of conductive components | Bidirectional power flow | IGBTs | Diodes | Number of isolated gate driver supplies |
|---|---|---|---|---|---|
| MC | 6 | Yes | 18 | 18 | 9 |
| IMC | 7 | Yes | 18 | 18 | 8 |
| SIMC | 9 | Yes | 15 | 18 | 7 |
| VSIMC | 9 | Yes | 12 | 30 | 10 |
| USIMC | 9 | No | 9 | 18 | 7 |
| MC with inverter stage | 9 | Yes | 14 | 14 | 11 |

Kolar et all.[5] also made a comparative study between the deferent topologies of AC-AC converters in term on used components ( IGBTs, Diodes, Isolates gate drive supplies …) (table I.2)

**Table I-2 Comparison between deferent AC-AC converters**

| | V-BBC | C-BBC | IMC | MC |
|---|---|---|---|---|
| IGBTs | 12 | 12 | 18 | 18 |
| Diodes | 12 | 12 | 18 | 18 |
| Isolated gate driver supplies | 8 | 8 | 10 | 9 |
| Devices in current path | 4 | 8 | 6 | 4 |
| Min current sensors needed | 4 | 3 | 2 | 2 |
| Min voltage sensors needed | 4 | 6 | 3 | 3 |
| Intermediate storage | $C_{DC}$ | $L_{DC}$ | NO | NO |
| Max. output voltage | $\approx U_1$ | $>= U_1$ | $0.86\ U_1$ | $0.86\ U_1$ |

Kolar et all.[5] extracted from the table many interesting points comparing between the MC and V-BBC (after excluding the C-BBC due high conduction losses compared to other ) :

- The MC has a limited output voltage range (86.6% of the input voltage) while the V-BBC can go higher (MC exhibits a buck type characteristic and V-BBC a boost type one)[24].
- The V-BBC has an input which is separately controlled from the output while in the MC it can’t be controlled separately. Thus, the control scheme of the V-BBC enables a higher degree of freedom and typically offers a more robust solution[24].

- The volume of passive components including the EMI input filter of the V-BBC is bigger than the MC's (by 2.5 for a switching frequency of 5kHz) [25].

Both structures ensure sinusoidal input currents, sinusoidal output currents, and bidirectional power transfer. Thus, the deference does not appear in the basic functionality but with regard to the possible operating range, the behavior in characteristic operating points, or the implementation effort[24].

This fact is reflected in the research on MCs that are still being investigated for a wide range of applications using various control strategies such as model predictive control, which has been extensively investigated for MC[26], [27], [28].

A further trend in recent research on MCs is the investigation of the MC topology for aircraft applications which is investigated in [29], [30].

## I.2 Three Phases AC Induction Machines:

For industrial applications, 3-phase AC induction motors are the prime movers for the vast majority of machines. These motors can be operated either directly from the mains (the main supply) or from adjustable frequency drives (Variable Speed Drives). In the last decade, it has become increasingly common practice to use 3-phase squirrel cage AC induction motors with variable speed drive (VSD) [3]. To clearly understand how the VSD system works, it is necessary to understand the principles of operation of this type of motors.

### I.2.1 Induction Machine Equations:

#### I.2.1.1 Simplifying assumptions:

The generally accepted assumptions in the asynchronous machine model according to [31],[32] are :

- The machine is perfectly symmetrical.
- Saturation and losses in the magnetic circuit are not considered (Losses by hysteresis and Eddy currents are negligible)
- The spatial distribution of magnetic fields along the air gap is sinusoidal.

- The rotor in short circuit is equivalent to a three-phase winding mounted in a star.
- Power is supplied by a symmetrical three-phase voltage system.
- The skin effect is overlooked.
- The stator resistance is considered constant.

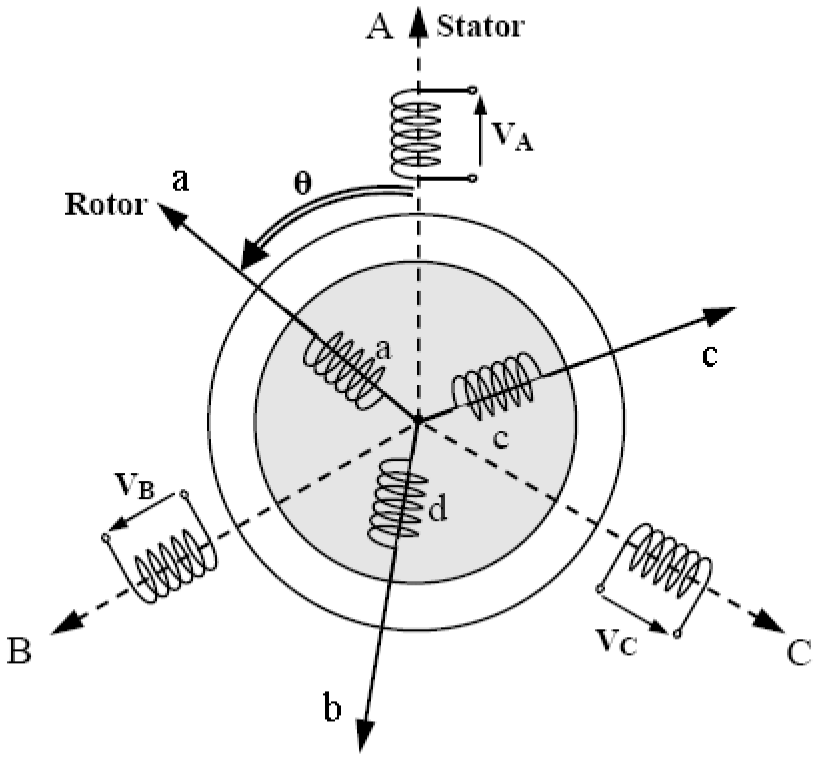


**Figure I-7 induction machine**

### I.2.1.2 The Machine's Equations :

The concerned machine is a squirrel cage AC induction machine which can be modeled with the following equations:

**a) Electric Equations**

- For the stator

$$[V_S] = R_s[I_s] + \frac{d}{dt}[\varphi_s] \tag{I.1}$$

$\boldsymbol{V_s}$ and $\boldsymbol{I_s}$ are the three stator voltages and currents respectively and $\boldsymbol{\varphi_s}$ is the flux vector through the three phases of the stator:

With $[V_s] = \begin{bmatrix} V_{sa} \\ V_{sb} \\ V_{sc} \end{bmatrix}$ $\quad [I_s] = \begin{bmatrix} I_{sa} \\ I_{sb} \\ I_{sc} \end{bmatrix}$ $\quad [\varphi_s] = \begin{bmatrix} \varphi_{sa} \\ \varphi_{sb} \\ \varphi_{sc} \end{bmatrix}$

- For the rotor

$$[V_r] = R_r[I_r] + \frac{d}{dt}[\varphi_r] \tag{I.2}$$

With $[V_r] = \begin{bmatrix} V_{ra} \\ V_{rb} \\ V_{rc} \end{bmatrix}$ $\quad [I_r] = \begin{bmatrix} I_{ra} \\ I_{rb} \\ I_{rc} \end{bmatrix}$ $\quad [\varphi_r] = \begin{bmatrix} \varphi_{ra} \\ \varphi_{rb} \\ \varphi_{rc} \end{bmatrix}$

**b) Magnetic equations:**

The relation between the flux and the current is as follows:

- For the stator

$$[\varphi_s] = [L_{ss}][I_s] + [M_{sr}][I_r] \tag{I.3}$$

- For the rotor

$$[\varphi_r] = [L_{rr}][I_r] + [M_{rs}][I_s] \tag{I.4}$$

With

$$[L_{ss}] = \begin{bmatrix} l_s & M_s & M_s \\ M_s & l_s & M_s \\ M_s & M_s & l_s \end{bmatrix}, \quad [L_{rr}] = \begin{bmatrix} l_r & M_r & M_r \\ M_r & l_r & M_r \\ M_r & M_r & l_r \end{bmatrix}, \quad [M_{sr}] = M \begin{bmatrix} cos(\theta) & cos(\theta - \frac{4\pi}{3}) & cos(\theta - \frac{2\pi}{3}) \\ cos(\theta - \frac{2\pi}{3}) & cos(\theta) & cos(\theta - \frac{4\pi}{3}) \\ cos(\theta - \frac{4\pi}{3}) & cos(\theta - \frac{2\pi}{3}) & cos(\theta) \end{bmatrix}$$

Where:

- $\theta$ designates the angular difference counted in the direction of rotation between the phases of the stator and the rotor.

- $M$ is the mutual inductance when the axes of the two windings considered coincide: $[M_{sr}] = [M_{rs}]^T$
- $M_s$ is the mutual inductance between two stator phases
- $M_r$ is the mutual inductance between two rotor phases
- $M_{sr}$, $M_{rs}$ are the mutual inductances between stator phases and between rotor phases.

**c) Mechanical equation**

The equation of rotation of the machine is governed by its dynamic equation that follows:

$$\frac{d\Omega}{dt} = \frac{1}{J}(C_{em} - C_r - f_k\Omega) \tag{I.5}$$

Where

$C_{em}$: electromagnetic torque

$C_r$: resistive torque

$\Omega$: the rotor's speed

$f_k$: viscous friction coefficient

$J$: rotor's inertia

### I.2.2 Park's model

To replace the differential equations whose coefficients are functions of time by simpler differential equations and with constant coefficients, a transformation mostly used for the asynchronous machines known as Park transformation is used. It allows to pass from an alternative three-phase system to a two-phase system (reference d, q, o). The stator and rotor quantities are then expressed in the same frame of reference (direct axis d and quadrature axis q). The transformation is written as follows:

$$[X_{dqo}] = [P(\theta\ )][X_{ABC}] \tag{I.6}$$

Where $[P(\theta\ )]$ is the park transformation matrix, as following:

$$[P(\theta)] = \sqrt{\frac{2}{3}} \begin{bmatrix} cos(\theta) & cos(\theta - \frac{2\pi}{3}) & cos(\theta + \frac{2\pi}{3}) \\ sin(\theta) & sin(\theta - \frac{2\pi}{3}) & sin(\theta + \frac{2\pi}{3}) \\ 1/\sqrt{2} & 1/\sqrt{2} & 1/\sqrt{2} \end{bmatrix} \quad (I.7)$$

We can schematize this transformation by the following figure I.8

For what follows we take:

- $\theta$ is the angle between axis a and A.
- $\theta_r$ is the angle between axis A and d.
- $\theta_s$ is the angle of the stator between a and d.
- $\omega_a$ is the angular speed of the axis system (d, q).
- $\omega_r$ is the electrical rotor angular speed

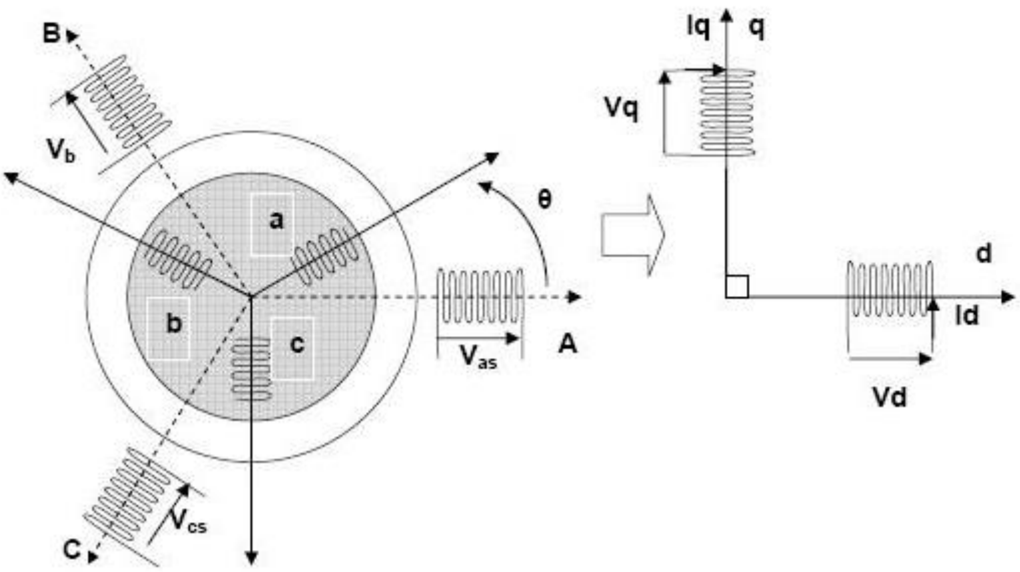


**Figure I-8 park transformation model**

### I.2.2.1 The machine's equations in park's model

In this frame reference the equations are in a 2 phase system (d,q)

**a) Voltage Equations**

$$\begin{cases} V_{sd} = R_s I_{sd} + \frac{d}{dt}\varphi_{sd} - \omega_a \varphi_{sq} \\ V_{sq} = R_s I_{sq} + \frac{d}{dt}\varphi_{sq} + \omega_a \varphi_{sd} \\ V_{rd} = 0 = R_r I_{rd} + \frac{d}{dt}\varphi_{rd} - (\omega_a - \omega_r)\varphi_{rq} \\ V_{rq} = 0 = R_r I_{rq} + \frac{d}{dt}\varphi_{rq} + (\omega_a - \omega_r)\varphi_{rd} \end{cases} \quad (I.8)$$

**b) Flux Equations**

By applying park's transformation, the flux equations of the machine become a diagonal matrix as follows:

$$\begin{cases} \varphi_{sd} = L_s I_{sd} + L_m I_{rd} \\ \varphi_{sq} = L_s I_{sq} + L_m I_{rq} \\ \varphi_{rd} = L_r I_{rd} + L_m I_{sd} \\ \varphi_{rq} = L_r I_{rq} + L_m I_{sq} \end{cases} \quad (I.9)$$

With $L_s = l_s - M_s$ $\quad L_r = l_r - M_r$ $\quad L_m = \frac{3}{2}M$

Where:

Ls : is the cyclic stator inductance

Lr: is the cyclic rotor inductance

Lm: is the mutual cyclic stator-rotor inductance

**c) Electromagnetic Torque Equation:**

The electromagnetic torque can be expressed by the following relationships:

$$\begin{cases} C_{em} = p(I_{sq}\varphi_{sd} - I_{sd}\varphi_{sq}) \\ C_{em} = p\frac{L_m}{L_r}(I_{sq}\varphi_{rd} - I_{sd}\varphi_{rq}) \\ C_{em} = p\frac{L_m}{L_s}(I_{rq}\varphi_{sd} - I_{rd}\varphi_{sq}) \end{cases} \quad (I.10)$$

**d) Choice of reference**

There are three possibilities of reference system, the choice of the reference depends on the studied problem

- Reference linked to the stator or reference α / β. This repository is used for DTC. It results in the conditions: $\frac{d\theta_s}{dt} = 0 \quad \omega_a = \frac{d\omega}{dt} = -\omega_m$
- Reference linked to the rotor where: $\frac{d\theta_s}{dt} = \omega \quad \omega_a = \frac{d\omega}{dt} = 0$
- Reference linked to the rotating field

**e) The State Equation expressed in the frame of reference ($\alpha, \beta$) linked to the stator**

$$\begin{bmatrix} \dot{I_{s\alpha}} \\ \dot{I_{s\beta}} \\ \dot{\varphi_{s\alpha}} \\ \dot{\varphi_{s\beta}} \end{bmatrix} = \begin{bmatrix} -\frac{1}{\sigma}(\frac{1}{T_s} + \frac{L_m^2}{L_s L_r T_r}) & 0 & \frac{L_m}{L_s L_r T_r} & \frac{L_m}{\sigma L_s T_r}\omega \\ 0 & -\frac{1}{\sigma}(\frac{1}{T_s} + \frac{L_m^2}{L_s L_r T_r}) & -\frac{L_m}{\sigma L_s T_r}\omega & \frac{L_m}{L_s L_r T_r} \\ \frac{L_m}{T_r} & 0 & -\frac{1}{T_r} & -\omega \\ 0 & \frac{L_m}{T_r} & \omega & -\frac{1}{T_r} \end{bmatrix} \begin{bmatrix} I_{s\alpha} \\ I_{s\beta} \\ \varphi_{s\alpha} \\ \varphi_{s\beta} \end{bmatrix} + \begin{bmatrix} \frac{1}{\sigma L_s} & 0 \\ 0 & \frac{1}{\sigma L_s} \\ 0 & 0 \\ 0 & 0 \end{bmatrix} \begin{bmatrix} V_{s\alpha} \\ V_{s\beta} \\ 0 \\ 0 \end{bmatrix} \quad \text{(I.11)}$$

$T_s = \frac{L_s}{R_s}$ stator time constant

$T_r = \frac{L_r}{R_r}$ rotor time constant

$\sigma = 1 - \frac{L_m^2}{L_s L_r}$ The dispersion coefficient.

### I.2.3 The equivalent circuit

To understand the performance of an AC induction motor operating using AC-AC converter, it is useful to electrically represent the motor by an "equivalent circuit". This clarifies what happens in the motor when stator voltage and frequency are changed or when the load torque and slip are changed. There are many different versions of the equivalent circuit, which depend on the level of detail and complexity. The stator current *I*S, which is drawn into the stator windings from the AC stator supply voltage *V*, can be predicted using this model[3].

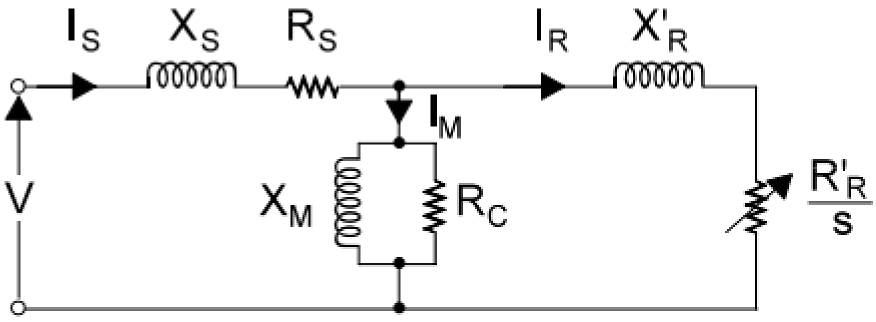


**Figure I-9 simplified equivalent circuit of an AC motor.**

Where:

V is the Stator supply voltage

$R_S$ is the Stator resistance

$X_S$ is the Stator leakage reactance at 50 Hz

$X'_R$ is the Rotor leakage reactance (transferred to the stator)

$X_M$ is the Magnetizing inductance

$I_S$ is the Stator current

$I_R$ is the Rotor current

$I_M$ is the Magnetizing current

$R_C$ is the Core losses, bearing friction, windage losses, etc

s is the slip

$R'_R/s$ = is the Variable rotor resistance (depends of the slip s)

Figure I.9 represents the simplified equivalent circuit of the AC motor; the rotor resistance is represented by an element that is dependent on the slip s. This represents the fact that the induced rotor voltage and consequently current depends on the slip. Consequently, when the induction motor is supplied from a power source of constant voltage and frequency, the current $I_S$ drawn by the motor depends primarily on the slip**[3]**.

From the previous equivalent circuit, the electromagnetic torque's equation can be written as following:

$$T_{em} = \frac{3R'_r {V_s}^2}{s\Omega_s} \frac{1}{\left(R_s + \frac{R'_r}{s}\right)^2 + X_1^2 \omega_s^2} \qquad \text{(I.12)}$$

Where $X_1^2 = X'_R + X_S$.

This formula is the base of the scalar control method (V/f = constant).

## I.3 State Of The Art Of Control Methods Applied To The IM Drive

In this section the widely used control techniques will be discussed

### I.3.1 V/f constant Control Method

This process is carried out by varying the supply frequency while keeping the ratio ${Vs}/{\omega s}$ constant (which means, keeping the flux $\boldsymbol{\varphi_s}$ constant). If the stator voltage drop is neglected, the electromagnetic torque can be written as a function of $\boldsymbol{\varphi_s}$ as follows:

$$T_{em} = \frac{3R'_r {V_s}^2}{s\Omega_s} \frac{1}{\left(\frac{R'_r}{s}\right)^2 + X_1^2 \omega_s^2} \qquad \text{(I.13)}$$

Furthermore, in the useful operating area where s is close to 0, the torque can be written as:

$$T_{em} = \frac{3p}{R_r} \varphi_s^2 \omega_r \qquad \text{(I.14)}$$

Where: $\varphi_s^2 = \frac{V_s^2}{\omega_s^2}$

Note that this method can only be applied when we can neglect the stator‘s voltage drops.

By varying the supply frequency and voltage the following characteristic is found (figure I.10)

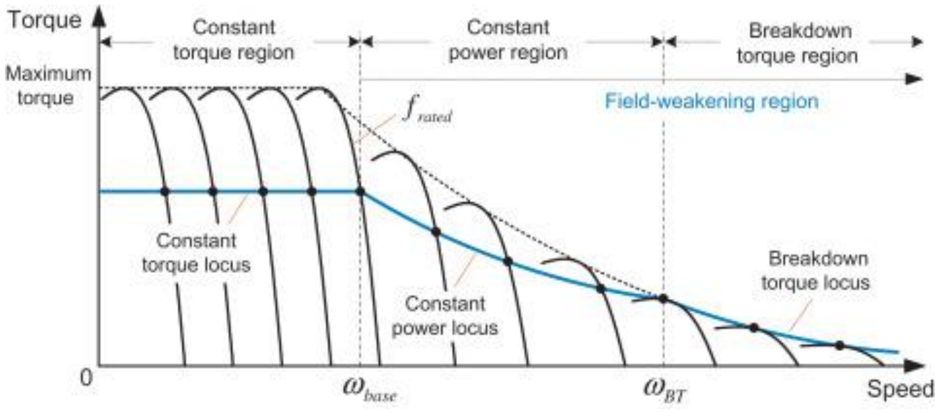


**Figure I-10 V/f Control overview.**

In overspeed mode, the increase in frequency cannot be accompanied by an increase in voltage, since the nominal voltage cannot be exceeded. Thus, the flux is then reduced ( defluxing ), it allows to avoid magnetic saturation.

Figure I.11 represents a global schema of the V/f control:

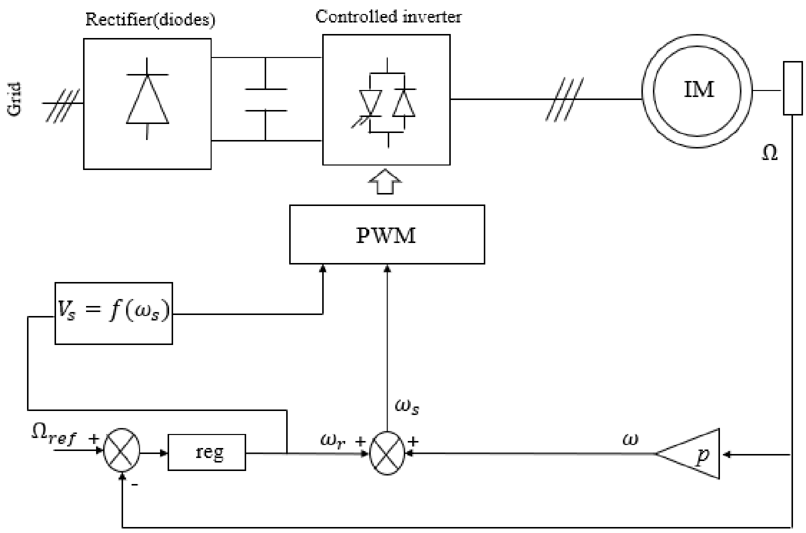


**Figure I-11 Global schema of the V/f control.**

So according to this characteristic and figure 1.10 it can be concluded that this method is adequate for controlling steady-state conditions and simple applications, such as pumps, fans and conveyors, which allow a lot of time for speed changes from one level to another and where the consequences of the changes in the process are not severe[3].

One of the biggest problems of this control method is low speed applications. therefore, stator voltage drop cannot be neglected.

High performance drives, such as robotics and rolling mills require fast and precise torque response. To achieve this, the dynamic structure of the machine has to be taken into account[33]. Several methods have been proposed to obtain fast torque response with flux regulation. However, the emerging consensus is to use field-oriented control (FOC) or DTC[33].

### I.3.2 Field-Oriented Control (FOC)

The concept of Field-Oriented Control (FOC) was introduced by Siemens company. Its implementation is based on transferring the vector from a rotating reference to a stationary one. This method has a good dynamic response[33].

FOC provides a decoupling between the magnetic component of the current (produces the flux) and the torque component (produces the torque)[33]. Thus, the two components can be controlled separately, generally the magnetic component varies slowly or kept as a constant for fast response and the torque varies rapidly[33] (figure I.12). Therefore, it provides independent control of torque and flux, which is similar to a separately exited dc motor[33].

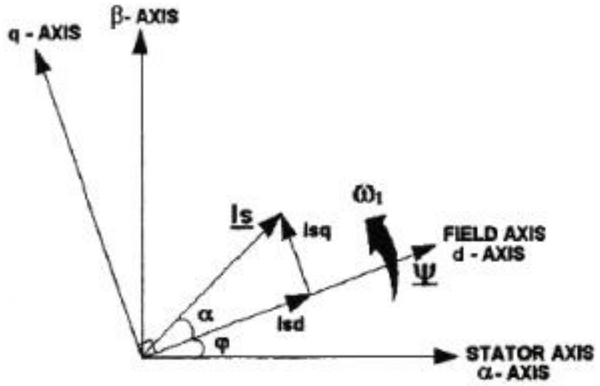


**Figure I-12** Stator current components in d-q Frame.

The FOC is achieved by aligning the rotor flux linkage vector along the d axis of the reference frame, when this condition is achieved the decoupling is realized and the control of the induction machine can be similar to a DC machine where $I_{sq}$ analogous to the armature current and $I_{sd}$ analogous to the field excitation.

### I.3.3 Direct Torque Control (DTC)

DTC for induction machines was proposed in the middle of 1980s by Takahashi [34]and Depenbrock [35]. This method ensures a dynamic performance equivalent to that obtained by the DC machine.

The basic principle of DTC is that stator voltage vectors must be chosen directly according to the differences between the torque and stator flux references and their actual values. Current controllers followed by a PWM comparator are not used in DTC control systems as well as the machine's parameters except for the stator resistance of the motor. Thus, DTC has the advantage of being less dependent on machine parameters and has a simpler configuration [36], [35]

The stator flux can be expressed in a frame of reference linked to the stator of the machine by the following equation:

$$\varphi_s(t) = \int_0^t (V_s - R_s I_s)dt + \phi_{s0} \tag{I.15}$$

In the case where a non-zero voltage vector is applied the voltage drop due to Rs is neglected compared to Vs. Thus, the equation I.16 that follows:

$$\varphi_s(t) = \phi_{s0} + V_s T_e \tag{I.16}$$

Where the non-zero voltage is applies for an interval of [0, Te]

So, the flux can directly be controlled and fixed by applying a suitable voltage vector. The following figure (figure I.13) shows an example of the evolution of the end of the stator flux vector with the chosen voltage vector.

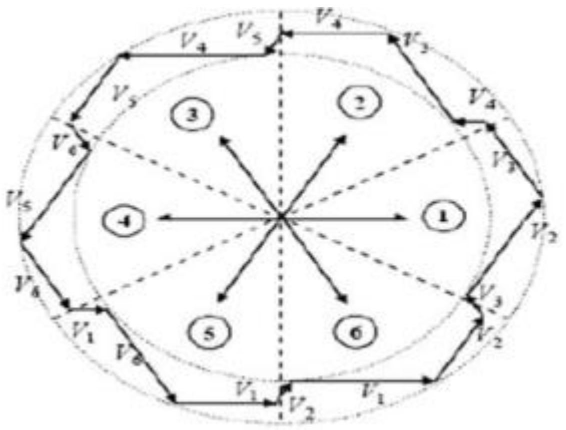

**Figure I-13 Evolution of the flux vector**

The basic DTC scheme uses a switching table in order to determine the switching state selection and a proper estimation of the stator flux vector and the torque[34].

Following the diagram presented by Takahashi in his paper the DCT requires two hysteresis controllers, the stator flux controller that imposes the period of active voltage vector and the torque controller to determine the zero voltage vectors so as to create a band of hysteresis and keep the motor's torque within it[34].

## I.4 Industrial Application of AC-AC Converters

Given the need for AC-AC converters, progress has been noted in the speed of their development, for their capability in fixed/variable voltage at rated/variable frequency[37].

In fact, they possess a total flexibility of independently converting voltages and frequencies and delivering reasonably sinusoidal voltages/currents to the load. Its applications differ with every topology and control techniques[37].

### I.4.1 Direct AC-AC Converters applications

#### a) Matrix Converters

The MCs are used in several fields, and particularly suitable for applications that require a compact volume and low weight. However, their applications in industry are limited. In [38] an investigation of MC application areas has been summarized as showed in Table 1.3

**Table I-3 Summarized information of investigated applications areas of MC**

| | Input and output frequency | Applied control methods | Investigation breadth | Comments |
|---|---|---|---|---|
| Motor Drive | Very different | DTC, MPC, FOC | Very wide | Promising and developed |
| UPFC | Same | SVM, SMC | Wide | Developing |
| Wind Turbine | Very different | SVM, SMC, SVD | Medium | Developing |
| Utility Supply | Different | SVM, genetic algorithm, repetitive control | Medium | Developing |
| Grid interface (smart grid) | Same or similar | MPC | Narrow | Promising and underexplored |

#### b) Cyclo-converters

Cyclo-converters convert a constant voltage, constant frequency AC waveform to another AC waveform of a lower frequency, this characteristic makes them used for high-power low-speed ac motor drivers with constant frequency input applications.

Cyclo-converters are used also in controllable VAR generators for power factor correction and ac system interties linking two independent power systems. [37]

### I.4.2 Indirect AC-AC Converters applications (with a DC-link)

They are mainly used for power conversion from a three-phase main system to a three-phase load with an arbitrary voltage amplitude and frequency. With the DC link energy storage element an advantage for both of the converter stages, making them controlled separately . [5]

These converters are applicable also in power distribution network to exchange power between different countries that also help to stabilize the network frequency, or to provide the specified country frequency if there is a difference between the country's frequency.

In [39] it is stated that the indirect AC-AC converters are used also for High-Power Wind Energy Conversion Systems (WECS). But there is some requirement that must be met which are mentioned in the same reference.

In [40] a solution was proposed so as to use an AC-DC-AC topology as a power electronics converters for variable speed pump storage. Thus, one of the main uses of Indirect AC-AC converts it pump applications. The following figure presents one of the proposed topologies for the application mentioned in [40].

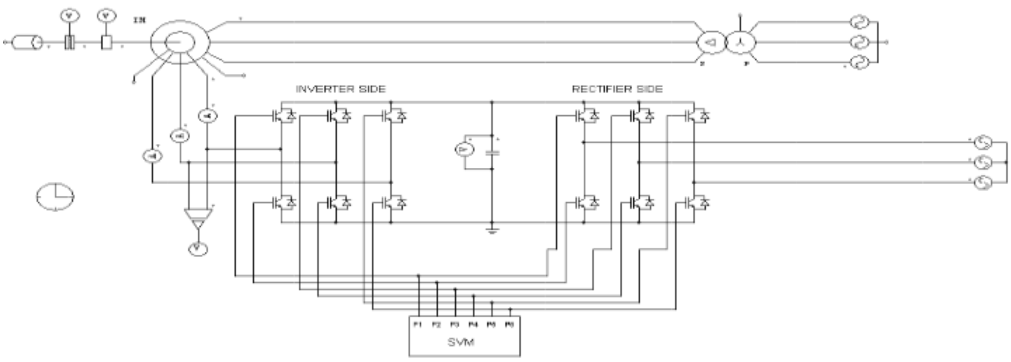


**Figure I-14 indirect AC-AC converter with PWM control system**

Another application for the variable speed drives is the use of this last for conveyor-belt system. ABB as one of the leading companies presented "A project report of the revamp of a lignite conveyor line" with quality criteria that meets high standards [41]

## I.5 VSDs Market , Evolution and Major Industrial Companies

**“Markets and Markets”** predicts that the Variable Speed Drive (VSD) market will grow from USD 20.73 billion in 2018 to USD 27.57 billion by 2023, at a Compound Annual Growth Rate (CAGR) of 5.87% during the forecast period. The major factors that are expected to be driving the VFD market are increased usage of VFDs across major industry verticals, rapid industrialization and urbanization, along with increasing investments on infrastructure development, and shifting focus on energy efficiency. [42]

In what follows a small forecast about the VSD market based on type, application, range power ,end user and region. [42]

Figure 1-15 shows the growth in the VSDs market over the past recent years with a prediction in the next three years

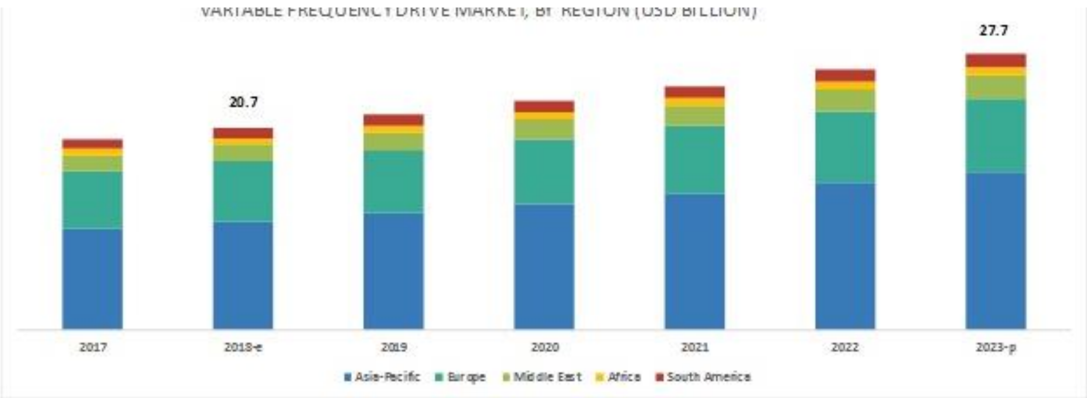


Source: Investor Presentation, Secondary Literature, Expert Interviews, and MarketsandMarkets Analysis

**Figure I-15 The growth of VSDs market (USD Billion)**

### I.5.1 Segmentation of VSDs Market

The VSDs market can be divided to five segments as shown in the figure 1.16,each segment plays a role to its development due to its influence not only in the industrial side but also in our everyday applications[43]

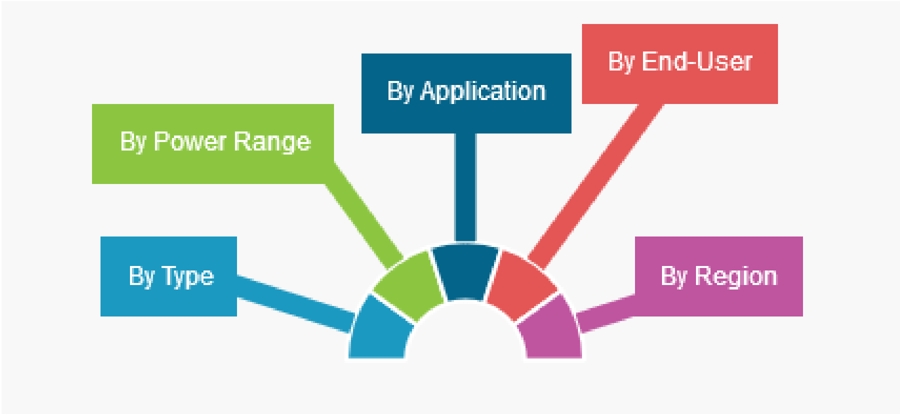


**Figure I-16 Variable Speed Drive Segments**

a) **By type:** based on the input type it can be divided in three sections AC drives, DC drives and servo drives. [43]

Based on the market study done by [43] it is well established that AC drivers acquire a large share in the market in addition to that VSDs can significantly reduce the overall cost by changing the speed.

As a result and as it is mentioned in the study : "AC drives are anticipated to possess the dominating position during the forecast timeframe"

b) **By power range:** the power range can be divided in four categories that are: Micro, Low, Medium and High power. Long operational life, compact size and adaptability to provide better control, power and energy saving has catered the market size of medium power VSD. As shown in figure 1.17 the market share by power range , medium size are the most sold then we can see that micro is just below it but have a great growth potential in the future .[43]

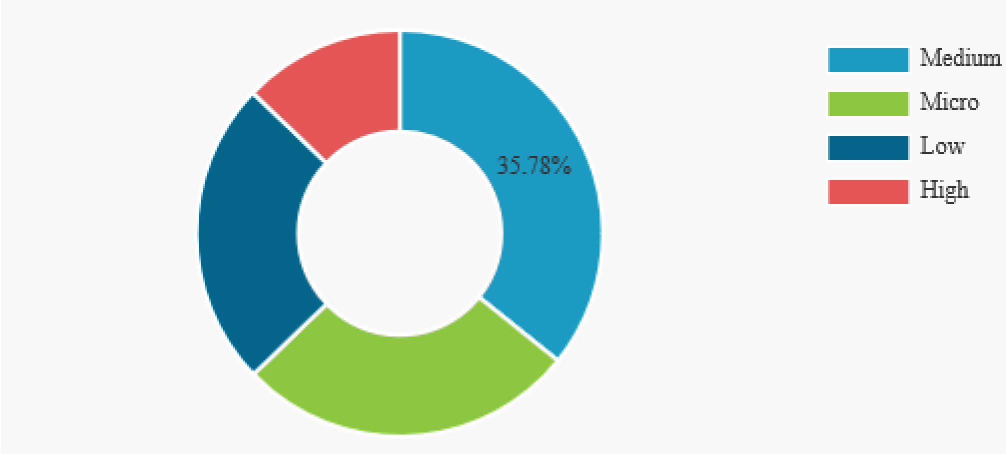


**Figure I-17 : Global VSD market share by power range 2018**

c) **By Application:** in this segment the VSDs market can be broadly divided into pumps, conveyors, HVAC, electric fan, extruders … etc. Pumps are the leaders in the market due to their wide range of application. HVAC is showing also a growth due to its adoption to energy-efficient strategy. [43]

d) **By End-Users:** This market is primarily divided into food & beverage, oil & gas, power generation, infrastructure, agriculture, mining … etc. Oil & gas market is the major in this segment. [43]

e) **By Regional Analysis:** Geographically, the VSDs market has been divided into five major regions which are North America, Europe, Middle East and Africa, Asia Pacific and Latin America. [43]

As it can be seen in figure 1.18 Asian Pacific has the major share of the VSD market due to its exponential development in industrial infrastructure, oil & gas, agriculture … etc and as leading countries China, India, Japan, Australia. [43]

North America also expects an increase in the VSDs market with the discovery of new hydrocarbon reserves and industrial growth. [43]

Europe intends to grow also in this market by establishing new norms for energy-efficient infrastructures those achieving an energy efficiency target of 32.5% by 2030. [43]

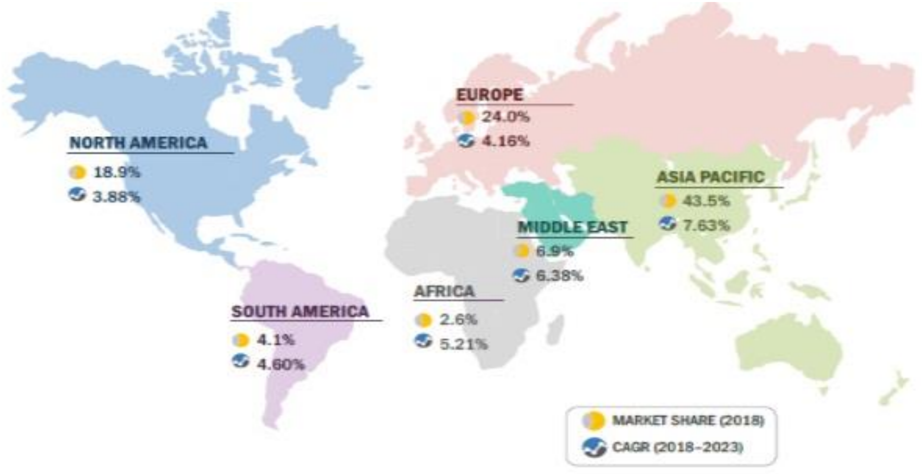


**Figure I-18 Global VSD Market Share (%) 2017**

### I.5.2 Industry key Players

The VSDs market has observed different regional and international participants, those procuring many products and now are introducing innovative products to many sectors to expands its usage. [43]

The leader companies of the VSDs market are [43]:

- Eaton
- Hitachi Hi-Rel Power Electronics
- Rockwell Automation
- Johnson Controls
- Anaheim Automation Inc
- WEG
- ABB Electrification
- Nidec Motor Corporation
- Siemens
- Danfoss Drives
- Honeywell International Inc
- TMEIC
- FUJI Electric Corp. of America

- Schneider Electric
- Yaskawa, Inc – Drive & Motion Division
- Toshiba International Corporation
- Mitsubishi Electric Automation, Inc.

## I.6 Trends in Speed Variation

Today manufacturers face many challenges to meet with their customers demand for more innovative products at lower price. Thus, benefiting from advanced automation systems that offer greater flexibility, reliability and productivity. [44]

Future Market Insights (FMI)[44] describes the VSDs trend benefits as:

- Energy efficiency: by using a VSD the motor rotation can be adjusted according to the needed requirements, resulting into energy savings [44]
- Advanced functionality: Modern VSDs come equipped with sensors that gauge important parameters to prevent damages on the motor [44]
- Improved Load Control: VSDs allow for smooth operation and acceleration as they prevent load swings in travers motions [44]
- Lower Starting Current: VSDs by powering the motor with less starting current prevent its impact on the motor and energy grid, thus reducing the probability of electric equipment failure [44]
- Regenerative energy: VSDs can create regenerated energy to be sent to the grid thus saving it from being wasted as heat. [44]

VSDs trends can be focused in 4 aspects:

- **Safety:** Considered as the first major trend. Safety functions are included as Safe Torque off, Safety Limited Speed and Safe Brake Control. As a result, production plants obtain greater levels of safety while requiring less overhead to integrate the drives into fail-safe, automation, and drive environments because safety is handled over the network [44]

- **Flexibility:** As a second major trend, having one drive product to fit all applications is appealing, as having to always change the drive for every application isn't cutting anymore and a standardized one is more beneficial [44]
- **Decentralization:** in this approach, a motor has the drive built into it, with just a communication line sent to the unit, reducing many costs due to space saving, air conditioning, wires diminution and maintenance. [44]
- **Pre-developed code:** Such code can support advanced functionality by loading it directly to drives on industry-specific machines, speeding and simplifying integration. [44]

## Conclusion

In this chapter a state of art about the AC-AC converters topologies has been presented with a small comparison between them. These topologies are divided into several families which are Indirect AC-AC converters where a power storage element must be included in the DC link, Direct AC-AC converters where we have the Cyclo-converters and the Matrix converters. Then, a simplified model of the induction machine (taking the Simplifying assumptions into account) was also presented with Park's model and the simplified equivalent circuit of the IM as well.

Another state of art about the control methods where V/f constant control, FOC and DTC methods were slightly presented.

A study on the VSDs market was presented, as well as its trends and some future predictions very clear that the VSDs market is rising due to its various applications in the industrial world.

The VSDs are found in various applications using all the topologies presented before. The Indirect AC-AC converter takes large share of its own in the market due to its robustness, simplicity, low price and its ability to provide a sinusoidal output that can be filtered to obtain a low THD.

Therefore, the optimal solution in the industrial field is to use a VSI based VSD that can provide all these while providing as well a control with maximum torque unlike the CSI that suffers from many insufficient such as the torque ripple.

# Chapter

# II

# CHAPTER II: POWER CIRCUIT STRUCTURE AND SIZING

## Introduction

In the first chapter a stat of the art about the VSD and its various topologies were presented and a brief market study was discussed.

The various topologies presented in the previous chapter are a basic view of the VSD. But in fact, a VSD construction is way more complicated since there are more important circuits included. These circuits are not replaceable as they contain basic functions of a VSD such as the pre-charge circuit and the braking circuit that will be presented later in this chapter.

In addition to that, this chapter will present the sizing of the power components and some other components (filters, snubbers…etc.) in the purpose to determine the basic criteria of choice of components of the VSD.

## II.1 Variable Speed Converter

From the previous chapter a VSI based variable speed drive has been chosen, this drive is composed of many parts that will be shortly presented here and discussed in detail later in the same chapter.

As presented in the previous chapter the ac-ac VSI consists of two stages a front-end diode rectifier and an inverter stage between them there is a DC link with a storage capacitor.

In addition to that, the chosen topology contains an input filter in order to reduce the EMI interferences, a pre-charge circuit for the DC link capacitor and a braking circuit.

In the following a brief introduction about each part is presented:

### II.1.1 The Input Filter, DM and CM

Comes right after the input supply, the main purpose of this filters is to minimize the pollution and noises coming from the common mode (CM) and the deferential mode (DM) that are presented as follows in figure II.1:

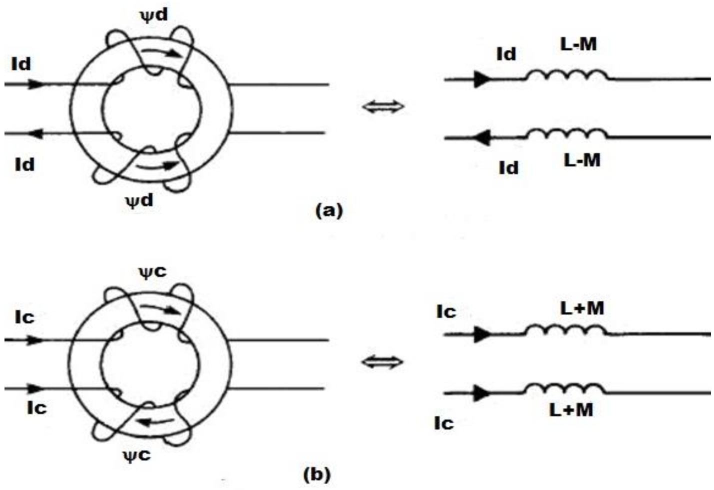


**Figure II-1 DM and CM noises**

Figure II-1-a represents the differential mode noise which is a current that appears on two lines of a closed loop, but current flow is in opposite directions. This kind of interference essentially appears in series with the desired signal. The solution is an inductor in series with the high side (and/or low side) of the line and a shunt capacitor across the lines (X type capacitors).

Figure II-1-b represents the common mode noise which appears on the two lines simultaneously in the same direction. The signal on each line returns through a common ground via a leak capacitor. The solution is to put a common-mode choke that produces equal and opposite magnetic fields that cancel one another. A capacitor from each line to ground is also used.

### II.1.2 The rectifier

As presented in the previous chapter the VSD contains two stages, the rectifier is the first stage and it contains many topologies depending on the application domain and the required specifications, for the very high-power applications (over 3MW) a thyristor-based rectifier is used when for low power IGBT or Diode rectifier is used (the choice will be presented in detail later this chapter).

### II.1.3 DC link capacitance and the charging circuit

To maintain a good DC Voltage with almost no ripples, a DC capacitor must be added to the DC link. This capacitor will be sized and chosen later in this chapter along with a specific circuit in order to charge this capacitor so as to assure the protection of the system and the DC voltage at all time.

### II.1.4 Braking circuit

When the speed setting in the VSDs is reduced, the braking circuit is used to dissipate the energy transferred from the motor or regenerate it depending on the braking circuit type used.

### II.1.5 The inverter

An inverter is a static converter assuring continuous – alternative conversion. The inverter output ensures an alternative supply with a specified frequency and amplitude that is needed. For VSDs, IGBT is used in the inverter due to its superior characteristics combining the high-speed switching performance of a power MOSEFT with the high-voltage/high-current handling capabilities of a bipolar transistor.

### II.1.6 Protection circuits

A protection device is required in the VSDs to provide thermal protection, over-voltage , overcurrent and short-circuit protection. Thus, protection devices can be: fuses, varistors or other type of circuits as snubber.

### II.1.7 Measurement circuits

To have a closed loop control of the AC motor some parameters are needed as the output current and voltage, here the measurement circuit has the role to give their value to the controller.

## II.2 Input filter

In order to eliminate DM and CM modes noises the industrial world came up with many topologies of filters, the basic filter is presented in [45] this filter contains two indictors and two capacitors in order to eliminate both types of noises as presented in figure II-2 where the type X capacitors are used for the differential mode and the type Y capacitor are used for common mode

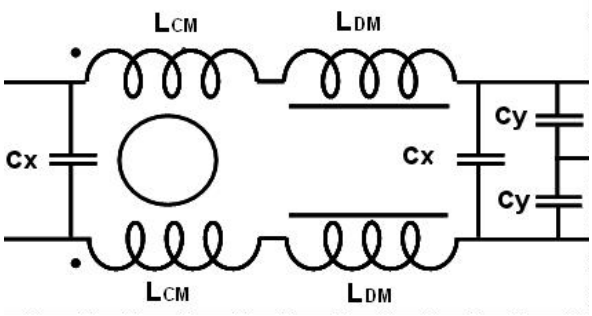


**Figure II-2 the basic filter for both DM and CM mode**

This filter is the basic filter for DM and CM noises, an improvement has been added to the inductors of this filter. Since the differential mode inductor is very low compared to the common mode inductor, usually in the industry, a common mode chock inductor is chosen where the leak is equal to the calculated deferential mode current. [46]

Another type of filters called AC shunt source side filter presented in [47]. This filter is used to decrease voltage distortion and harmonics and to correct the power factor. (figure II-3)

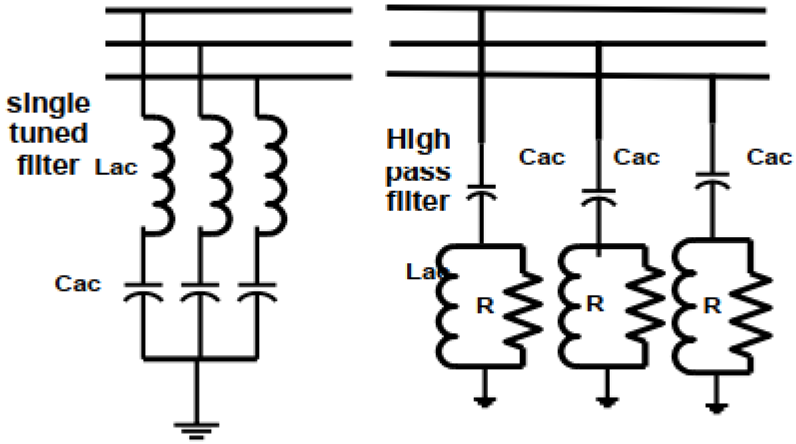


**Figure II-3 shunt source side filter**

There are many different input filter topologies used in the industrial world. We present two of them in Figure II-4 [48]:

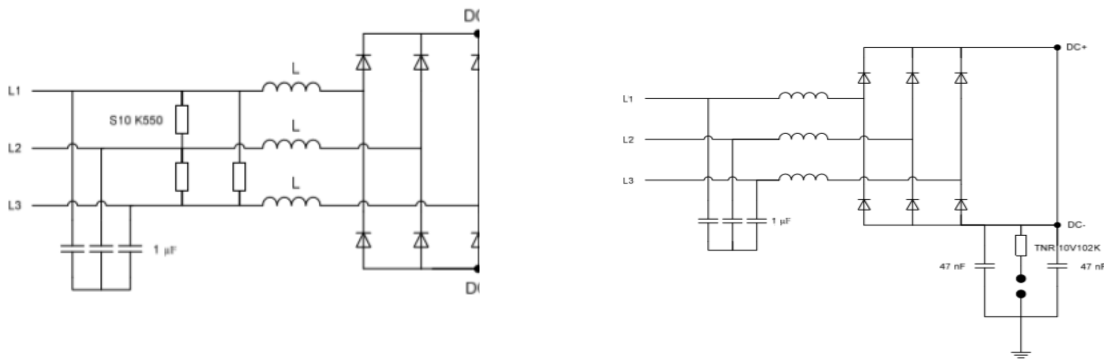


(a) (b)

**Figure II-4 some industrial input filter topologies (a) EMI filtering of Danfoss VLT MircoDrive FC51, Circuit diagram of Hitachi X200 EMI filtering**

From Figure II-4-a we can see that basically the input filter is generally a CL filter where only Y type capacitors are used and that’s because usually the dominated noise is the common mode noise, As for (figure II-4-b) a Y type capacitor is added in the DC link in order to eliminate the differential mode noise the additional capacitor in the DC link and not in the input has a major advantage of eliminating the additional noise coming from the diodes commutation according to [49].

So, according to the comparison, in order to minimize the cost one inductor will be chosen and since the rectifier is a diode rectifier the selected input filter is a traditional CL filter (as seen in figure II-4-b) in order to avoid the diode rectifier noise.

### II.2.1 Input filter sizing

In order to size the input filter a spectrum analyses for the output current is needed since it's the carrier of the differential mode current (coming from the commutation frequency), this analysis gives the harmonics with high amplitude in order to choose an appropriate cut off frequency.

$$f_c = \frac{1}{2\pi\sqrt{LC}} \qquad \text{(II.1)}$$

After choosing a good $f_c$ , the CL filter inductor is chosen first since it causes a voltage drop. This voltage drop must be under 5% in the industrial norms recommended by the NEC [50]. The value of L can be extracted.

$$U_L = L\frac{di}{dt} \qquad \text{(II.2)}$$

Therefore, from II.2

$$L = \frac{U}{\frac{di}{dt}} \qquad \text{(II.3)}$$

That being said it is impossible to determine an inductance value theoretically due to the non-linearity of the current which results a variable di/dt. So, in order to find the proper value a series of tests on different values are done so as to choose the appropriate inductor.

Which means that usually the input filter inductor in chosen experimentally.

As for the capacitor, from II.1 we have:

$$C = \frac{\left(\frac{1}{2\pi f_c}\right)^2}{L} \tag{II.4}$$

## II.3 The Rectifier Bridge

There are many types of rectifier topologies that can be used depending on the used power semiconductor (diodes, thyristor, GTO, IGBTs…) as seen in figure II-5.

The thyristor rectifier is used for application with very high power usually over 3MW because thyristor can support it but in the same time they can't go high in frequency. Meanwhile the IGBTs works as opposite since they can go very high in frequency but they can't support high power due to its commutation.

Usually the controlled rectifiers (thyristor, GTO, IGBTs…) are used in VSD where the regenerative braking is possible, in the other hand applications that do not require regenerative braking system with low power, the most appropriate rectifier is a diode-based rectifier where the rectification can be done with high efficiency and low cost.

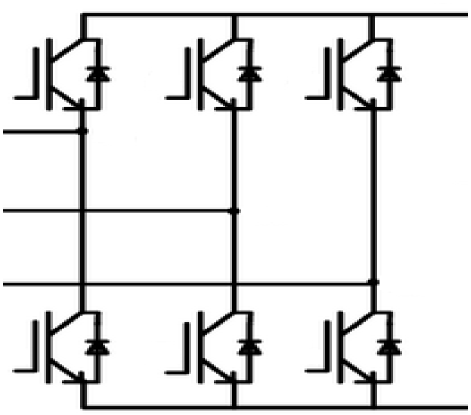

a-IGBT Based rectifier

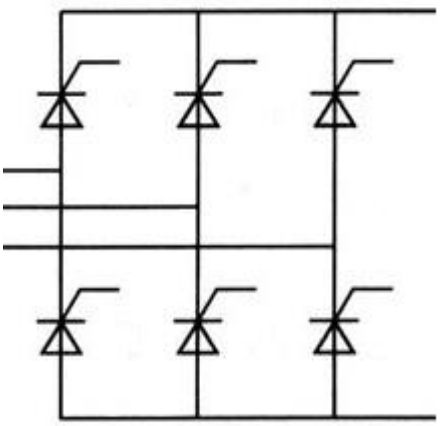

b-Thyristor based rectifier

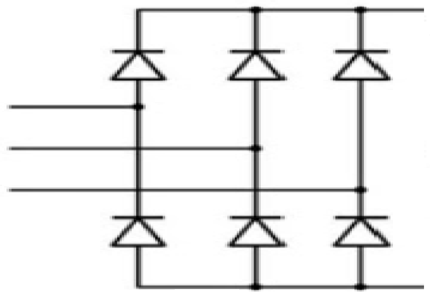

d-Diode based rectifier

**Figure II-5 basic rectifier designs**

Other rectifier topologies exist and they basically use IGBTs. Most of them are used to design the rectifier of the Matrix converter such as the spars MC, the very spars MC..., these topologies were already presented in chapter one in figure I-3.

The specifications of this project give a power of 2.2kW which is relatively a small power so thyristors are not the appropriate choice, and since the braking system is not regenerative so the use of IGBTs will be additional cost, therefore the most appropriate choice it to choose a diode rectifier which suitable for standard application and the cheapest as well.

### II.3.1 The rectifier sizing

The rectifier gives an output voltage where its mean is calculated as follows:

$$V_{DC} = \frac{2qV_{max}}{\pi}\sin\left(\frac{\pi}{q}\right) \tag{II.5}$$

Which means $V_{DC} = 660V\ with\ V_{max} = \sqrt{2} \times 220$. With q=3.

This value goes between 600V and 1200V (the values that exists in industrial world) so the chosen value is 1200V bridge rectifier

These diodes need to support a current that goes to a nominal value of

$$I = \frac{P_{load}}{V_{DC}} = \frac{2200}{660} = 3.33A$$

## II.4 The DC Link Capacitor

In all practical topologies in use, the inverter used in the dc-ac conversion stage which injects high frequency current ripple to the dc bus. In the other hand the rectifier bridge injects low frequency current ripples. Therefore, many investments have been made to decrease the effects of these noises.

In the industrial world there are many topologies of the DC link filter, presented and explained in [51], [52], [53]. The following figure (figure II-6) presents some of these filters.

In figure II-6-a a C type filter is presented, this is the most basic filter in a DC link (DC link Capacitor) [51], which is still the most common structure in the industrial applications, in this filter a large electrolytic capacitor is used to store the energy and to supply the inverter with a low voltage ripple. But, the use of electrolytic capacitor makes the structure bulky.

In figure II-6-b a second type is presented where the electrolytic capacitor is replace with a film capacitor which is rather smaller in size according to the same reference [51], this type of filter gained more attention also because of its longer life compared to the first filter. But the film capacitors cannot store high levels of voltages which leads to a large ripple and thus it will affect the inverter control technique in order to overcome this variation (according to the same reference).

Another filter is presented in Figure II-6-c which is an active filter called EI structure ( Electronic Inductor ), this filter is used to improve the line current harmonic distortion , in this filter the inductor is controlled in a manner to provide a constant current in the DC terminal according to [51]

Figure II-6-d presents the Z source topology. It was presented in [54] the Z-source inverter allows the system output voltage to be stepped down or up as desired by inserting a unique X-shaped *LC* impedance network.

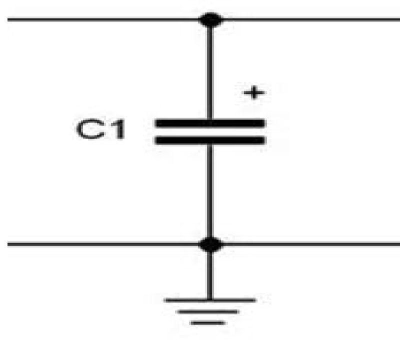


a- a C filter

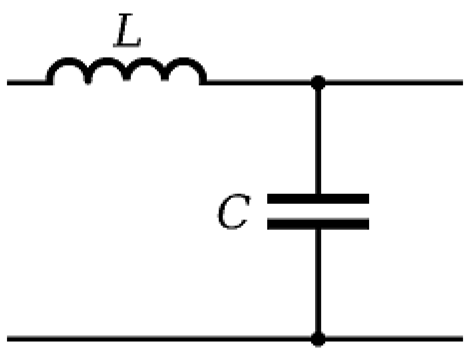


b- LC filter

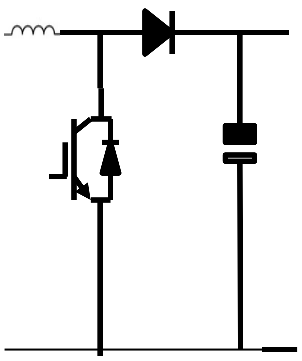

c- EI filter

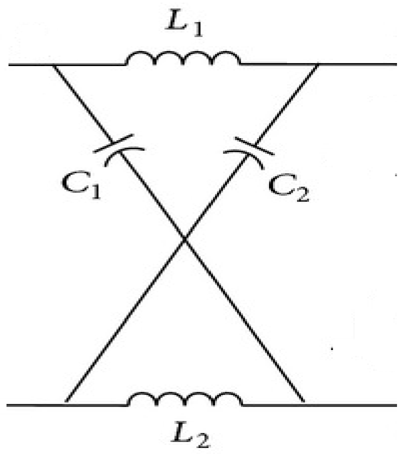


d- Z source

**Figure II-6 DC Link filters topologies**

Since the specification of the project states that the inverter is a VSI so the controlled variable is the voltage with a DC link value that exceeds 600V which is relatively high. So, in order to provide a very good DC link voltage a C type filter is used for its possibility to withstand the voltage and for its low cost.

### II.4.1 Sizing the DC link capacitor

The dc bus capacitor $C_{DC}$ receives harmonic current from both the rectifier (Irh, LF) and inverter (Iih, HF) sides. Therefore, the dc bus capacitor current ripple rms value is calculated as in [52]

$$I_c = \sqrt{I_{rh}^2 + I_{ih}^2} \quad \text{(II.6)}$$

Since the drive is a VSI drive that means the dc bus voltage ripple should be minimized which means that an electrolytic capacitor is preferred due to its high capacitance/volume ratio as follows [52].

According to the same reference the DC link capacitor is calculated using the following formula where $P_{load}$ is the rated load power and $V_{s_{rms}}$ is the grid voltage rms value and $f_{re}$ is the grid's frequency.

$$C_{dc} = \frac{Pload}{240 V_{ripple} V_{s_{rms}} fre} \quad \text{(II.7)}$$

Where the $V_{ripple} = 0.5\% \; of \; V_{DC}$

That means $C_{dc} = 416 \; \mu F$

## II.5 DC Bus Charging Control System

When the power is first connected to the input terminals of the VSD, very high inrush currents would occur, those currents are injected directly across the DC bus charge (capacitor). While the diodes in the rectifier module and the capacitors may be able to withstand these high currents, a possibility that upstream fuses or circuit brakers would trip out the VSD [55].

Therefore, provisions are made to limit this inrush currents, a DC bus pre-charge circuit is provided [55]

There are two main approaches to solving the problem of inrush current:[55]

• Pre-charge resistors, with a bypass contactor, either on AC side or DC side of the AC/DC rectifier bridge.

• The AC/DC rectifier can be a controlled rectifier bridge instead of an uncontrolled diode bridge.

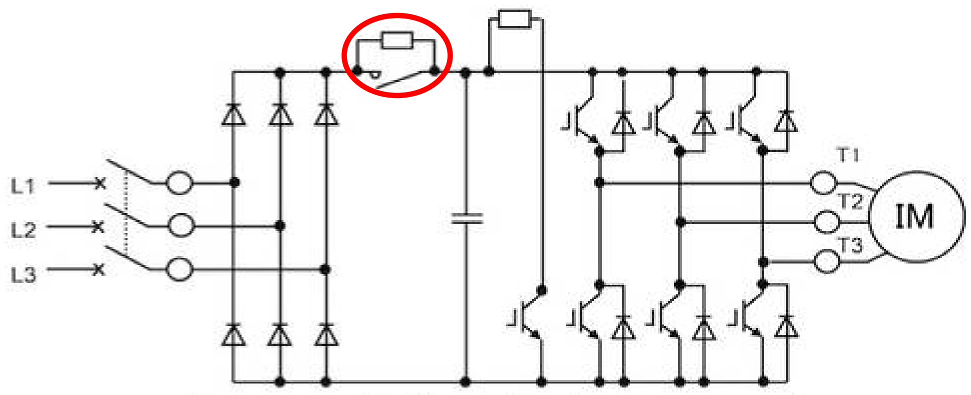


**Figure II-7 Example of a DC bus pre-charging circuit**

In figure II-7 charging resistors are inserted between the rectifier bridge and the capacitor to limit the current when the power is first applied. [55]

Once the capacitor is charged the resistors introduce additional losses in the VSD that are preferable to avoid by bypassing them using a relay (for small VSDs) or contactors (for large VSDs).[55]

In case of a bypass contactor, it’s control can be done by two different methods. The first one using a simple timer circuit with a fixed time delay between power being applied and the inverter stage being enabled. The other one is by monitoring the DC bus voltage and the bypass relay is closed after a certain voltage level has been attained .[55]

The main advantages of this method are:[55]

• Simplicity of the control circuit

• Cheap and easy to implement

The main disadvantages of this method are:[55]

• The losses associated with the relay contacts and coils

• The physical size of these components

### II.5.1 DC Bus charging sizing

As for the time pre-charging time, it is well known that

$$\tau = RC \quad \text{(II.8)}$$

In order to slow down the charging speed of the capacitor so as to have a long longevity the pre-charge time is chosen as 1.5s which means $3 \times RC = 1.5s$ in order to fully charge the capacitor

So, $R = 1k\Omega$

As for the power. this resistor needs to absorb all the power that can be absorbed by the capacitor, that means

$$E = \frac{1}{4} C{V_{dc}}^2 \quad \text{(II.9)}$$

And knowing that

$$P = \frac{\Delta E}{\Delta t} \quad \text{(II.10)}$$

With $\Delta t = 1.5s$

At the end we get $P = 13.6W$

## II.6 The Inverter Stage

There are many types of inverter topologies that can be used depending on the gate-controlled device that become available in the past decade, which are divided into two main groups of components[56]:

- Those based on thyristor technology such as Gate Turnoff Thyristor GTO and field Controlled Thyristor FCT.
- Those based on transistor technology such as the Bipolar Junction Transistor BJT, Field Effect Transistor FET and the Insulated Gate Bipolar Transistor IGBT.

As seen in figure II-8 many inverter topologies using different gate-controlled device are proposed.

Nowadays, like seen in figure II-9 [56] each power semiconductor has his own range in power and frequency.

As a conclusion VSDs use IGBT as gate-commutated device for its performance in both switching frequency range and power.

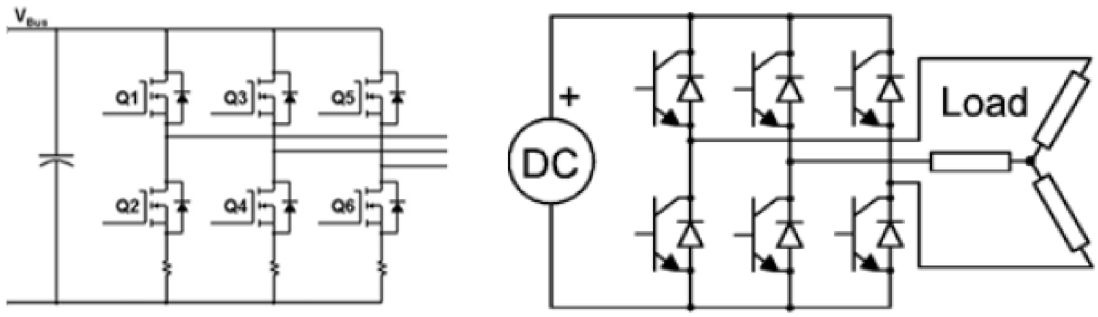


a- MOSFET inverter b- IGBT inverter

**Figure II-8 Inverter topologies**

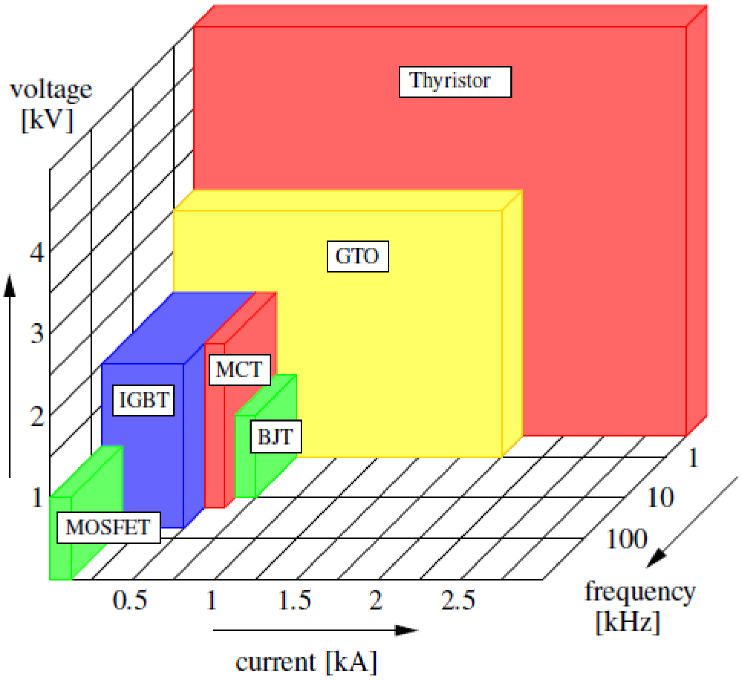


**Figure II-9 Summary of power semiconductor device capabilities**

### II.6.1 Driver circuit

Driver Circuit is equipment used to turn-On (conduct) and turn-Off (commutate) the power semiconductor by giving them the appropriate current pulse.

Drivers are usually used to regulate current flowing through a circuit. In addition to that, if the driver itself contains an optocoupler that means it also creates an isolation between the power semiconductors and the control circuit.[57]

The main purpose of the driver circuit is to amplify the control signal so as to be able to trigger the IGBT’s gate.

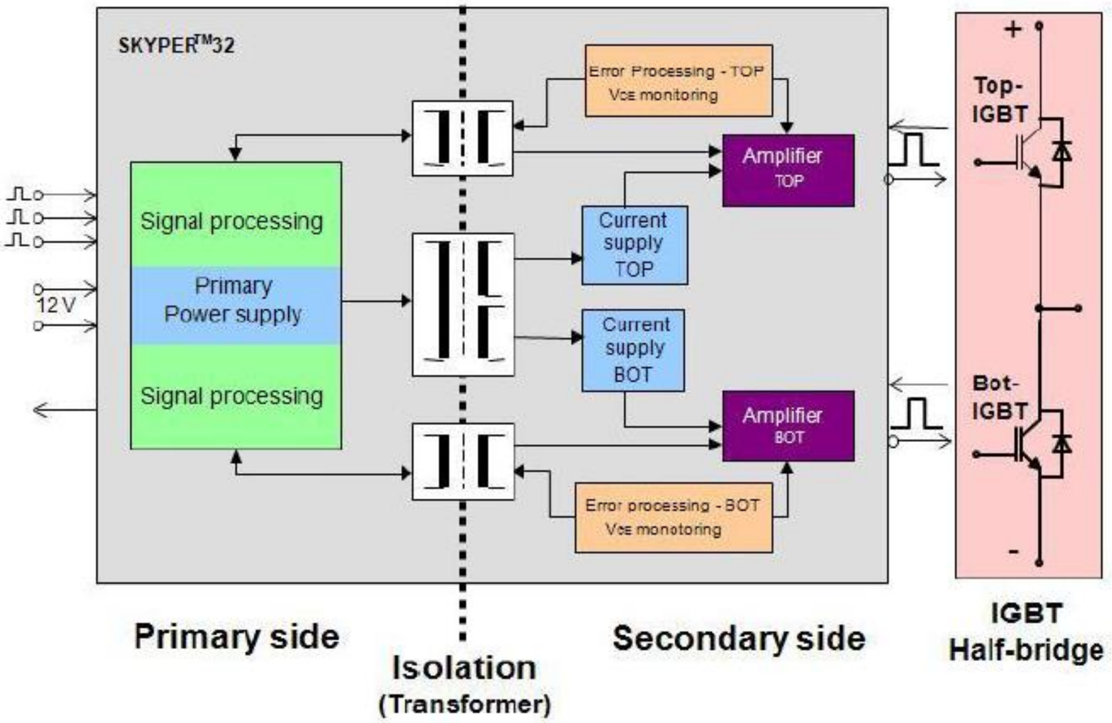


**Figure II-10 Block Diagram of half – bridge Gate Driver**

- **Opto-couplers:** An opto-coupler is basically used in the place of isolation transformers making it also a protective piece thanks to its property of isolating between the control and power circuits as seen in figure II-10. By generating light beams that are modulated by input current then received at the output side thus generating the necessary impulse to operate the semiconductor ( IGBT ). [57]

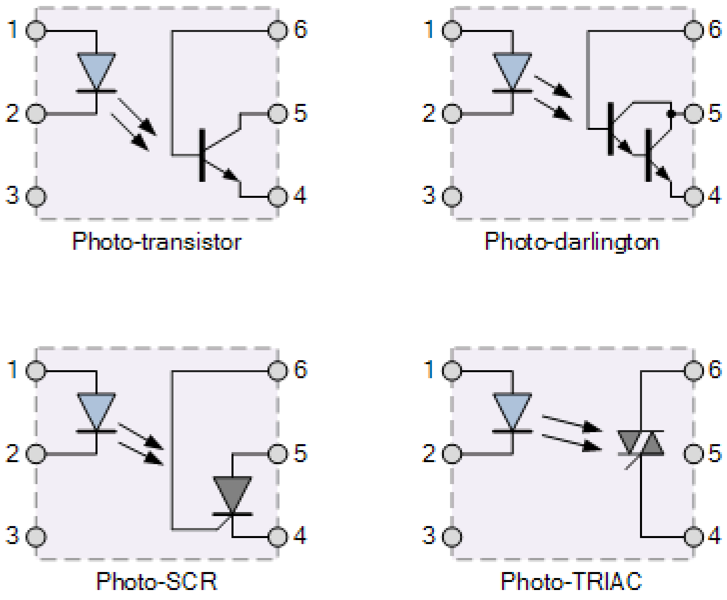


**Figure II-11 Optocoupler types**

As figure II-11 shows there are many types of Optocoupler the basic ones are the ones presented in the figure.

For the photo-transistor and photo-Darlington, they are mainly used in DC application since they ensure the one directed flow of current in them. The SCR and TRIAC based optocouplers are usually used in AC application thanks to the ability to control the fire angle and/or the bidirectional flow of current.

Optocouplers and opto-isolators can be used on their own, or to switch a range of other larger electronic devices such as transistors and TRAICs providing the required electrical isolation between a lower voltage control signal, for example one from an Arduino or micro-controller, and a much higher voltage or mains current output signal.

### II.6.2 Comparison between IPM and IGBT Module

- IGBT Module: IGBT module is a device required for inverter use in many types of industrial equipment, and has driven the trend towards high currents and high voltage since 1990, thus increasing its stability, durability, size reduction, energy saving and cost reduction. IGBT module with its development have seen many configurations as seen in figure II-12.[58]

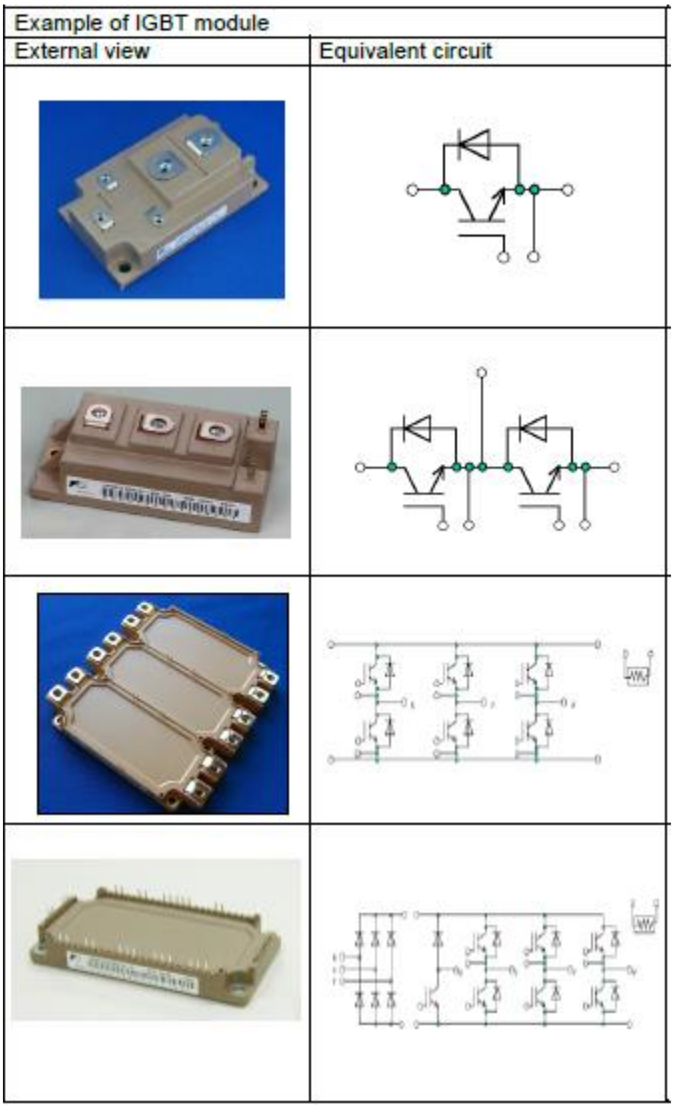


**Figure II-12 IGBT Modules**

- IPM (Intelligent Power Module) : is a high-performance module that mounts a dedicated drive circuit for drawing greater performance from an IGBT chip. IPM come equipped with control IC possessing IGBT drive circuits and protection circuits, and therefore, it is easy to design peripheral circuits and possible to ensure high system reliability. It is suitable for applications such as those using AC servos, air conditioning equipment, and elevators.[59]

The new generation IPM come equipped with some protection like overcurrent protection, short circuit protection, control of power voltage drop protection, and overheating protection for better function , performance and a less size .[59]

## II.7 Braking Circuit

There are several methods of decelerating and stopping a motor [55]:

• **Coast to stop**, where the kinetic energy is dissipated in the load itself.[55]

• **Mechanical braking**, where the kinetic energy is converted to heat due to friction.[55]

• **Electrical braking**, where the kinetic energy is initially converted to electrical energy before being transferred back to the power supply system or dissipated as heat in the motor or a resistance.[55]

Most fixed and variable speed drives are stopped by removing the power and then allow the driven machine to coast to a stop after a natural deceleration time as shown in Figure II-15 , but this natural deceleration is used in some typical applications as conveyers, funs … etc . However, there are some applications where additional braking is required to provide a shorter deceleration time as shown in figure II-13.[55]

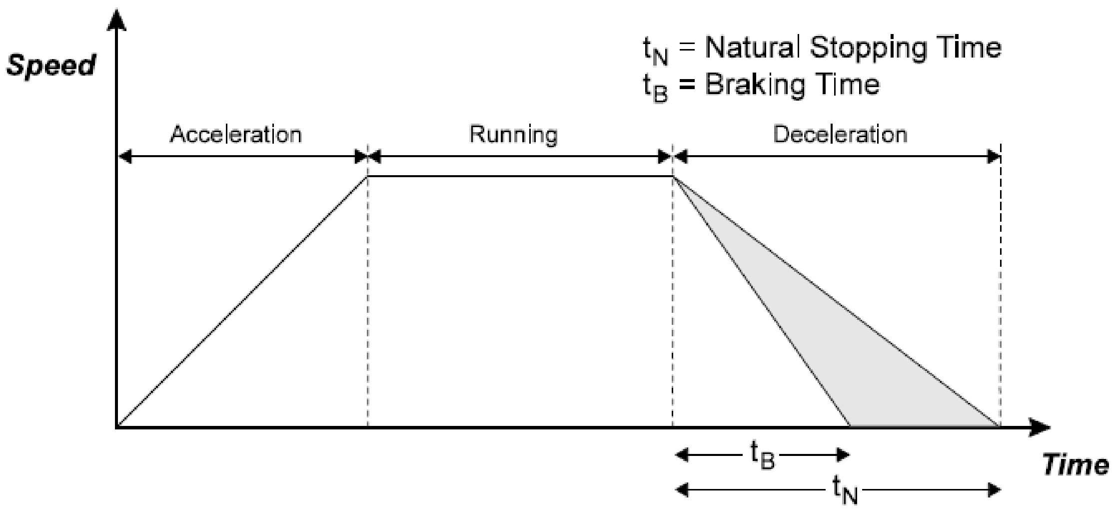


**Figure II-13 Braking times for rotating drives**

The traditional approach was by using mechanical braking, but this requires considerable maintenance for both the mechanical parts and the brake pads.[55]

For modern variable speed drive systems, electrical braking is the preferred method. Electrical braking system rely on temporarily using the motor as an induction generator driven by the mechanical load.[55]

• In the **motoring mode**, the inverter output frequency will always be higher than the rotor speed[55]

• In the **generating (braking) mode**, the inverter output frequency will be at a frequency lower than the rotor speed. The braking torque produced during deceleration is dependent on the slip of the motor.[55]

During electrical braking, energy conversion takes place from mechanical energy to electrical energy [55]

Electrical braking has several advantages over mechanical braking [55] :

• Reduction in the wear of mechanical braking components

• Speed can be more accurately controlled during the braking process

• Energy can sometimes be recovered and returned to the supply

• Drive cycle times can be reduced without any additional mechanical braking

### II.7.1 Dynamic Braking:

When the speed setting in the VDS is reduced, the output frequency supplied to the motor is also reduced and the synchronous speed will decrease to fit the new frequency. However, this does not mean an immediate change in speed. Any change in the motor depend on external mechanical factors, particularly the inertia of the rotating system.[55]

Figure II-14 an illustration of the change in motor torque when a braking occurs.

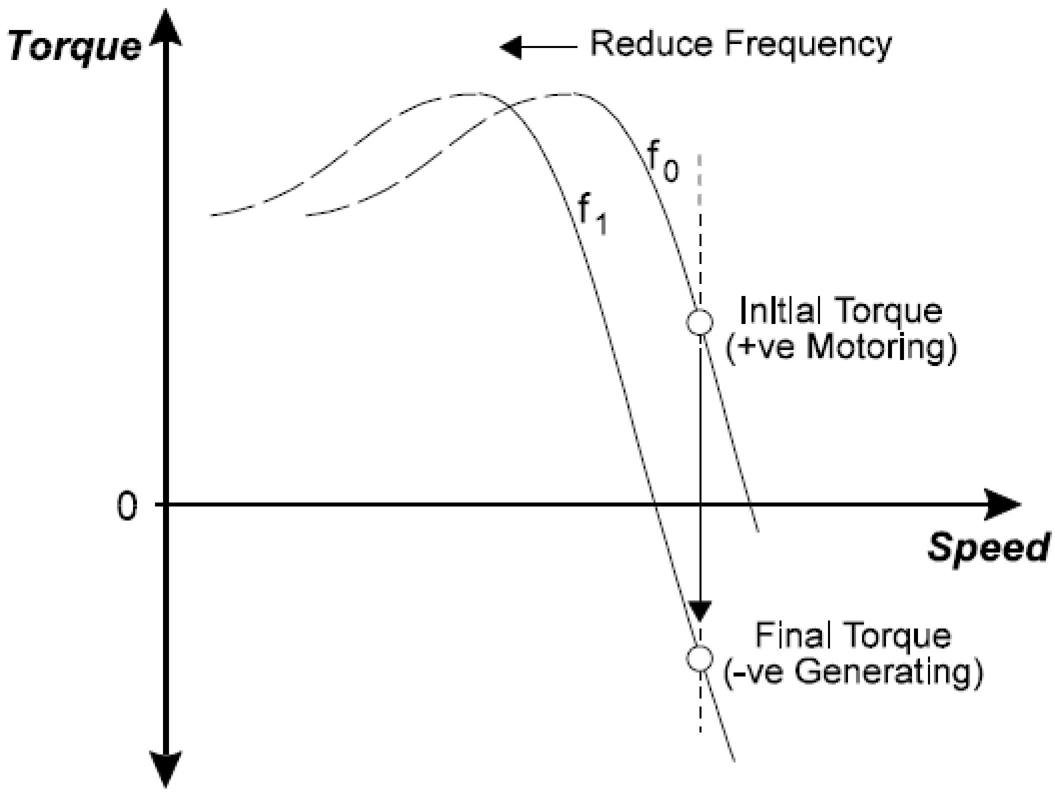


**Figure II-14 Torque–speed characteristics of an induction motor when braking (frequency is reduced from f0 to f1)**

In practice the output frequency supplied to the motor when braking is reduced slowly to avoid the large braking currents that would otherwise flow.[55]

During braking, the converter must have a mean to deal with the energy transferred from the motor. Since the DC bus voltage does not change during braking, the direction of the DC bus current reverses. With the use of a diode rectifier bridge, the braking current is blocked from returning to the power supply, thus this energy being absorbed by the DC capacitor resulting in a rise of the DC bus voltage to destructive levels. [55]

When Braking**,** the energy is dissipated in a braking resistor connected across the DC bus as shown in figure II-15.[55]

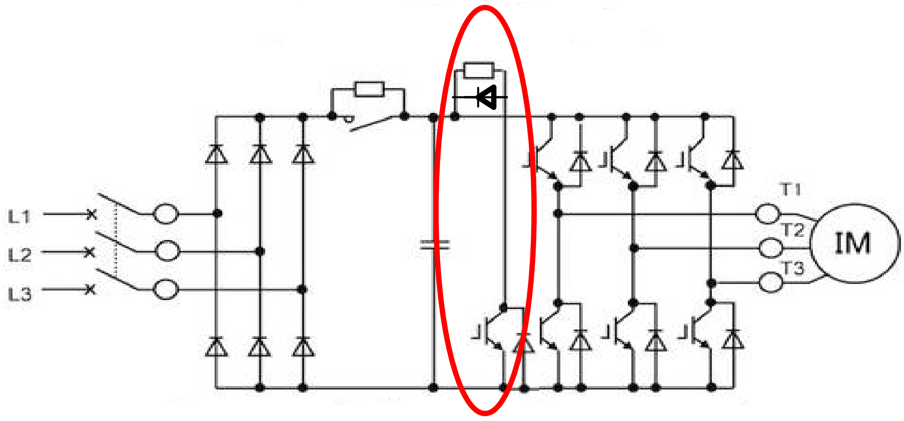


**Figure II-15 Ac converter with a DC link Dynamic brake.**

This braking circuit is the same used in electrical braking

### II.7.2 Dynamic braking sizing

The resistor of the dynamic braking can be found as [60]:

$$R = \frac{V^2{}_{mean}}{P} \qquad (II.12)$$

$$R = 198.9612\ \Omega$$

For the resistor power, by using a wire wound power resistor it can handle about 20 times its rated power for 3 seconds [60] , the resistor power can be calculated as :

P=2200/20=110W.

## II.8 Protection Circuits

### II.8.1 Varistors

The overvoltage peaks are attenuated by varistors between supply phases. The varistors are non-linear resistors whose resistance changes according to the voltage applied on it (figure II-16)

When the varistor is properly dimensioned and the supply voltage is within normal limits, virtually no current flows through the varistor. When the voltage exceeds the intrinsic voltage level of the component, its resistance suddenly collapses and short-circuits the interference current back into the return conductor.

The varistor is a simple and inexpensive protection against surges. However, the varistor only carries a limited amount of energy and therefore does not protect against transient surges. Its properties also deteriorate with repeated overvoltage peaks.

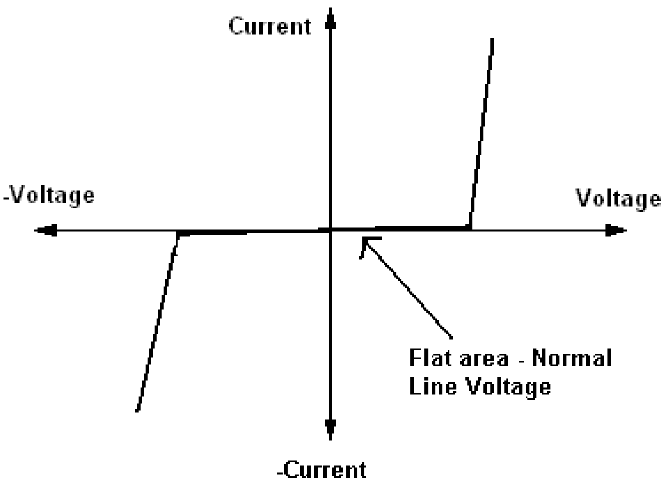


**Figure II-16 varistor's characteristics**

### II.8.2 Snubbers

In any circuit that contain power semiconductors, the existence of the snubber circuit is inevitable because they play a major role in the protection as well as improving the performances. According to [61] the snubber circuit can:

- Reduce or eliminate voltage or current spikes
- Limit dI/dt or dV/dt
- Shape the load line to keep it within the safe operating area (SOA)
- Transfer power dissipation from the switch to a resistor or a useful load
- Reduce total losses due to switching
- Reduce EMI by damping voltage and current ringing (ringing means sur-oscillation that happens when there is a quick transition to the signal)

There are many topologies of snubber circuits, the most common ones are the resistor capacitor (RC) damping network and the resistor-capacitor-diode (RCD) turn-off snubber figure II-17.

RC snubber circuit RCD snubber circuit

**Figure II-17 Snubber Circuits**

RC snubbers is used to reduce the peak voltage at turn-off and to damp the ringing, RC snubbers are very useful for low and medium power applications [61].

RCD snubbers can reduce the total losses of the circuit in addition to the peak voltage but holed a major disadvantage that makes the effective value of the damping resistor during the charging is equal to 0 because of the diode which makes some optimized RC snubbers better than this one according to [61].

#### II.8.2.1 How does snubber circuit work

RC snubber is commonly used in switching converters to limit the voltage spike on the switching device into a safe level

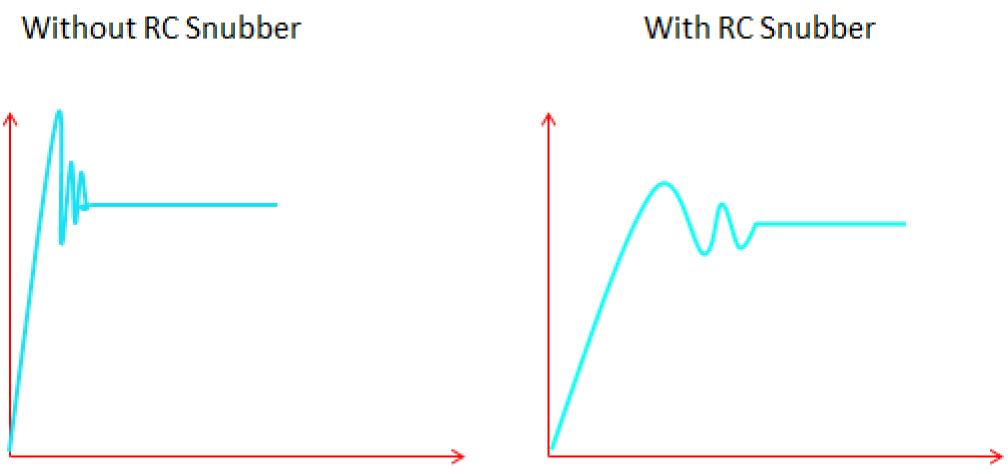


**Figure II-18 RC snubber effect**

RC snubber works by lowering the voltage spike level. The capacitor acts as charge storage and the resistor provides a discharge path. For instance, in the below circuit, the RC snubber R1 and C1 protects the MOSFET Q1 from voltage spike on the drain (same for the IGBT). When the MOSFET is OFF, the snubber capacitor will charge through R1. When the MOSFET turns ON, the capacitor will discharge through R1 to the MOSFET and to the circuit ground. The cycle will repeat with the capacitor is empty. The resistor is the one dissipates power. In a single switching cycle, there are two times where current flows to the resistor. Below illustration called the currents as charge and discharge currents.

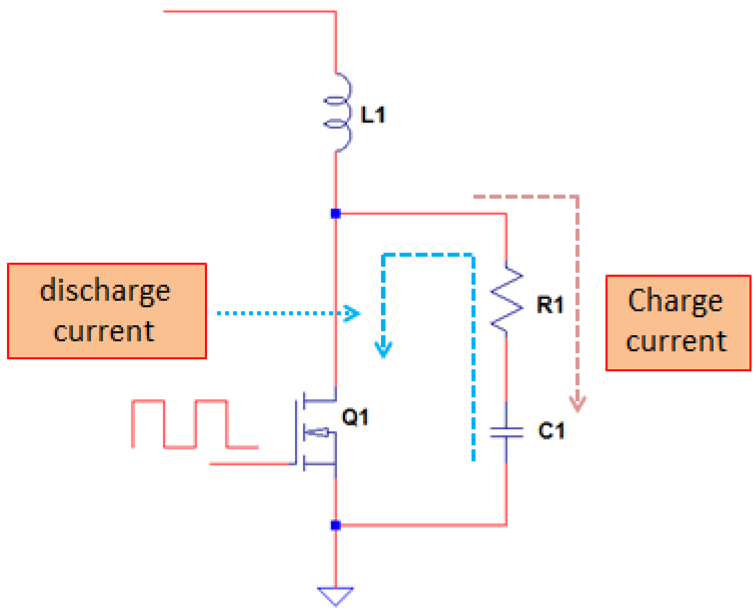


**Figure II-19 RC snubber circuit working principle**

In [62] a quick way to design a snubber has been suggested as follows.

For the current to flow through the resistor without requiring a voltage overshoot, Ohm's Law says the resistance must be[62]:

$$Rs \leq \frac{Vmean}{I}$$

⇨ $Rs \leq \ 198.1982\ \Omega$

The resistor's power dissipation is independent of the resistance Rs because the resistor dissipates the energy stored in the snubber capacitor that is $E = \frac{1}{2*Cs*Vmean^2}$ for each voltage transition. The capacitor must be chosen to let the resistor dissipate half of its power ratting (1Watt) in two times fs (switching frequency) per second:

$$1 = (\frac{1}{2*Cs*Vmean^2}) * 2fs \qquad \text{(II.11)}$$

From II.10 we have:

$$\Rightarrow \; Cs = \frac{1}{Vmean^2 * fs} \tag{II.12}$$

Where fs is the switching frequency that is 5KHz in this case.

$$\Rightarrow \; Cs = \; 4.5914e - 10\,F$$

## Conclusion

In this chapter a study of the motor speed drive circuit has been made where its principal components were given whilst doing the sizing of these components.

Both filters (input filter and DC link filter) were chosen and sized in the same time with some specific circuits that have different roles such as the Charging Control System that works as prevention against the inrush current and the braking circuit to decelerate or stop the motor.

In addition to that protection circuits were presented as well in order to protect the devise such as the varistors and the snubber circuits.

In order to see the results (simulation) of these circuits and the system as whole other circuits must be presented as well which are the measurements circuits and the IPM supply circuits.

These circuits as well as the results will be presented later in the next chapter.

# Chapter

# III

# CHAPTER III: HARDWARE CHOICE

## Introduction

In the previous chapter a study of each part of the VSD was presented in term of calculus in case of input filter, DC link and snubber circuits or a comparison between some of the exciting components such as IPMs, diode modules …etc.

Some notion that have deep impact in the main structure of the VSD were also presented such as the braking circuit, the pre-charge circuit and the EMI filters that plays an important role in eliminating the electromagnetic pollution and reduces its interference in the circuit in order to generate better quality signals.

But the industrial world is full of many manufactures that produce many products in different technologies, sizes and functionalities. So, choosing a component over another one must not be random, but under some rules and considerations that decides the most suitable one among all the other existing ones.

In the following chapter the choice of every component of the VSD with the detailed circuits are presented while doing some comparison between the already existing components.

Finally, this chapter is concluded with the results of the simulation with a chosen control type and the estimated price for the VSD.

## III.1 Input filter

In order to determine an appropriate EMI input filter a simulation without the is conducted to identify the higher harmonic components of the input current (figure III-1)

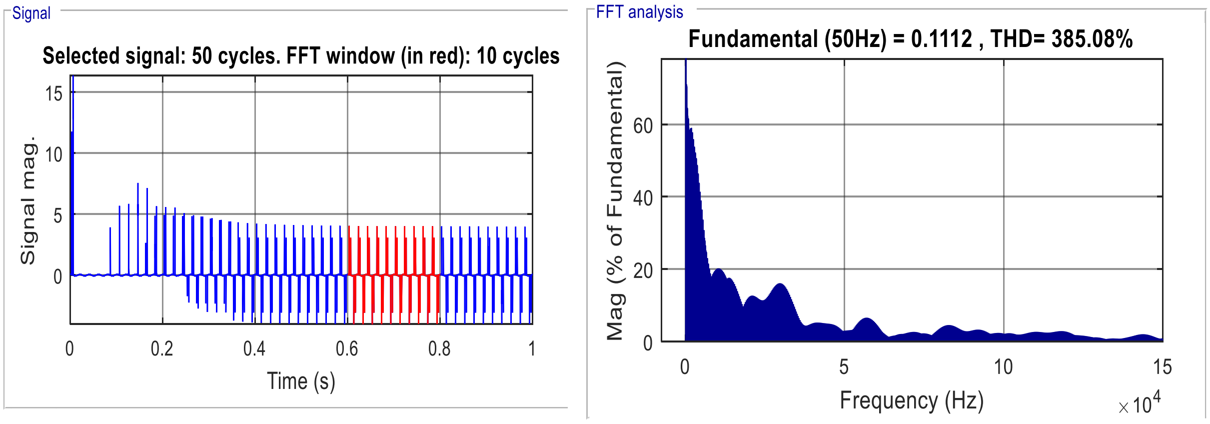


**a) Input current** **b) Spectrum analysis (FFT)**

**Figure III-1 input current before (without) the filter**

From the figure above, we can see a great THD that goes to about 385.08% which is really high because of the harmonic components due to CM and DM modes.

From figure III-1-b it is observed that the highest harmonic components are low frequency components due to the diode rectifier bridge (gives the harmonic orders represented by $n = 6n \pm 1$). these harmonics are not part of EMI harmonics. Where the need of either another filter or to change the non-controlled rectifier with a controlled one using IGBT's so as to eliminate the low frequency harmonic components.

According to[63] for better performances, the cut off frequency must be chosen in a way that it's so small than the commutation frequency. Since the simulation was done with a commutation frequency of 5kHz so the cut off frequency was chosen to be 3kHz give or take few hundreds.

### III.1.2 Inductor design

As presented in the previous chapter , the inductor must be calculated experimentally, various theoretical formulas were tested, their result were not acceptable in the sense of the volume of the filters.

So, the solution is to choose an inductor that was chosen for an EMI filter for HITASHI X200 with inductance value L=2 mH (reverse engineering).

### III.1.3 Capacitor design and choice

Using the previous formula provided in chapter II we find that $C = 1.407\ \mu H$ so an B32923C3155M189 capacitor with 1.5uF is enough but since it's close to price to B32923C3225M capacitor with 2.2uF this late is chosen since it gives far more adequate results.

These types of capacitors are known as X type capacitors (Figure III-2)


**Figure III-2 B32923C3225M X2 type capacitor.**

These types of capacitors are called EMI suppression capacitors and according to the file given by illinoiscapacitor [64]. They are divided into two categories X and Y type capacitors and in each type there are 3 sub-categories (X1,X2,X3….). According to the same reference the appropriate one is X2 (figure III-3).

So, with this the new cut off frequency is according to equation II.1

$$f_c = \frac{1}{2\pi\sqrt{LC}} = \frac{1}{2\pi\sqrt{2 \times 12^{-3} \times 2.2 \times 10^{-6}}}$$

$$f_c = 2399.4Hz \approx 2.4kHz$$

The results of this filter are provided in figure III-3 where it can be seen that the THD value dropped to 53.11% which is a relatively good result for an EMI filter.

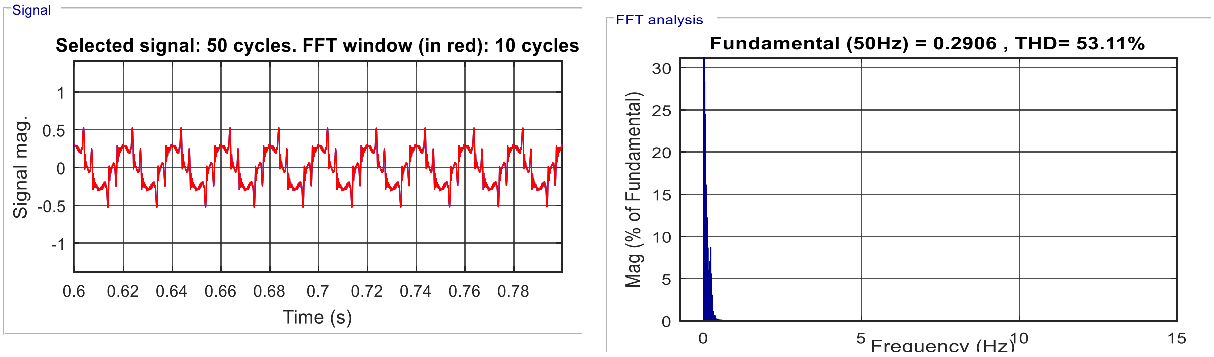


**a) Input current** **b) Spectrum analysis (FFT)**

**Figure III-3 input current with (after) the filter.**

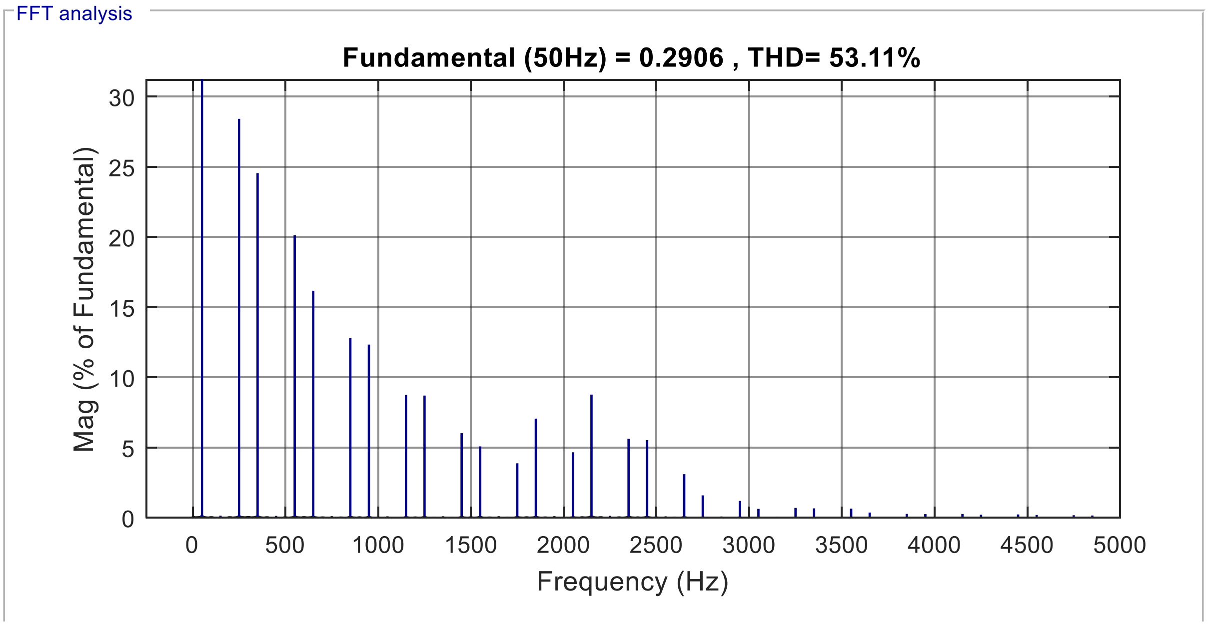


**Figure III-4 a zoomed view of the spectrum**

As it can be seen from figure III-4 all the harmonics above the frequency of about 2.5kHz are almost gone which goes well with the calculated value of the filter.

## III.2 Rectification stage choice

The rectifier is a diode-based rectifier that must have a reversed voltage of 1200V and which can support a max current of 10A.

Mouser has provided many rectifier bridges with those characteristics such as **VUO30-12NO3** and **VUC36-12GO2.** These rectifier bridges satisfy the condition but they are oversized a lot. Thus, they are more expensive. But, one of them was the most appropriate due to its relatively small volume and price which is **VUO28-12NO7** presented in figure III-5 bellow.

**Figure III-5 VUO28-12NO7 rectifier bridge module**

This rectifier bridge module can support a reversed peak voltage ok 1.2kV, a max surge current of 28A and a temperature that goes till 150 °C with a price of 11,75 € per unit.

## III.3 DC Link design

In order to choose the DC link capacitor there are some criteria to be met.

First, the capacity that was calculated in the previous chapter ($C_{dc} = 416\ \mu F$ ) ,since it is an electrolytic capacitor that means it cannot go over 500Vdc [52]. Plus, it must support the calculated ripple current

As it was mentioned in the second chapter (equation II.7), in [52] a method of calculating the ripple current is presented

$$I_c = \sqrt{I_{rh}^2 + I_{ih}^2}$$

$$I_r = \frac{P_{load}}{10V_{s_{rms}}} \qquad \text{(III.1)}$$

$$I_r == \ 0.55\text{A}$$

As $I_{ih}$ is related to the controlled part. So, it is basically neglected in front of the rectifier ripple current that comes from low frequency harmonics

Many components that fills these conditions were found such as ALF80G911EH400, LNX2G102MSEF, and some were even similar in term of volume such as LGG2G102MELC50 and LGL2G102MELC50. But, the factor of price makes the last one the most appropriate choice.

**Table III-1 Comparison between some DC link capacitors**

| | ALF80G911EH400 | LNX2G102MSEF | LGG2G102MELC50 | LGL2G102MELC50 |
|---|---|---|---|---|
| capacitance | 910 uF | 1000 uF | 1000 uF | 1000 uF |
| Voltage rating DC | 400 VDC | 400 VDC | 400 VDC | 400 VDC |
| Temperature | -40°C ~ 105°C | -25°C ~ 85°C | -25°C ~ 105°C | -25°C ~ 105°C |
| Dimension | 60mm*40mm | 51mm*70mm | 35mm*50mm | 35mm*50mm |
| Ripple current | 4.04 A | 5A | 2140 mA | 2.2A |
| Price/unit | 30,34 € | 26,59 € | 13,64 € | 13,53 € |


**Figure III-6 LGL2G102MELC50 capacitor**

This chosen capacitor has a max DC voltage of 400V so in order to make the capacitor support the DC link another capacitor must be added in series which means $400 + 400 = 800V$. In this way they can support the DC link, and since the needed capacitance is $416\ \mu F$ that means two capacitors of $1000\ \mu F$ will make an equivalent of a $500\ \mu F$ capacitor which respects the conditions.

## III.4 Braking circuit design

In case of braking, the induction machine works as a generator, which means we have a reversed flow of energy and since the rectifier stage is based on diodes (which is not bidirectional), this energy must be dissipated in an external resistor called dynamic braking resistor.

The power components of the braking circuit are basically an external resistor and an IGBT for the control system as shown in figure III-7.

The detailed circuit of the control system will be presented later in this chapter.

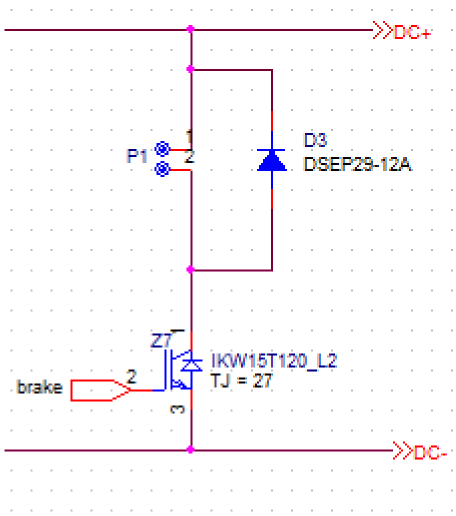


**Figure III-7 Braking circuit**

## III.5 Inverter stage design

The inverter is the controlled part of the VSD. Thus, its main component is IGBTs, but as seen in chapter II, IGBTs can be either districted and for each IGBT we have to associate the driving circuits…etc. Or, it can be as a module (IPM) which may well or may not contain the driving circuits as well as protection circuits.

### III.5.1 Using IPM

Digikey, Infineon and mouser provided many intelligent power modules (*IPMs*). These lasts have many topologies and various constructions. Some of them contain only an IGBT module with the drivers, some others include the braking circuit as well and may or may not contain the drivers (as shown in the following figure) and others include also the rectifier bridge.

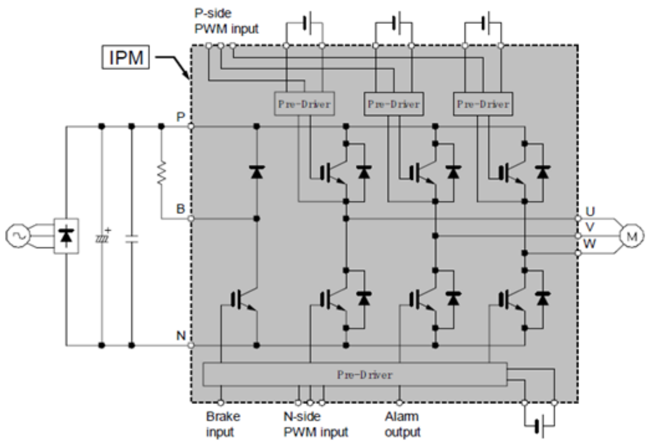


**Figure III-8 an IPM with braking circuit and drivers included**

This variety in this product give multiple choices in building a VSD according to the techno-economic study so as to choose the proper choice taking into consideration the performance, volume and price.

In the following some products will be presented that include all the given categories, these chosen products respect the principal criteria of the project (reversed voltage of 1200V forward current greater than 10A) so the comparison will take into account other factors such as the structure, the circuits included, price, protections…etc.

For example:

FUJI ELECTRIC in [65] presented an IGBT IPM that contains the drivers as well as overheating protection with a price of 175.44€.

ON SEMICONDUCTOR in [66] another IGBT IPM is presented that also contains the IGBT drive circuits , we can find also many protections such as short circuit protection with only 30.65 €.

Infineon in [67] also presented an IGBT IPM that includes the drivers as well as many types of protections (Under-voltage lockout, Programmable fault clear timing and enable input , Cross-conduction prevention …etc.) according to the datasheet it is well suitable for electrical motors in many applications such as pumps. Its price is 27.69 €.

Another interesting choice is provided by STMicroelectronics [68] which is also an IPM but it has many interesting circuits included within (Short-circuit protection, Smart shutdown function, Built-in temperature sensor, Comparator for fault protection, Fully isolated package …etc.) with a price of 17.36 € which makes it an intriguing choice.

In [69] Infineon presents another module that contains the inverter as well and the rectifier but excluding the braking circuits that must be added with a price of 35.81€

Lastly, there is a module presented by IXYS in [70] that contains the rectifier, braking circuit and the inverter stage as well including the temperature sense. But, in the other hand this module contains only the power module. So, the driver circuits are excluded which means they must be added externally. This solution costs 51.05€.

### III.5.2 Discrete IGBT module

Previously the case of using various modules were discussed, another solution is to build the module from scratch by using IGBTs.

In this solution a proper IGBT that respects the essential criteria of voltage and current must be chosen in addition to that a proper driver circuit must be add as well.

In mouser an IGBT that goes well with the conditions was found which is the IKW15T120 with a price of 5.15 € per unit.

### III.5.3 Comparison

The following table represents the some propositions with their main characteristics for a comparison between them:

**Table III-2 Comparison between IPMs, IGBT modules and IGBTs**

| | FSBB15CH120D(fuji) | IM818MCCXKMA1(Infineon) | FP15R12W1T7_B3(Infineon) | MUBW10-12A7 (IXYS) | IKW15T120 Infineon |
|---|---|---|---|---|---|
| Characteristic | IPM<br>$V_{CC}$=15<br>$f_{PWM}$=20kHz<br>$I_{MAX}$=15A | IPM<br>$V_{CC}$=15<br>$f_{PWM}$=20kHz<br>$I_{MAX}$=20A | IGBT module and rectifier without drivers<br>$V_{CC}$=15<br>$f_{PWM}$=100kHz<br>$I_{MAX}$=15A | IGBT module, rectifier and braking system with no drivers<br>$V_{CC}$=15<br>$f_{PWM}$=100kHz<br>$I_{MAX}$=20A | IGBT<br>$V_{CC}$=15<br>$f_{PWM}$=100kHz<br>$I_{MAX}$=15A |
| Temperature | -40°C ~ 150°C | -40°C ~ 125°C | -40°C ~ 175°C | -40°C ~ 125°C | -40°C ~ 150°C |
| Size (mm) | 44.2×27 | 36×23 | 63×34 | 82×45 | 20.9×15.9 |
| Protections | Under Voltage Lock Out – Short Circuit Protection | Over current shutdown- Under voltage lockout- Cross-conduction prevention Programmable fault clear timing and enable input | 2.5 kV AC 1min insulation. | Thermal protection | none |
| Certifications or qualifications | UL Certified No.E209204 | tests of JEDEC 47/20/22 | Not mentioned | Not mentioned | Not mentioned |
| Application | Motion Control – Industrial Motors | Fan drives and active filter for HVAC, pumps, and low power motor drives | Auxiliary inverters- Air conditioning- Motor drives. | Three phases synchronous or asynchronous motor- electric braking operation | Frequency Converters- Uninterrupted Power Supply |
| Others | Low loss -very low thermal resistance – single ground power supply. Works also with 3.3/5 V logic | Integrated bootstrap functionality- Built-in NTC thermistor for temperature monitor- Lead-free terminal plating; RoHS compliant Works also with 3.3/5 V logic | High power density- Compact design- Solder contact technology. | Input from single or three phase grid- Fast rectifier diodes for enhanced EMC behavior- Temperature sense included- | high ruggedness, temperature stable behavior- Low EMI- Low Gate Charge- Very soft, fast recovery anti-parallel Emitter Controlled HE diode. |
| Price | 25,54 € | 27,69 € | 34.61 € | 51,48 € | 5,15 €/ unit |

From the previous data an IPM IGBT is preferable to the circuit since it has the protections needed and the driver circuit that we don't find in a simple IGBT module making it easier to use and reliable as well. For the price the IGBT Module is cheaper but this price comes without the driver's circuits and the protections existing in the IPM. As a conclusion and as seen in an existing VSD the Hitachi X200 [48] the use of an IPM is more efficient .

Based on the table as well the chosen IPM is **IM818MCCXKMA1** because it satisfies all the requirements, contains driving circuit and many protections, suitable for the application, adaptable to 3.3V logic and relatively has a good price. The following figure (figure III-9) represents the configuration of the chosen IPM.

Another solution is presented here as well. This solution is based on using discrete IGBTs. The chosen IGBTs for this solution are the ones presented in the table (IKW15T120 by Infineon).

The use of discrete IGBTs require the addition of another circuit called the driving circuit which will be presented next.

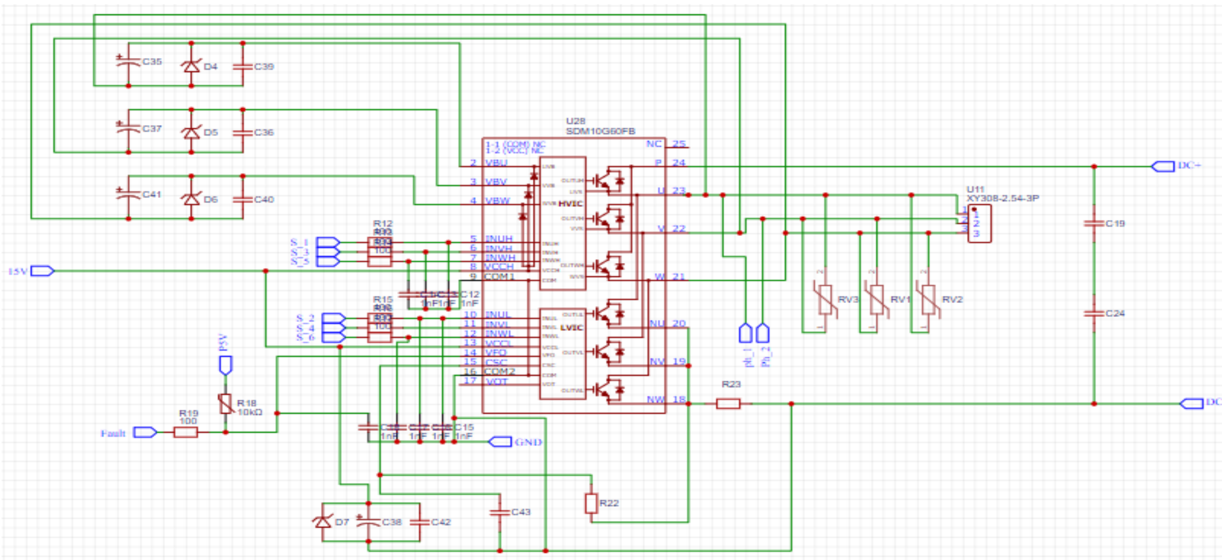


**Figure III-9 IPM Configuration**

#### III.5.3.1 Driver circuit design

In order to control an IGBT, a control signal must be sent to its gate, but the control signals are low power signals. In the other hand, the IGBTs are power electronic devices that deals with high currents, that means, the very low power control signal cannot trigger the IGBT. Hence, these signals need to be amplified.

The driver's circuits ensure the amplification of those signals to ensure the pic of gate current.

Here a brief description of two type of drivers:

- Leg driver IR2110
- ONE IGBT driver HCPL 3120

In the end a small comparison between the two types of drivers is presented.

**a) Using one leg driver**

According to the datasheet, the IR2110 driver is a driver that ensures the control of one leg IGBT (one upper IGBT and one lower IGBT as in figure III-10). From the datasheet, some of this driver's basic characteristics are

- ability to control 2 IGBTs (creates two grounds)
- compatible to 3.3V logic (STM32 case)
- suitable for high frequency applications
- low power dissipation

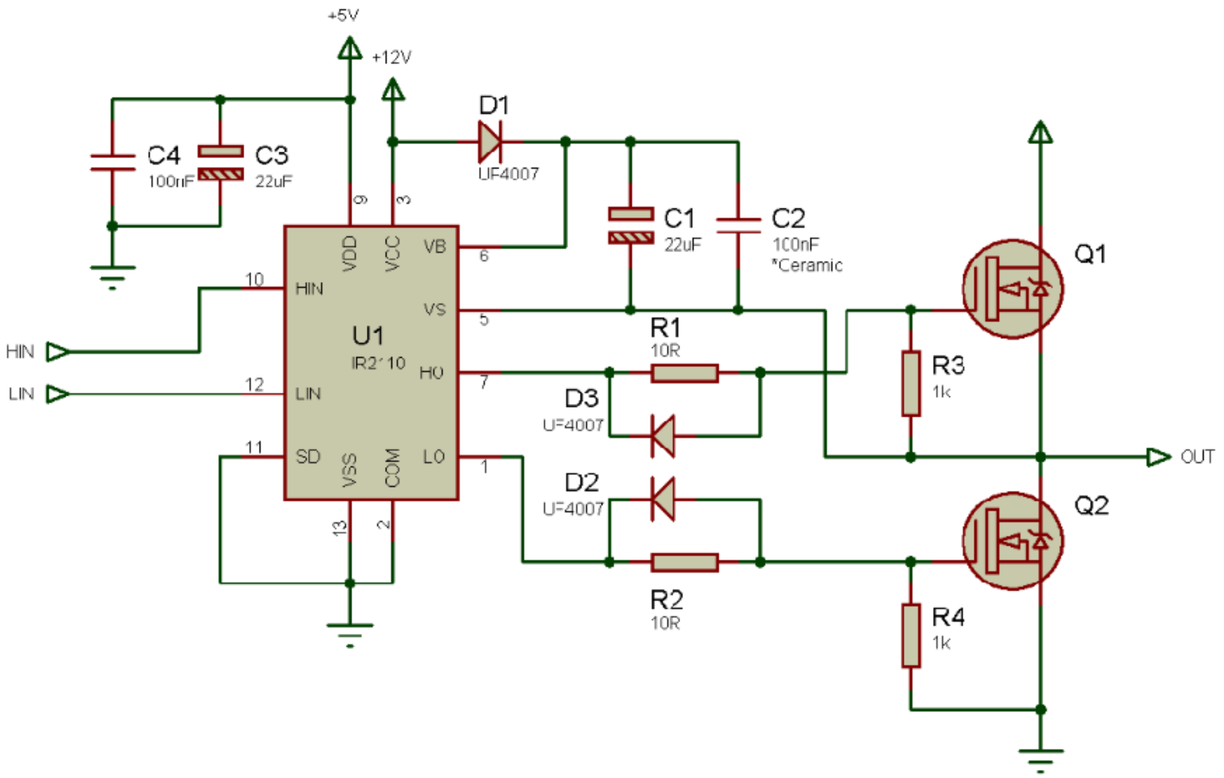


**Figure III-10 IR2110 IGBT drive circuit.**

According to the datasheet provided the IR2110 and IR2113 have almost the same proprieties except the $V_{OFFSET}$ (500V for IR2110 and 600V for IR2113) which makes the IR2110 cheaper.

Another candidate which is IR2112 but this one has a low $I_O$ where in the IR2110 and IR2113 series it can rich 2A.

The major inconvenient in this family is that they do not contain an optocoupler that guarantees the isolation between the power and the control system. Plus, the complexity of the circuit as seen in the previous figure.

TEXAS INSTRUMENTS gave another solution in leg drivers which is the **UCC21530** family. From it we chose **UCC21530DWKR** which is an interesting driver for its characteristics presented in the data sheet and the protections provided in it.

**b) Using one IGBT driver**

As the datasheet specifies, this driver is ideally suited for driving power IGBTs and MOSFETs used in motor control inverter applications. The HCPL-3120 series can be used to drive a discrete power stage so it drives the IGBT gate. And as figure III-11 shows this driver is used for a one IGBT (it provides one isolated GND).

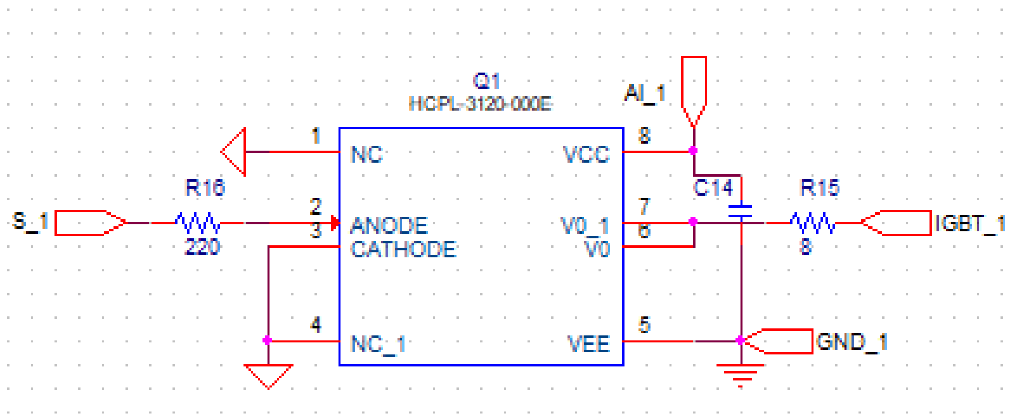


**Figure III-11 HCPL-3120 driver circuit.**

Another option which is the use of the **PS9552L2** driver circuit, a comparative study between the two drivers [71] shows that the **PS9552L2** is a good candidate to replace the HCPL-3120 since it has an equivalent performances to this last.

**TD351** is another solution from the TD35x family, presented by STMicroelectronics which is suitable for 1200 V IGBTs driving system.

The TD351 is an advanced IGBT driver with integrated control and protection functions. It has an active Miller clamp function to reduce the risk of induced turn-on in high dV/dt conditions and a 2 kV ESD protection but in the other hand it does not contain an optocoupler which means this last is needed in the circuit to assure the isolation.

As for the gate resistor of the HCPL, calculating it goes with three steps according to the datasheet of the HCPL3120.

Step 1 : Calculate Rg ( Gate resistor ) Minimum from the $I_{OL}$ Peak specification

$$R_g \geq \frac{V_{cc} - V_{ee} - V_{OL}}{I_{OL}} \quad \text{(III.2)}$$

The $V_{OL}$ value of 2V in the previous equation is a conservative value of $V_{OL}$ at the peak current of 2.5A

$$= \frac{Vcc-0-2}{2.5} = 5.2\Omega$$

⇨ $Rg \geq 5.2\Omega$

Step 2: Check the HCPL-3120 Power Dissipation and Increase Rg if Necessary. The HCPL 3120 total power dissipation (PT) is equal to the sum of the emitter power (PE) and the output

power (PO):

$$P_t = P_e + P_o \quad \text{(III.3)}$$

$$Pe = If \times Vf \times Duty\ Cycle \quad \text{(III.4)}$$

$$Po = Po(Bias) + Po(Switching) = Icc \times (Vcc - Vee) + Esw(RG, QG) \times f \quad \text{(III.5)}$$

For the circuit with $I_F$(worst case ) = 16mA , Rg=6Ω , Max Duty Cycle =80% , Qg=85nC,F=5KHz and $T_{Amax}$=85°C :

$$Pe = 16e - 3 \times 1.8 \times 0.8$$

$$\Longrightarrow Pe = 23mW$$

$$Po = 4.25e - 3 \times 15 + 1.5e - 6 \times 5e3$$

$$\Rightarrow Po = 71.25mW$$

Po<$Po_{max}$(85°C) so the Rg value can be used.

### c) Comparison

In the following table a comparison between four types of drivers in order to select the most appropriate one for the circuit.

**Table III-3 comparison between drivers**

| | IR2110 | UCC21530DWKR | HCPL3120 | TD351 |
|---|---|---|---|---|
| Number of used drivers | 4 | 4 | 8 | 8 |
| Turn-on rise time | 35 ns | 16ns | 100 ns | 100ns |
| Turn-off fall time | 25 ns | 12ns | 100 ns | 100ns |
| Complexity of circuit | Complex | complex | Simple | simple |
| Optocoupler existence | NO | YES | YES | NO |
| Price per Unit | 3.59 € | 3.94 € | 2.64 € | 2.06 € |
| Total price | 14.36 € | 15.76 | 21.12 € | 16.48 € |

From the previous table we can notice that the UCC21530DWKR is relatively the best choice since compared to the IR211x series it contains an optocoupler for the isolation and provides better performances according to the data sheet .But, it really has a very complex circuit which will increase the total price of the circuit, in the other hand the TD351 presents a good solution with a low price but similar to IR211x, it does not contain the optocoupler.

So, the chosen solution, will be the use of the HCPL-3120 despite the appearance of the high price but it has the isolation included with a simple circuit with a very good performance.

### III.5.4 Thermal protection (heat sink sizing)

The functionality of power semiconductor switches results that a part of the electrical energy to be transmitted as heat. So, in order to make the switches work in an acceptable temperature without damaging our device these energy losses must be well studied in order to make a heat sink that stops the temperature from going to higher degrees.

These losses can be categorized as two types of losses conduction losses and switching losses.

These two parameters are necessary in order to size the heat sink according to [72].

- **Conduction losses**

As the name states these losses occurs when the power semiconductor is on:

$$P_{CT} = u_{CEO} \times I_{Cavg} + r_C \times I_{Crms}^2 \tag{III.6}$$

$$P_{CT} = u_{CEO} \times I_o(\frac{1}{2\pi} + \frac{m_a \times \cos(\phi_1)}{3\pi}) + r_C \times I_o^2(\frac{1}{8} + \frac{m_a \times \cos(\phi_1)}{3\pi}) \tag{III.7}$$

As for the anti-parallel diodes the formula is as follows

$$P_{CD} = u_{DO} \times I_{Davg} + r_D \times I_{Drms}^2 \tag{III.8}$$

$$P_{CD} = u_{DO} \times I_o(\frac{1}{2\pi} - \frac{m_a \times \cos(\phi_1)}{3\pi}) + r_D \times I_o^2(\frac{1}{8} - \frac{m_a \times \cos(\phi_1)}{3\pi}) \tag{III.9}$$

Where

$u_{CEO}$ is the IGBT on-state zero-current CE voltage 0.6V

$u_{DO}$ on-state zero-current voltage drop across diode 1.1V

$r_C$ CE on state resistance = $\frac{\Delta u_{ce}}{\Delta I_c}$ = 0.05 Ω

$r_D$ Diode on state resistance = $\frac{\Delta u_D}{\Delta I_D}$= 0.035 Ω

$I_o = \sqrt{2} * I_{orms}$ (rms value of output current) (5A)

Ma Amplitude modulation index 1

$\cos(\phi_1)$ motor displacement factor 0.89

Both on state voltages and resistors are found in the date sheet using the output characteristics of the IGBTs and the forward current-voltage characteristic of the antiparallel diode.

- **Switching losses**

Same as on state voltages and resistors, switching losses are found in the datasheet using the energy loss graph for the IGBT and the average power dissipation given for the diodes

So, for the total losses of the two stages:

$$P_{tot} = P_{CT} + P_{CD} + P_{rectifier} \qquad \text{(III.10)}$$

$$P_{tot} = 16.4178W$$

Now the thermal dissipation from junction to ambient temperature must be calculated by the following formula:

$$\theta_{JA} = \frac{T_j - T_A}{P_T} \qquad \text{(III.11)}$$

$$\theta_{JA} = \frac{105° - 25°}{16.4178} = 4.8728°\ K\backslash W$$

Starting with the IGBTs, the thermal resistance of the junction and the diode is presented in the datasheet is 0.6346 K\W beside they are connected in parallel (note that the thermal resistance of the used IGBT junction is 1.1 K\W and the antiparallel diode is 1.5 K\W)

A “860 Silicone Heat Transfer Compound” [mouser] has a thermal resistivity of 1.5 K\W added to the IGBT’s thermal resistance to get 2.1346 K\W. This value is for one IGBT.

6 IGBTs are pasted together in a parallel way which makes the whole thermal resistivity 2.1346/6= 0.3558 K\W. Adding the thermal resistance of the diode bridge (2.5K\W) In parallel

So the total thermal resistance is 0.3115 K\W.

So the thermal resistance from the sink to the ambient is $\theta_{SA} = \theta_{JA} - (\theta_{JC} + \theta_{CS}) = 4.8728 - (0.3115 + 0.4) = 4.1613 K\backslash W$

According to “the heat sink design for thermal analysis” provided by Digikey [73] in order to calculate the length of the sink first we need to calculate the ratio between the desired thermal dissipation and the actual thermal resistance.

For better performances let’s take the desired dissipation as 4 K\W which means 4/4.1613=0.9612.

According the same reference the length is about 3.5 inches =8.89 cm.

## III.6 Protection circuit sizing

### III.6.1 Varistor sizing and choice

According to [74], to find the voltage rating of the MOV, allow for 20% head room to take into account voltage swells. In other way, the varistor must have a voltage rating value that exceeds the applied voltage by 20% (380×1.2). The voltage rating value can be found in the datasheet and it will determine the used varistor.

$380V_{AC}$ x 1.2 = $456V_{AC*}$

According to mouser the closest voltage rating value is 460 V

The chosen varistor is VDRUS10T460BSE presented in [75] (figure III.12 ) with a price of 1.19 € . By using 3 in the input and 3 in the output it becomes of a total price of 7.14€.

**Figure III-12 VDRUS10T460BSE**

### III.6.2 Over voltage protection

As it was calculated before the equivalent capacitor of the DC link support a DC voltage of 800V. In case of a braking phase the induction machine is assumed as a generator. Hence, the flow of the energy is reversed (from the machine to the DC link) at the same time the rectifier bridge is a diode-based rectifier that means the flow of energy is in one direction. As a consequence, the DC link capacitor’s voltage will rise exposing it to the risk of explosion in case the voltage surpasses the max voltage of the capacitor (800V). That’s why the braking circuit is added in order to dissipate the energy of the braking phase and prevent the reverse flow of energy back into the DC link capacitor.

The DC link voltage is measured by using Hall Effect sensors for an example LEM (LV25-P) or by the following circuit as shown in figure III-13. Where voltage divider is used as an entrance for the op-amp (operational amplifier) that gives a result which doesn’t exceed 3.3V in the output (STM32 ADC max voltage).

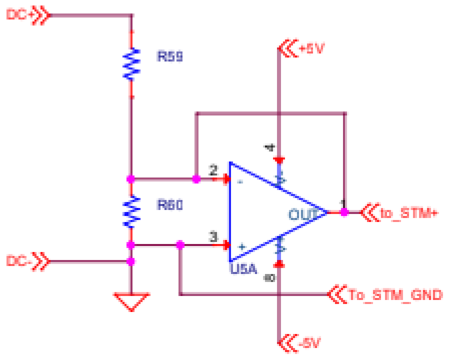


**Figure III-13 DC Link voltage measurement**

The measured value is compared then to a referenced value that represents the capacitor's voltage that is used to command the braking circuit.

The moment when the measured value surpasses the DC linked voltage (max allowed) the NE555 is activated and commands the IGBT of the braking circuit via the driver or via an opto-coupler connected to the driver in case of IR2112.

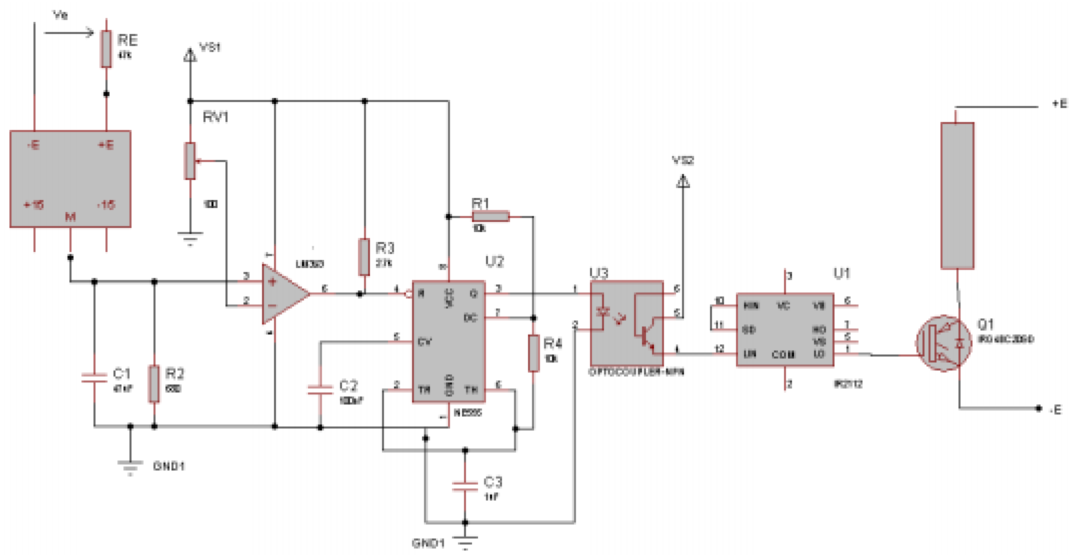


**Figure III-14 Over voltage and braking circuit.**

# III.7 Measurements circuits

## III.7.1 Current measurement circuit design

For the current measurement circuit, measuring two phases is enough while the third one can be extracted mathematically since $i_a + i_b + i_c = 0$ in a three-phase system.

After the C20 filter capacitor the measurement is taken as the voltage of R29, the signal goes directly to the op-amp. Since the output is 5V, a voltage divider is needed so as to respect the STM's 3.3V restriction.

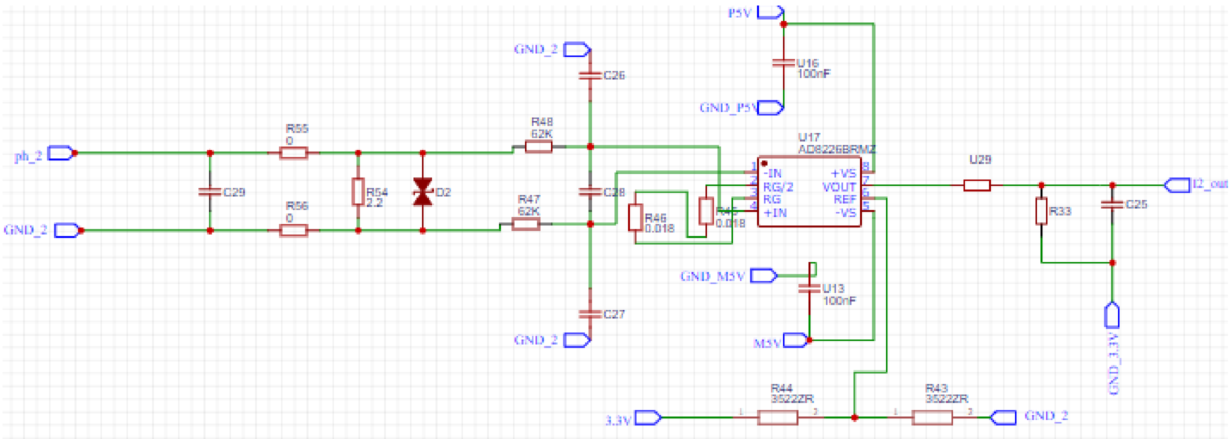


**Figure III-15 Current measurement circuit design**

# III.8 DC supply circuit

## III.8.1 Driver's supply design

To create a supply for all 8 IGBTs drives (case of district IGBTs) 5 separate grounds are needed (3 for the upper half in the inverter, one for the lower half and the braking circuit and one for the pre-charging circuit).

The following circuit is the driver's supply circuit; it was made and presented by BOUTOUCHE Hicham an engineer in GA-tech. In this circuit IC4 represent an HFT (High Frequency Transformer).

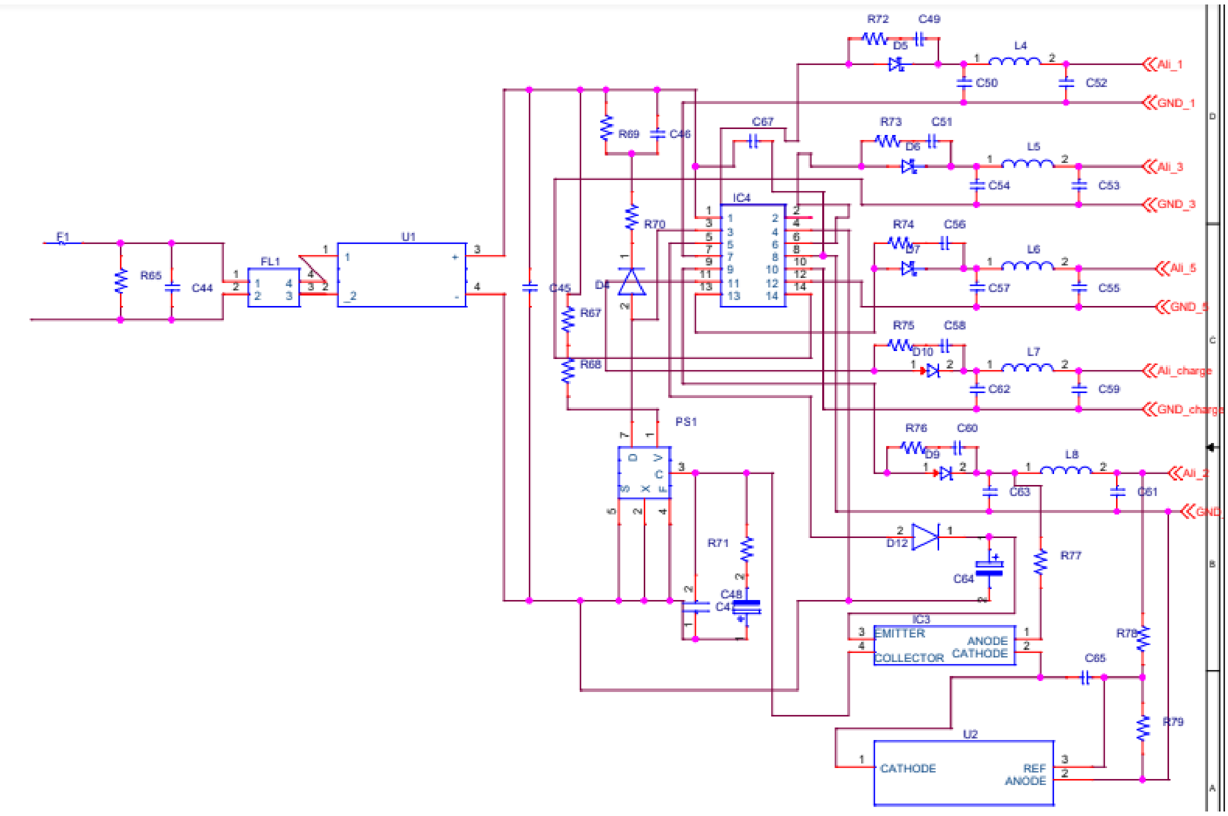


Figure III-16 driver's power supply design

## III.8.2 Micro controller supply design

The following circuit allows to generate the 3.3V using a step-down regulator this 3.3V is used to supply the STM Micro controller represented in the figure. The input (ali_2) comes from a 15V circuit.

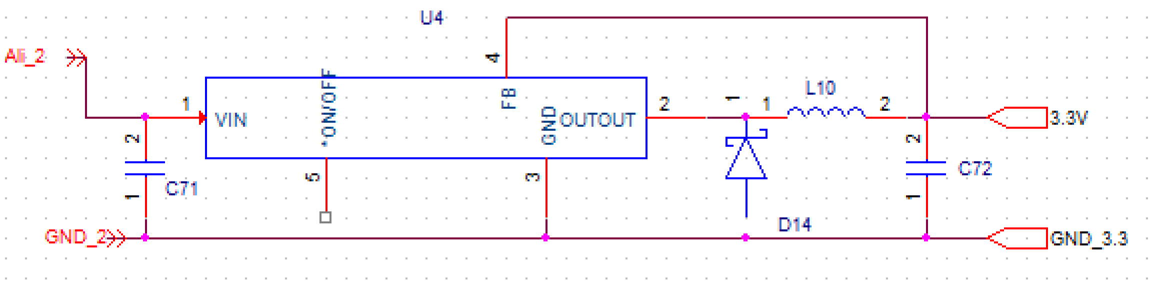


Figure III-17 STM's power supply circuit

### III.8.3 Current measurement power supply

Similar to the 3.3V circuit another regulator is used to create a 5V for the supply of the measurement circuits.

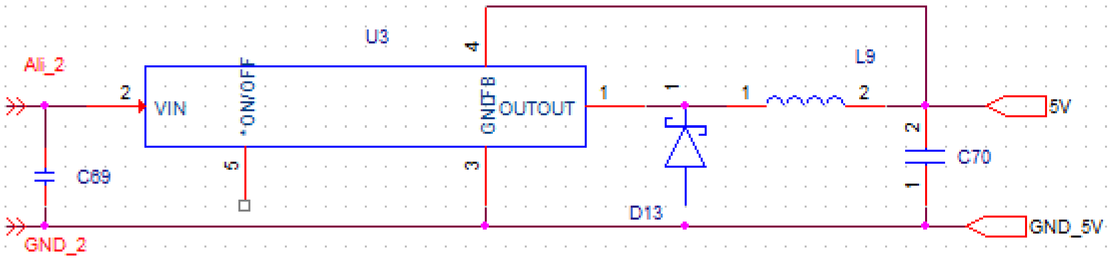


**Figure III-18 Current measurement power supply circuit**

The DC voltage and the output current measurements requires the 5V and the -5V as well that's why and additional circuit was added in order to generate them

The first solution is proposed considering that the 5V was already generated in the circuit shown in figure III-17 so to generate the -5V the following circuit is used (figure III-18)

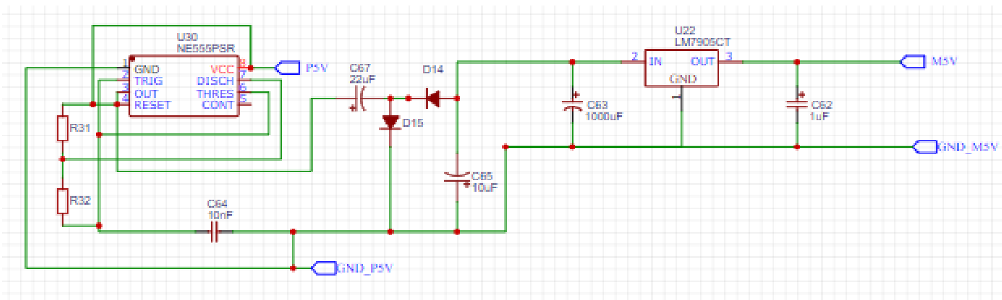


**Figure III-19 5V inverter circuit**

In this circuit a timer NE555 is also used after that the LM7905 is used in order to get the -5V.

Another solution is proposed, by using the well-known asymmetric power supply where: first, the 15V and -15V are generated using the LM7815 and LM7915 respectively after stepping down the voltage using a midpoint transformer then a rectifier bridge (Figure III-19), and from those two the +5V and -5V are generated using the LM7805 and LM7905 respectively.

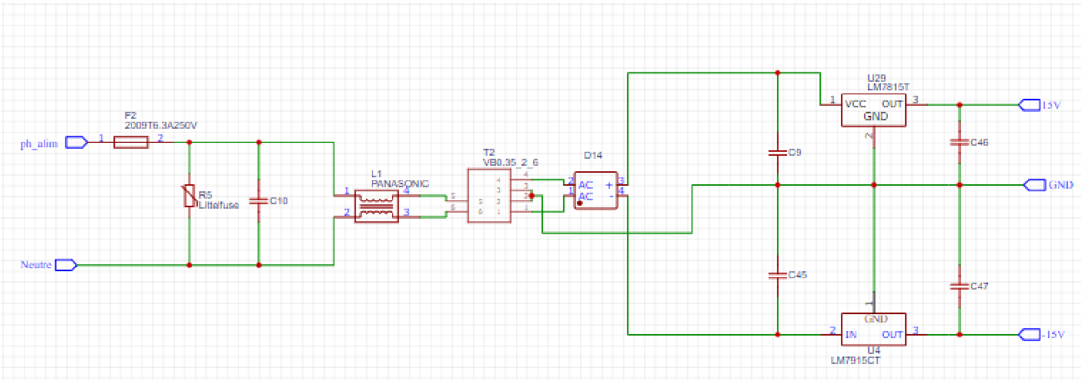


**Figure III-20 Asymmetrical power supply 15V -15V**

## III.9 STM32

As the core of all the circuits the STM32F4 was chosen as a microcontroller to control the entire circuit.

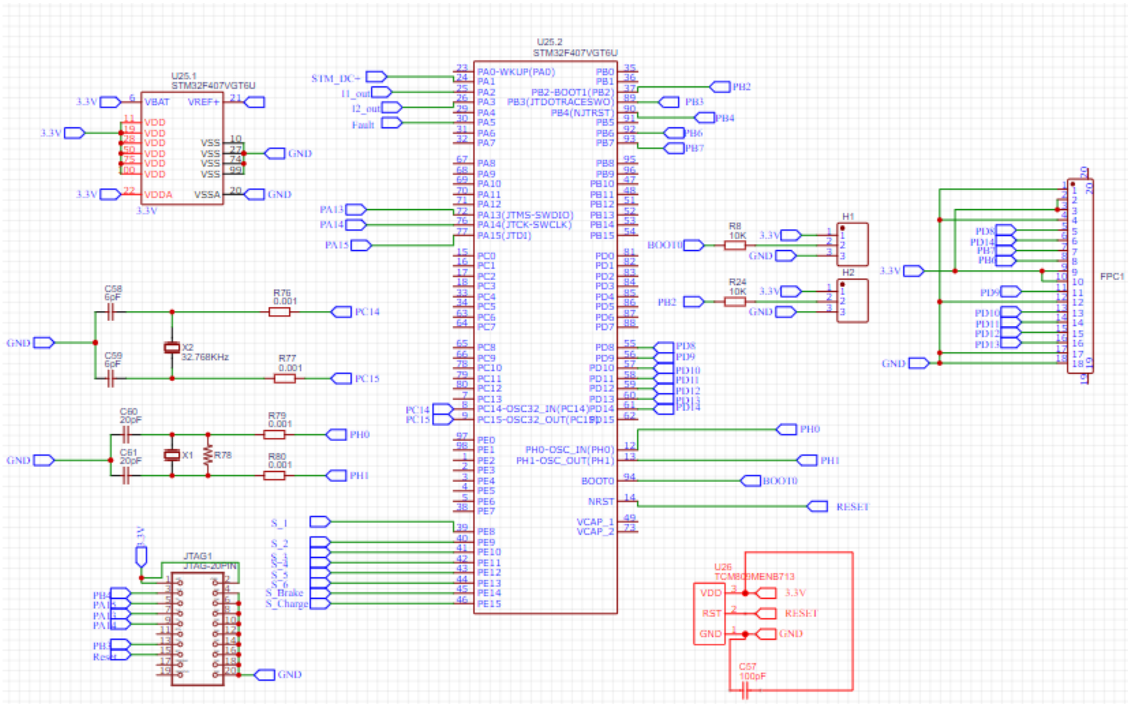


**Figure III-21 STM 32F4**

The figure before (Figure III-21) represents the STM32F4 microcontroller with the external oscillators (X1 and X2) a JTAG where all the control signals are and finally the screen represented by FPC1.

## III.10 EMI design considerations

With the increase use of PCB for high speed circuits, creating it became more challenging because of the noise coming for the EMI.

So, in order to reduce these noises many considerations were taken into account, CYPRESS semiconductors provided a document [76] where they discussed shortly about these considerations.

### III.10.1 Ground plates

Maximizing the area of the ground plates helps to minimize the inductance which is the most vital element when designing a PCB. Thus, one of the most recommended solutions is to have a full ground plane as it provides the lowest impedance as the current returns back to its source. Thus, a whole layer must be reserved for the ground. So, the PCB must be multi-layers.

This solution is impossible for two layers PCB. Therefor another solution is proposed in which ground grids are used as shown in figure III.22 (a) that follows

A third solution is the use of a faraday's cage by stitching the ground on the complete periphery of the PCB and not routing any signal outside this boundary figure III.22 (b). Thus, it limits the emission from and to the PCB.

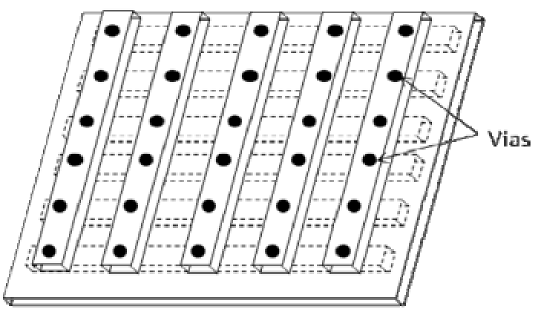


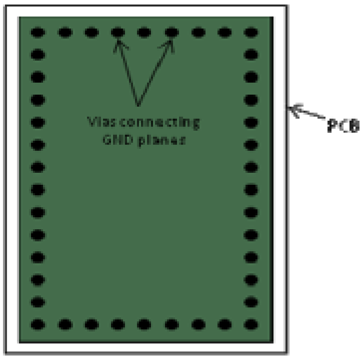

**a) Ground grid** **b) Faraday's cage**

**Figure III-22 Ground plate consideration**

### III.10.2 Component Segregation

The PCB components must be grouped according to their functionality such as analog, digital, power supply sections, low-speed circuits, high-speed circuits, and so on. Each group then is a sub system. And between the groups there are filters in order to have a better signal.

### III.10.3 Analog Circuits

Traces carrying analog signals must not interfere or come near high-speed or switching signals and must always be guarded with a ground signal that is not shared with the digital subsystem. A low pass filter should always be used to get rid of high-frequency noise coupled from surrounding analog traces

### III.10.4 Decoupling Capacitor

The decoupling capacitor is the one used in the input filter it is used to prevent any noise on the power supply which can alter the functionality of the operated devise this noise is usually high frequency. So, a bypass capacitor or decoupling capacitor is required to filter out this noise.

### III.10.5 Cables

One of the major problems in EMI is the existence of cables that carries the digital signals. The current enters a cable then leave it at the other end. Thus, emitting parasitic capacitance and inductance radiations.

In order to minimize the magnetic field that creates the parasites using a twisted pair cable is provided as a solution. Another solution being shield cables are presented in case of high frequency signals where the shielding is connected to ground both at the beginning and at the end of the cable

### III.10.6 Crosstalk

Crosstalk happens when two PCB traces re next to each other forming mutual capacitance and inductance that are proportional to the distance and according to the same document. In digital systems, crosstalk caused by mutual inductance is typically larger than the crosstalk caused by mutual capacitance. Therefore, increasing the spacing between the two traces or reducing the distance from the ground plane will reduce the mutual inductance.

## III.11 Cost estimation

After choosing the components using a comparative study in estimated value of the cost of the whole VSD is made

| component | Description | PCB footprint | Price per unit | quantity | price |
|---|---|---|---|---|---|
| Rectifier stage + pre-charge + braking. | | | | | |
| BR1 | Bridge Rectifiers 28 Amps 1200V | VUO2812NO7 | 11,75 € | 1 | 11,75 € |
| C1 C2 C3 | Safety Capacitors 2.2uF 20% 305Vac MKP X2, LS 21.5MM | CAP-TH_L26.5-W15.5-P22.50-D0.8 | 1,10 € | 3 | 3,30 € |
| R6 | Thick Film Resistors - Through Hole 100W 5K ohm 1% TO-247 | TO1016P521X1575X2451-2P | 15,21 € | 1 | 15,21 € |
| C6 C7 | Aluminium Electrolytic Capacitors - Snap In 400volts 1000uF | CAPPRD1000W170D3575H5200 | 13,53 € | 2 | 27.06 € |
| D3 | Single Diode 1200 V | TO254P482X1028X2284-3P | 2,44 € | 1 | 2,44 € |
| Z7 Z8 | IGBT Transistors LOW LOSS DuoPack 1200V 15A | PG-TO247-3-41_INF | 5.15 € | 2 | 10.30 € |
| Q7 Q8 | Logic Output Opto-couplers 2.0A IGBT Gate Drive | HCPL-3120-000E | 2,64 € | 2 | 5,28 € |
| R100 R101 | Thick Film Resistors - Through Hole RES TH TO220 6R 1% 50W | TO508P343X1041X1930-2P | 2,35 € | 2 | 4.70 € |
| Inverter IPM | | | | | |
| U28 | Gate Drivers CIPOS MAXI | | 27,69 € | 1 | 27,69 € |
| Inverter district IGBTs | | | | | |
| Z1~Z6 | IGBT Transistors LOW LOSS DuoPack 1200V 15A | PG-TO247-3-41_INF | 5.15 € | 6 | 30.90 € |
| Q1~Q6 | Logic Output Opto-couplers 2.0A IGBT Gate Drive | HCPL-3120-000E | 2,64 € | 6 | 15.84 € |
| R15, R17 R19, R21 R23, R25 | Thick Film Resistors - Through Hole RES TH TO220 6R 1% 50W | TO508P343X1041X1930-2P | 2,35 € | 6 | 14.1 € |

| | | | | | |
|---|---|---|---|---|---|
| DC supply | | | | | |
| R56 | Varistors 275V 80pF | | 0,486 € | 1 | 0,486 € |
| C44 | Safety Capacitors 275vac 0.1uF 10% | CAP_R46KI310000M1K_KEM | 0,432 € | 1 | 0,432 € |
| FL1 | Common Mode Chokes / Filters N Series Type 18N Line Filter | ELF18N016A | 4.20 € | 1 | 4.20 € |
| U1 | Bridge Rectifiers 1.0 Amp 600 Volt | DIP4_DFM_VIS | 0,504 € | 1 | 0,504 € |
| PS1 | AC/DC Converters Int Off-Line Switchr 86W/119W | TOP256EN | 1,60 € | 1 | 1,60 € |
| IC3 | Transistor Output Optocouplers Optocoupler Phototrans | DIP762W60P254L460H450Q4N | 0,252 € | 1 | 0,252 € |
| IC4 | Ferrite Cores & Accessories COIL FORMER RYNITE FR 530 | B66359X1014T001 | 1,45 € | 1 | 1,45 € |
| U2 | Voltage References Adjustable Precision Shunt Regulator | LP3_TEX | 0,378 € | 1 | 0,378 € |
| C (50 52 53 54 55 57 59 61 62) | Aluminium Electrolytic Capacitors - Radial Leaded 25volts 100uF 6.3X11.5 | CHEMI-F11 | 0,306 € | 9 | 2,754 € |
| STM 32 | | | | | |
| U25 | STM34F04 | QFP50P1600X1600X160-100N | 4,50 € | 1 | 4,50 € |
| JTAG | JTAG | 2X10_2.54MM_PTH | 8,20 € | 1 | 8,20 € |
| X1 | Crystals 49.152MHz | HC-49US_L11.5-W4.5-P4.88 | 0,531 € | 1 | 0,531 € |
| X2 | Oscillator | OSC-SMD_L3.2-W1.5 | 3,83 € | 1 | 3,83 € |
| Micro controller + measurement supply | | | | | |
| U4 | Switching Voltage Regulators 3A STEP-DOWN VLTG REG | TS5B_TEX | 3,01 € | 1 | 3,01 € |
| U3 | Audio Amplifiers 20-W Audio pwr Amp | T05D_TEX | 3.43 € | 2 | 6.86 € |
| Input and output varistors | | | | | |
| VR1 VR2 VR3 VR4 VR5 VR6 | Varistors 460V 4500A 10D Radial | VDRUS10T460BSE | 1,19 € | 6 | 7,14 € |
| | | | TOTAL PRICE with IPM | +others | 317.857 € |
| | | | TOTAL PRICE with IGBTs | +others | 351.007 € |

It is very clear the price using the IPM module is much less than using six IGBTs which makes it a better solution (verified in some industrial VSD). This estimation is by using the prices in case of buying one component. In the case of industrial manufacturing (series production) the price will be cheaper.

## Conclusion

In this chapter a detailed study on each circuit has been presented such as braking circuit design, current measurement circuits, DC voltage measurement, protection circuits…etc.

Driving circuits were also presented using different circuits in order to determine the most appropriate one. The impact of the EMI input filters was presented with simulation.

The choice of the component for the VSD was the main purpose of this chapter, as it was presented, many manufacturers have various candidates with very interesting performances. So, in order to choose the optimal solution, a comparison study was made with different possible candidate.

The criteria applied in the selecting process were to take in consideration the performances, the price and the volume of the components in order to have a good, not bulky VSD with a reasonable price.

In the end an estimated cost of the VSD was presented taking into consideration the main parts of it. This price being not accurate since it has some components not mentioned plus the price of the PCB layout which is basically the board where the circuit will be implemented.

The PCB layout is special board were the full circuit of the VSD will be printed. It has many characteristics that will be presented in the next chapter.

# Chapter

# IV

# CHAPTER IV: SIMULATION RESULTS AND PCB DESIGN

## Introduction

Electronics are present in all the devices we use every day, cars, cell phones, cameras and computers. All these applications require the production of electronic cards to ensure and manage the power supply and the connections of different components as in the case of this application.

An electronic card is a support in the form of a plate, making it possible to maintain and electrically connect a set of electronic components together, in order to create a complex electronic circuit for precise use. It is also known by the term: PCB (**Printed Circuit Board**).

After generating the component list of the circuit diagram, a design is usually carried out on the CAD system and symbols will be stored in the component library of this system. As the complexity of circuits increase, it became necessary to do a simulation first before trying in hardware.

In this chapter, we will follow and discus the steps taken in order to design the PCB of the VSD.

## IV.1 Simulation of the circuit with V/f constant with the braking

In total three simulations were proposed, the first one is the normal functioning of a three-phase system. The second one is a simulation with two phases (one phase is lost), and lastly a mono-phase simulation.

### IV.1.1 Three-phase simulation case

The whole circuit was simulated using MATLAB with the machine given in the following specifications:

- Input voltage: 400V
- Machine’s power: 2.2kW.

- Input filter: $C_f = 2.2\mu F$ , $L_f = 2mH$

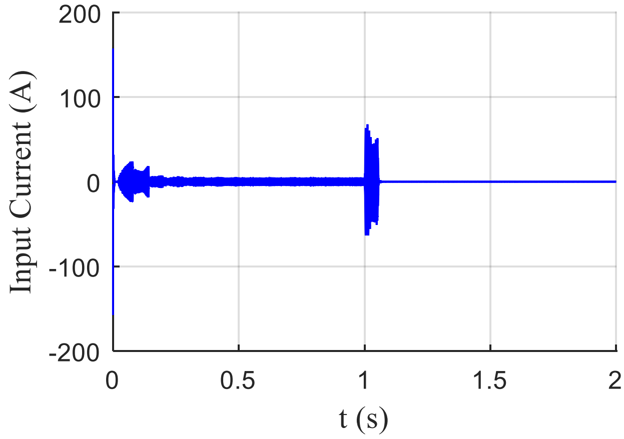


(a)

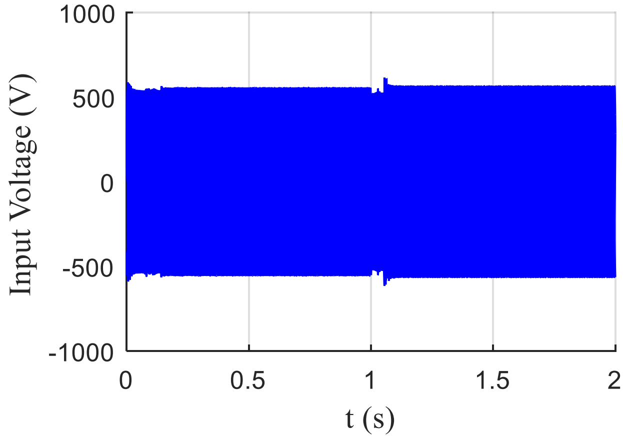


(b)

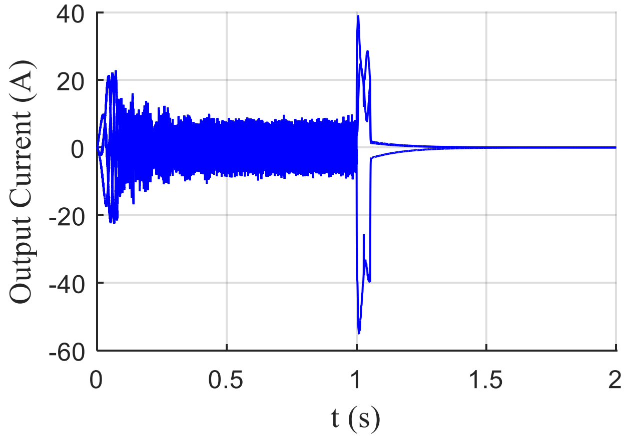


(c)

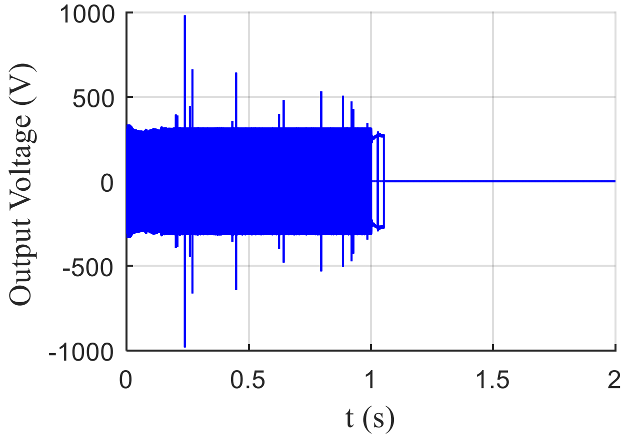


(d)

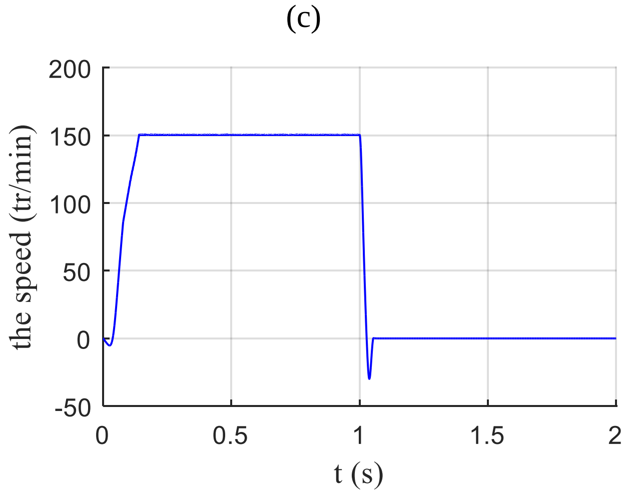


(e)

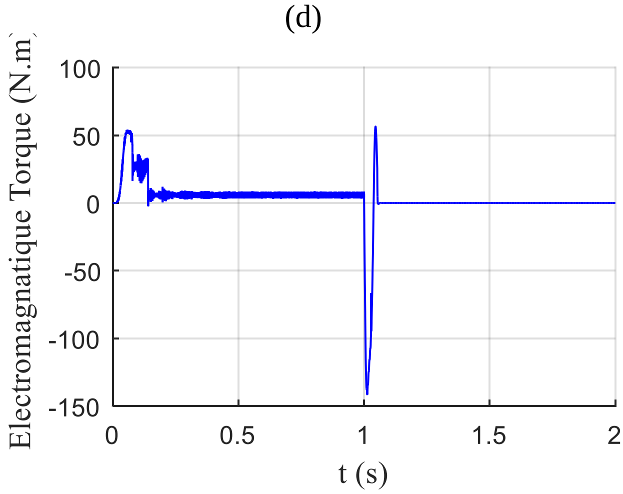


(f)

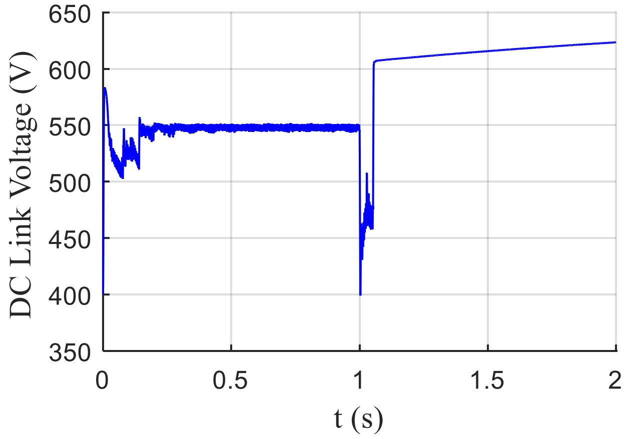


(g)

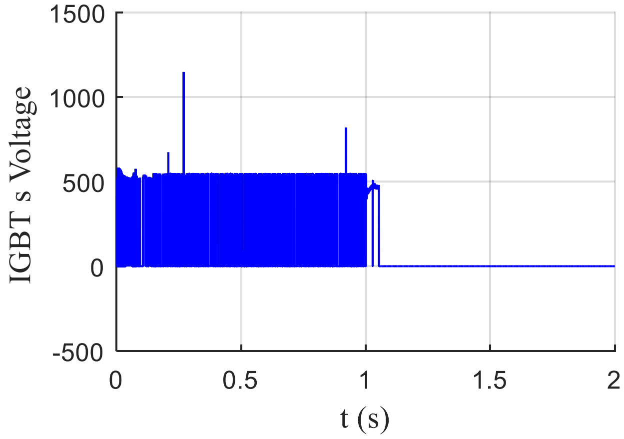


(h)

**Figure IV-1 Three-phases simulation results**

Figure IV-1 represents the simulation results for the VSD in a three-phases supply case

The performed simulation contains two phases: the first one is the start of the motor and maintaining its speed at the nominal value (from t=0s to t=1s), while the second phase which is the braking phase took place from t=1s to t=2s.

An assumption is made which is that the DC link capacitor is charged at the beginning of the simulation.

Multiple results were extracted from MATLAB/Simulink where:

Figure IV-1 (a) and (b) represent the input current and voltage, an inrush current is seen at the beginning which represents the staring current. When the machine gets to its nominal speed the current stabilizes until the next change, which is at t=1s (represents the moment of braking), another inrush current comes till the machines stops and then the control technique is stopped as well which makes the current zero. Figure IV-1 (e) represents the speed of the motor in the two described phases.

Figures IV-1 (c) and (d) represent the output current and voltage, the same phenomenon is observed there the current and voltage goes down to 0 when the system brakes. The zero value of both voltage and current can be justified by the absence of the control in order to brake the motor, this absence can also be justified by Figure IV-1 (h) where it can be clear that after the moment of braking, there is no commutation in the IGBT which is maintained opened.

Figures (e) and (f) represent the output characteristics of the motor, the speed goes from 0 to the nominal value directly, in t=1s it drops to zero causing the motor to stop due to the dynamic braking. Since the motor is braking and inverted flow in energy exists which can be justified by the existence of the negative value torque at the moment of braking.

Lastly, figures (g) and (h), these two figures demonstrate the energy balance, figure (g) represents the DC link voltage that can be seen constant in about 550V that is needed in the control. But after the end of this phase it goes up to the nominal value of the calculated rectified voltage (660V). Figure (h) of the IGBT voltage shows that there is no control applied after t=1s.

### IV.1.2 Two phases simulation case

In this part it is assumed that the machine works with only two phases and the third one is down due to a fault.

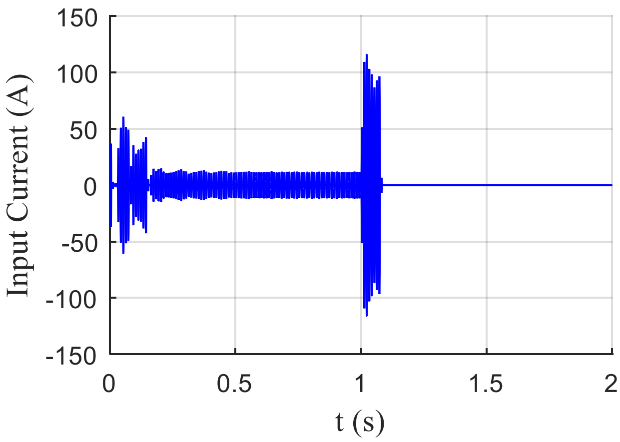

(a)

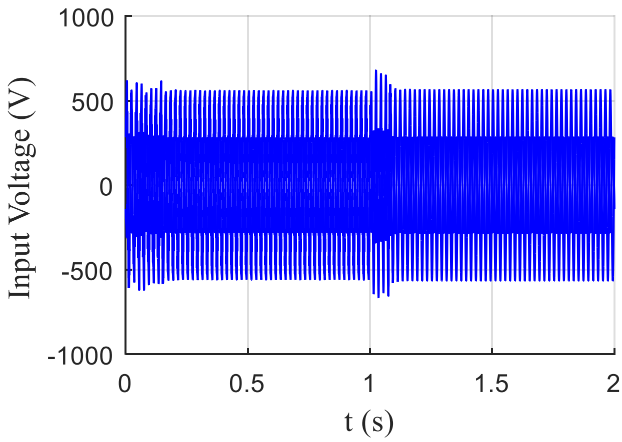

(b)

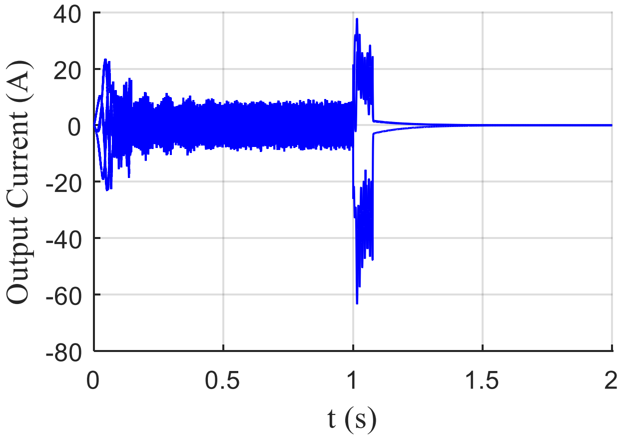

(c)

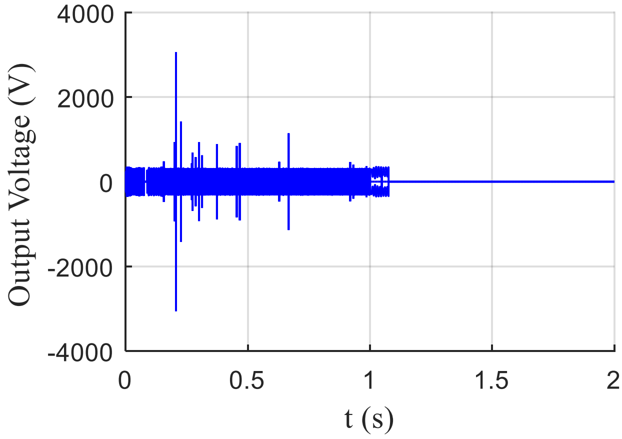

(d)

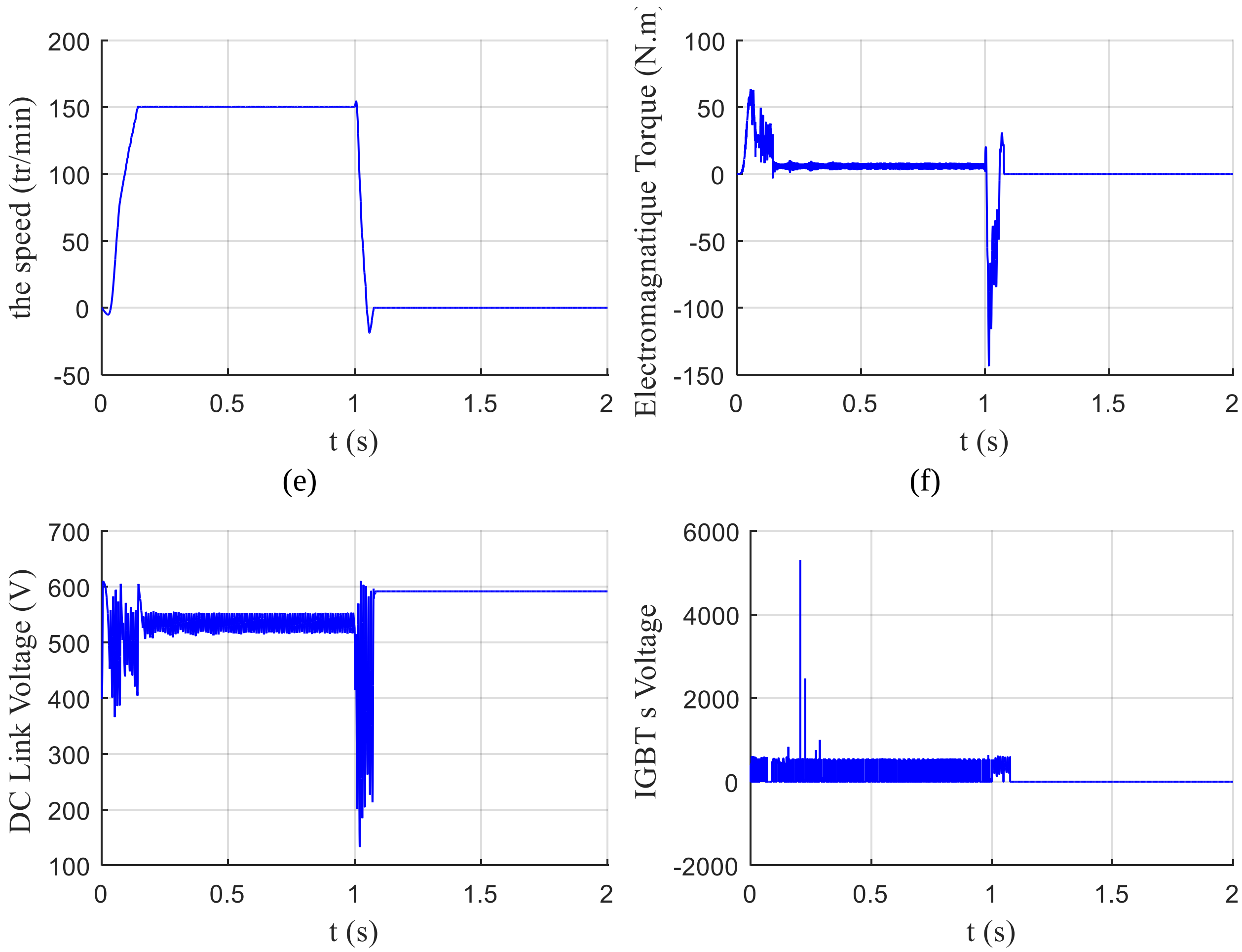


**Figure IV-2 Two phases simulation results**

The same logic of functioning applies in the two phases case, here the braking is also applied in t=1s, but since the VSD is working with only two phases, its consumer a bigger value (input current) -figure IV-2 (a)- in order to move the same load as the three-phase case.

The max value of the DC link has dropped as well due to the loose of one phase.

### IV.1.3 Single-phase simulation case

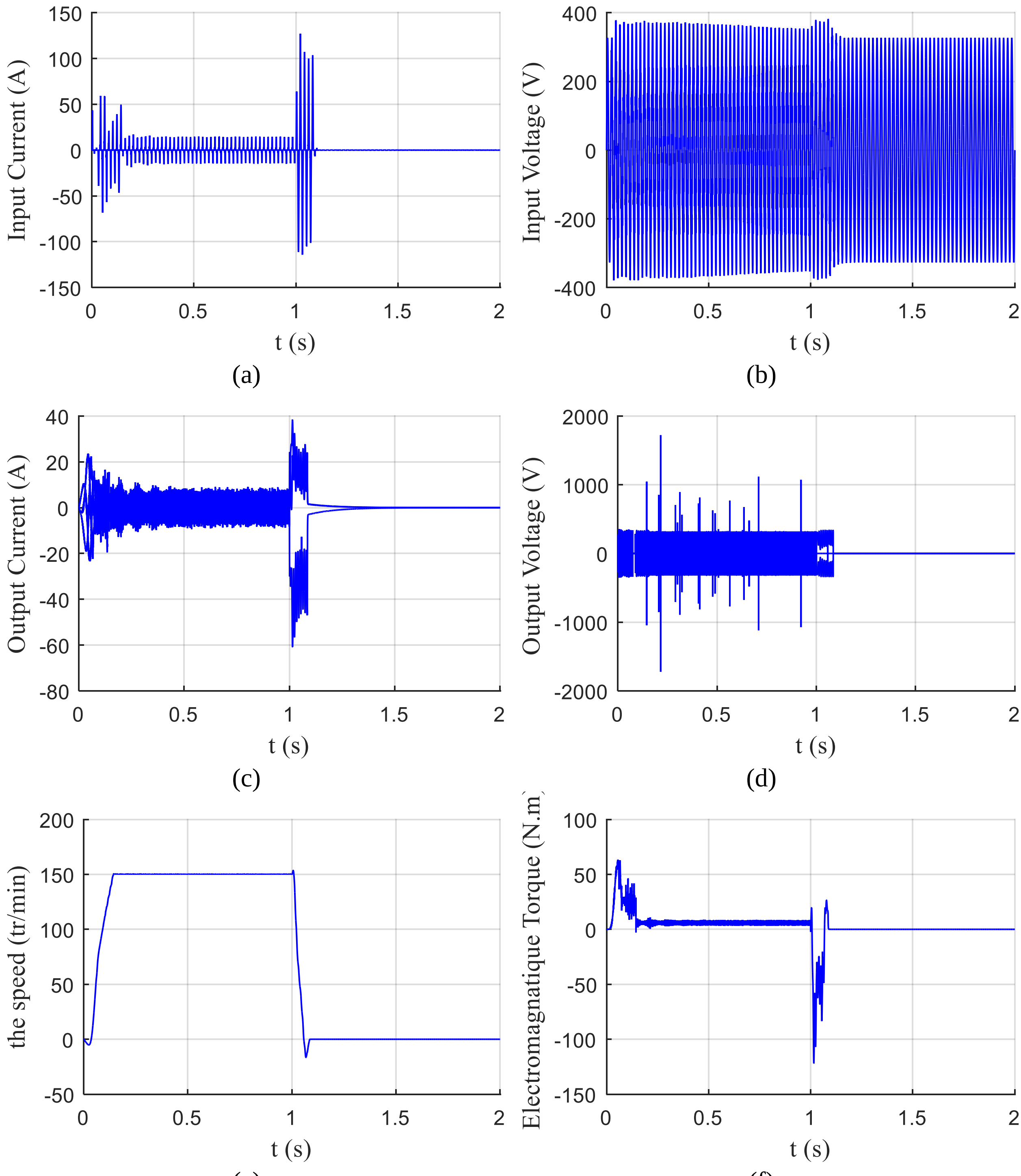

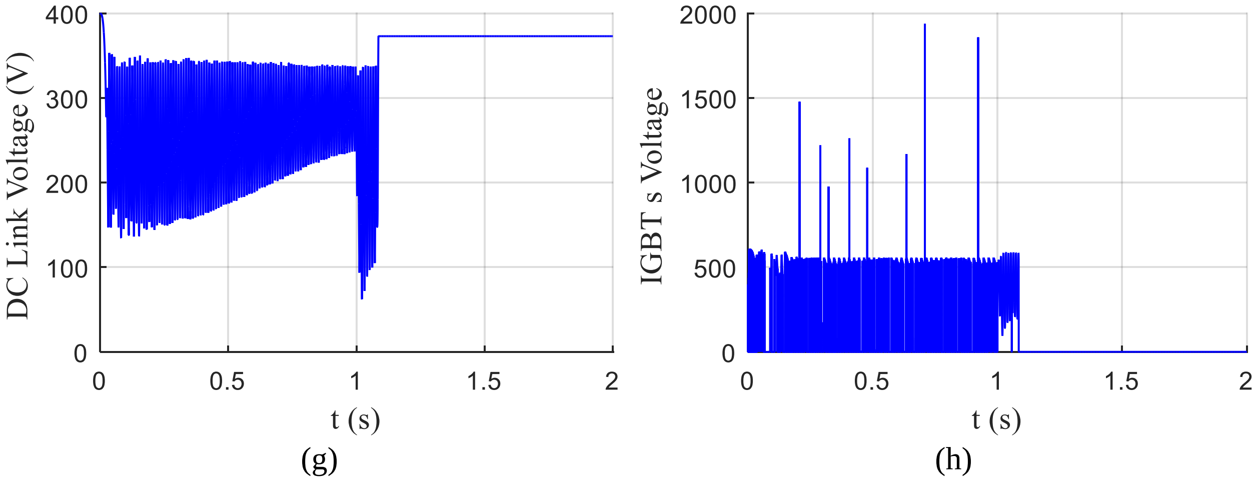


**Figure IV-3 Single-phase simulation results.**

In the mono-phase case, we can see that the DC link voltage drops more as it can be seen in figure IV-3 (g).

In conclusion, the three-phase functioning is the most appropriate one, since in the bi-phase and the mono-phase cases, the unbalanced system will rise the number of harmonics (the harmonic multiple of three will reappear).

In general a three-phase VSD usually works as three-phases only, and in case of any kind of faults the system is shuts-down and the whole system stops.

From the results presented, we can see that the VSD can work in both modes (three phases input supply and single phase input supply).

## IV.1.4 Important Notions about circuit design

### IV.1.4.1 The Schematic

Before designing any electronic card for any application, we must first draw a schematic diagram of the overall circuit with precision and a good choice of component values. The connections between the components of the circuit result in conductive material tracks at the electronic card.

The optimal choice of components as well as their arrangements and the shapes of the tracks considerably affect the size and reliability of the electronic card and. therefore its construction price.

#### IV.1.4.2 The Netlist

A Netlist is essentially a list of "Nets" connections that correspond to the electrical circuit diagram made by the CAD environment. It also contains the list of components, component manufacturers, component footprints and other information such as the names assigned to the connections ... etc.

The Netlist is used to facilitate the design of printed circuits, because it allows the importation of all the information necessary for the design environment. Thus, saving considerable time and effort.

### IV.1.5 Ground plane

The ground plane is fundamental for the operation of many circuits. There are several techniques to set it up. These techniques can be integrated into any design:

Use of copper: The larger the metal surface is, the lower the impedance gets, which is desirable for various electrical reasons.

In the case of a multi-layer design, it is preferable to dedicate one layer for the ground plane. Sometimes it is necessary to use holes to minimize the impedance of the tracks using the ground plan.

### IV.1.6 Surface Mounted Components

This is a method of mounting components on an electronic board, hence a surface mounted component. Previously, the circuit board design method included drilling the board to solder the components placed on the top layer. So, welding should be done on the back side. Therefore, traditional cards take up more space.

Using the surface mount technology, design engineers can install and weld components on both sides of the printed circuit board, allowing installation of larger circuits in a smaller space.

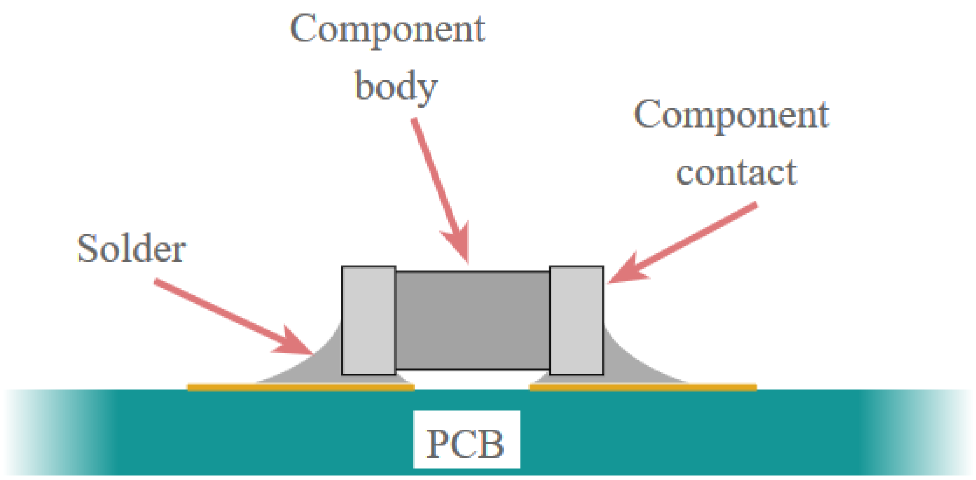


**Figure IV-4 Surface Mounted Components**

## IV.2 General guidelines

High quality design is essential. This means that the product must meet all specifications concerning electrical performance, reliability and service life, making it expensive. For this, it is important to:

- Choose the most suitable technology or combination of technologies and optimal partitioning.
- Choose reliable components for the application.
- Design for Manufacture: It is necessary to take into account that the design is made to be manufactured. High efficiency and low-cost production require, for example:
  - Use as few conductive layers as possible
  - Conductors must be as large as possible to support the given current (no fine line).
  - Use the minimum number of component types possible (standardization).
  - Robust electrical design.

- Design for testability: To minimize the level of defaults, it is important to have a test procedure that covers a lot of defects. The designers and test specialists should cooperate closely during product design to a good testing strategy[77].

## IV.3 PCB Conception Steps in OrCAD

There is many CAD software that can be used to produce electronic cards. In our application, the IT environments used for the design of our PCB are: OrCAD Capture and OrCAD PCB Designer[78]

### IV.3.1 Step 01: THE CIRCUIT'S WHOLE SCHEMATIC

The schematic of the overall circuit of VSD was made using OrCAD Capture as shown in the figure below:

The first one (figure IV-5) represents the global circuit using Discrete IGBTs which represents the first solution. While, the second one (Figure IV-6) represents the global circuits using IPM which represent the second solution.

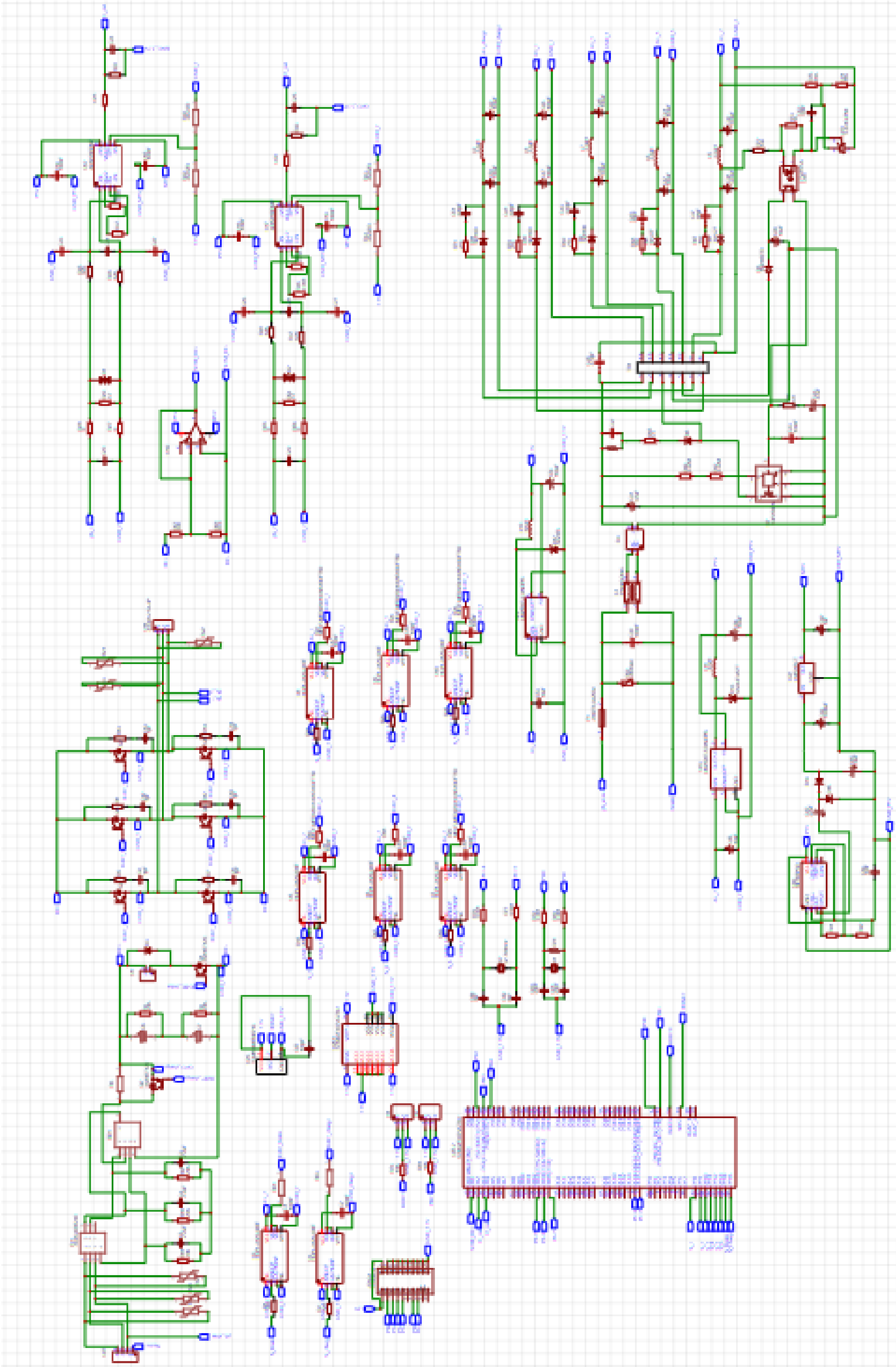

**Figure IV-5 Overall schematic using discrete IGBTs**

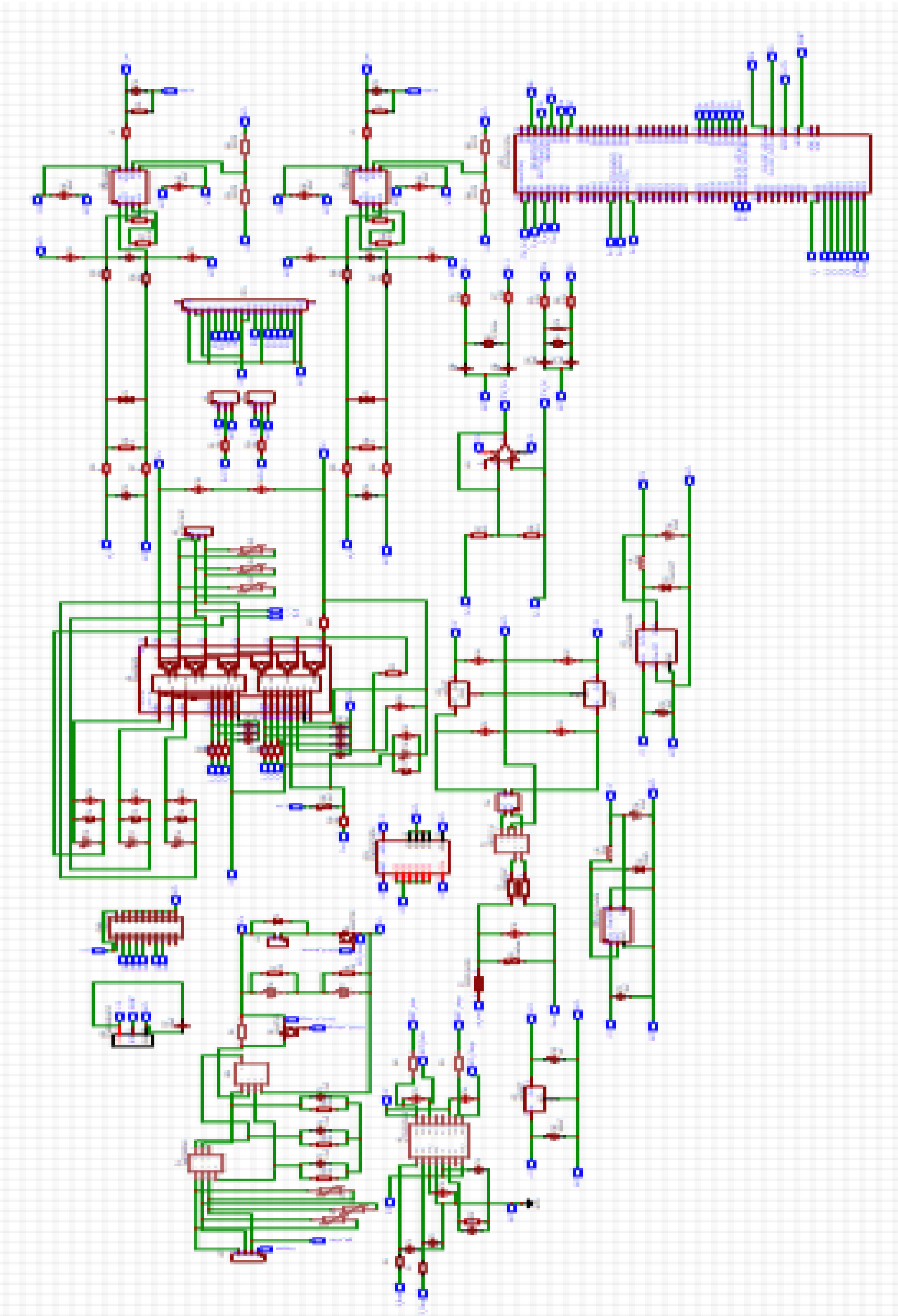

**Figure IV-6 Overall circuit using IPM**

### IV.3.2 Step 02: Components List:

This step was already done in the previous chapter where all the components, their footprints, their quantity and price were presented.

### IV.3.3 Step 03: From OrCAD Capture to OrCAD PCB Designer:

Once the circuit diagram is established, we go to the next step of electronic design automation process with the OrCAD PCB Designer tool.

The transfer of this circuit to the PCB tool will be done by the generation of the Netlist produced by OrCAD Capture, which includes all the information indicated in the designed circuit. In order to generate the Netlist, each used component must have a PCB footprint (1) that should exist in the PCB Designer's library. As shown in the previous chapter, each component must be referred with his own PCB footprint (figure IV-7)

(1) PCB footprint is the footprint that indicates the area of the layout of the components that will be physically attached and electrically connected to a printed circuit board.

| | | Reference | PCB Footprint | Power Pins Visible |
|---|---|---|---|---|
| 1 | ⊞ SCHEMATIC1 : rec : B | BR1 | VUO2812NO7 | ☐ |
| 2 | ⊞ SCHEMATIC1 : rec : C | C3 | B32923C3225M | ☐ |
| 3 | ⊞ SCHEMATIC1 : rec : C | C4 | B32923C3225M | ☐ |
| 4 | ⊞ SCHEMATIC1 : rec : C | C5 | B32923C3225M | ☐ |
| 5 | ⊞ SCHEMATIC1 : rec : C | C6 | CAPPRD1000W170D3575 | ☐ |
| 6 | ⊞ SCHEMATIC1 : rec : C | C7 | CAPPRD1000W170D3575 | ☐ |
| 7 | ⊞ SCHEMATIC1 : rec : C | C39 | CAP_3P2X2P5X2P1_PAN | ☐ |
| 8 | ⊞ SCHEMATIC1 : rec : C | C41 | CAP_3P2X2P5X2P1_PAN | ☐ |
| 9 | ⊞ SCHEMATIC1 : rec : D | D3 | TO254P482X1028X2284-3 | ☐ |
| 10 | ⊞ SCHEMATIC1 : rec : P | P1 | Jump2 | ☐ |
| 11 | ⊞ SCHEMATIC1 : rec : | Q7 | HCPL-3120-000E | ☐ |
| 12 | ⊞ SCHEMATIC1 : rec : | Q8 | HCPL-3120-000E | ☐ |
| 13 | ⊞ SCHEMATIC1 : rec : R | R3 | RESAD7500W80L4100D8 | ☐ |
| 14 | ⊞ SCHEMATIC1 : rec : R | R4 | RESAD7500W80L4100D8 | ☐ |
| 15 | ⊞ SCHEMATIC1 : rec : R | R5 | RESAD7500W80L4100D8 | ☐ |
| 16 | ⊞ SCHEMATIC1 : rec : R | R6 | TO1016P521X1575X2451- | ☐ |
| 17 | ⊞ SCHEMATIC1 : rec : R | R7 | RESAD7500W80L4100D8 | ☐ |
| 18 | ⊞ SCHEMATIC1 : rec : R | R8 | RESAD7500W80L4100D8 | ☐ |
| 19 | ⊞ SCHEMATIC1 : rec : R | R61 | RC05 | ☐ |
| 20 | ⊞ SCHEMATIC1 : rec : R | R62 | RESAD1590W60L630D24 | ☐ |
| 21 | ⊞ SCHEMATIC1 : rec : R | R63 | RC05 | ☐ |
| 22 | ⊞ SCHEMATIC1 : rec : R | R64 | RESAD1590W60L630D24 | ☐ |
| 23 | ⊞ SCHEMATIC1 : rec : Z | Z7 | PG-TO247-3-41_INF | ☐ |
| 24 | ⊞ SCHEMATIC1 : rec : Z | Z8 | PG-TO247-3-41_INF | ☐ |

**Figure IV-7 Footprint list**

In some cases, the PCB footprint is not found in the library which means it must be downloaded. Luckily there are many web sites that provide most of the PCB footprints such as ULTRA LIBRAIRIEN, Mouser, SnapEDA…etc. The downloaded file must be imported to the library via the following path Setup => User preferences => Paths => Library. The component will appear in the component library as shown below:

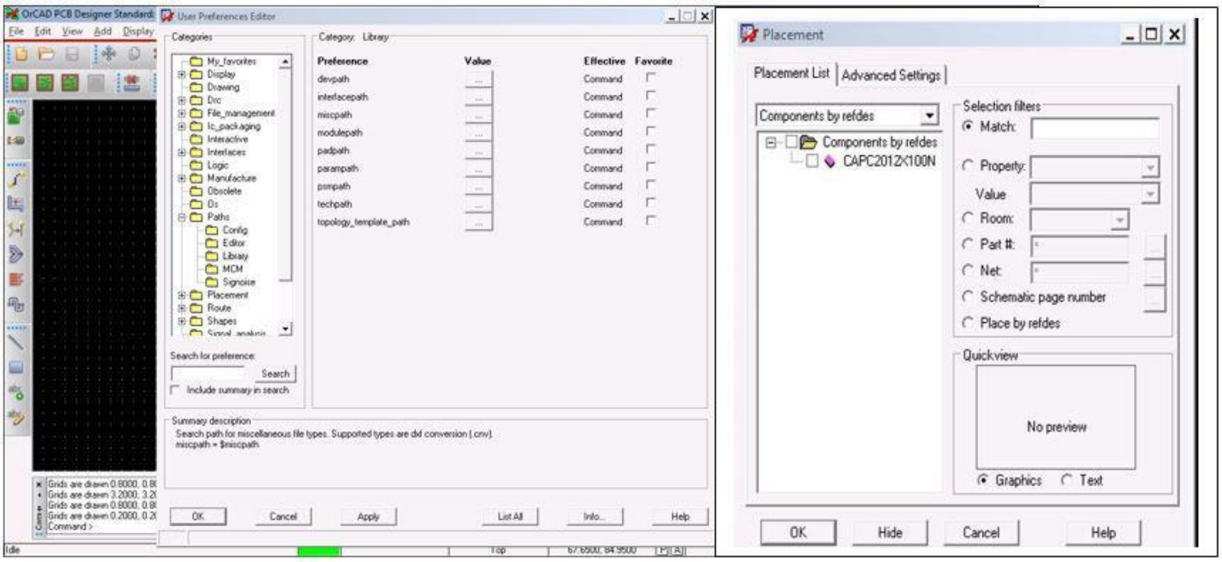


**Figure IV-8 Importing PCB footprints to OrCAD PCB designer**

### IV.3.4 Step 04: Netlist Generation:

Ones every component is referred by the PCB footprint, the Netlist can be generated as follows:

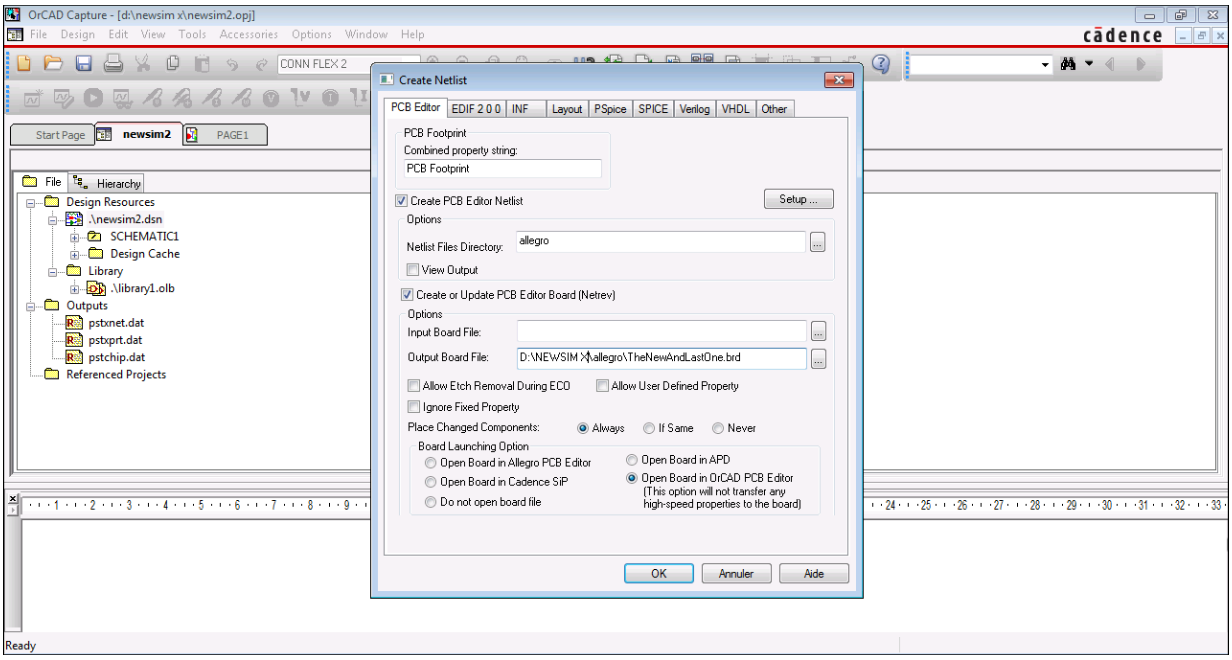


Figure IV-9 Creating the Netlist

Ones the Netlist is created, all components will be transformed to the PCB tool as follows:

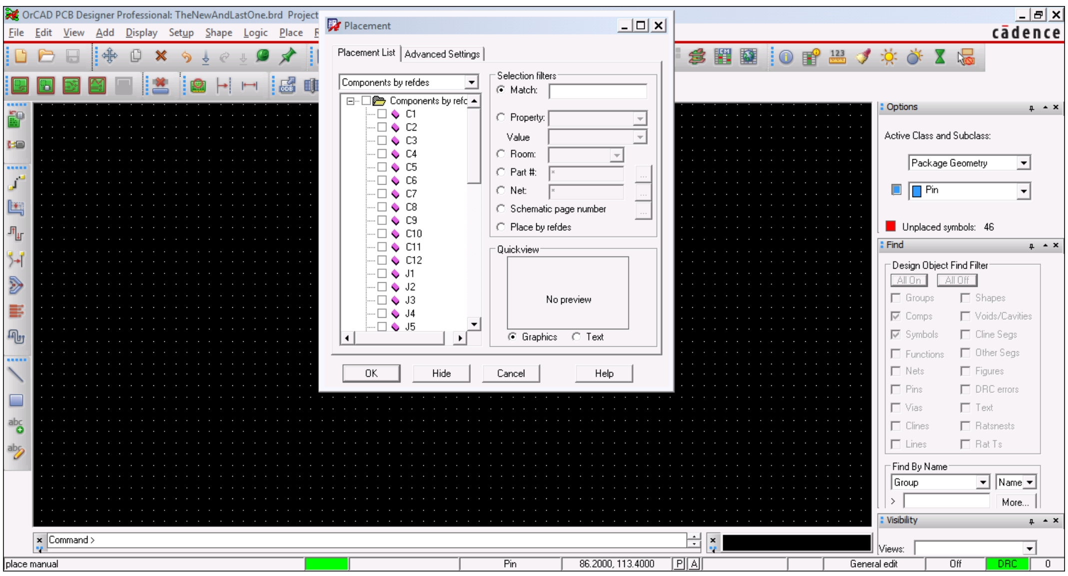


Figure IV-10 Transferring all components to PCB designer

### IV.3.5 Step 05: Components placement and framing:

Components placement by simply dragging the components from the library to the work surface after having checked the small box referring to them, then they are framed as presented in the following:

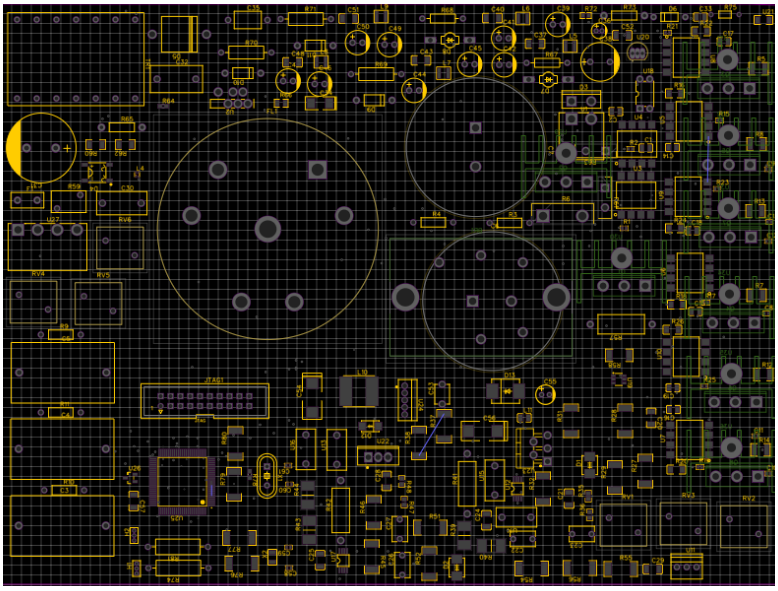

**Figure IV-11 Components placement**

### IV.3.6 Step 06: Routing:

After placing all the components, routing them will be recommended. The width of the tracks must correspond to the value of the current that crosses them ( The width was given by DigiKey calculator ). A cooper layer is then created to play the ground plate role .

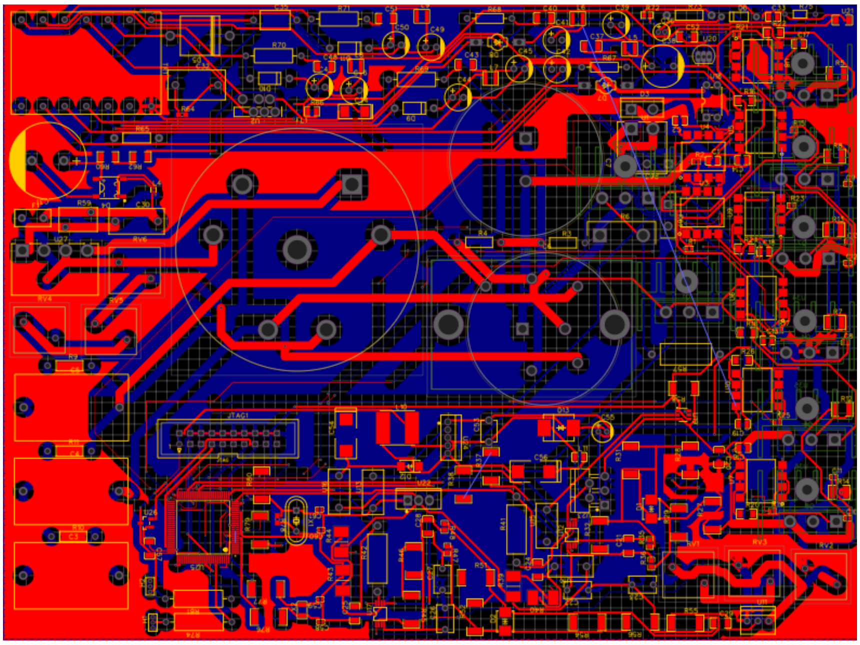

**Figure IV-12 The VSD circuit with rooting and ground plate**

## IV.4 Gerber file for the manufacture of the PCB

Ones the design is finished, the manufacturer must generate the Gerber folder using the OrCAD PCB designer and load it in CAM (Computer-Aided Manufacturing). The Garber folder contains all the information about the designed circuit such as: the description of the various layers, the location of each component, tracks and vias.

The Gerber file is universal, that means that the manufacturer receives a single type of file regardless of the software used which makes this file very interesting and useful.

Note that the Gerber folder includes files named "Artwork" which allows the manufacturer to draw the circuit on the printed board and place the information that the designer wants to put. For this project, the Gerber folder contains the files following:

- TOP Layer
- BOTTOM Layer
- SILKSCREEN_TOP
- SILKSCREEN_BOTTOM
- SOLDERMASK_TOP

- SOLDER MASK_BOTTOM
- OUTLINE
- DRILL

## IV.4.1 Definition

### IV.4.1.1 TOP/BOTTOM layer

As the name goes, it represents the top and the bottom side of the board, the tracks where the current flows. They are usually made by either aluminum or silver.

### IV.4.1.2 SILKSCREEN

Also goes by the components layer, it contains the contours of the components and their names (R1,C1..etc).

### IV.4.1.3 SOLDERMASK

It is called a "solder mask". It is a thin polymer layer that sits on the board and surrounds the component pins to avoid the unintentional electrical connection between two adjacent pins. This is essential for surface mount devices.

### IV.4.1.4 OUTLINE

It basically defines the boarders of the board. It can be modeled by the shape that the designer wishes. But usually it comes either square or rectangular. It is necessary to define the outline of the map for the manufacturer to know its dimensions.

### IV.4.1.5 DRILL

As the name suggests, this file contain information on the size and location of the drilling points on the electronic board. They represent vias, connectors as well as mechanical holes on the board.

## IV.4.2 Gerber files viewing

### IV.4.2.1 Artwork files viewing

Once the Gerber file is generated, it will be loaded into a software or an online site display of electronic PCB boards, in our case the EasyEDA is used.

The first case is the case of discrete IGBTs:

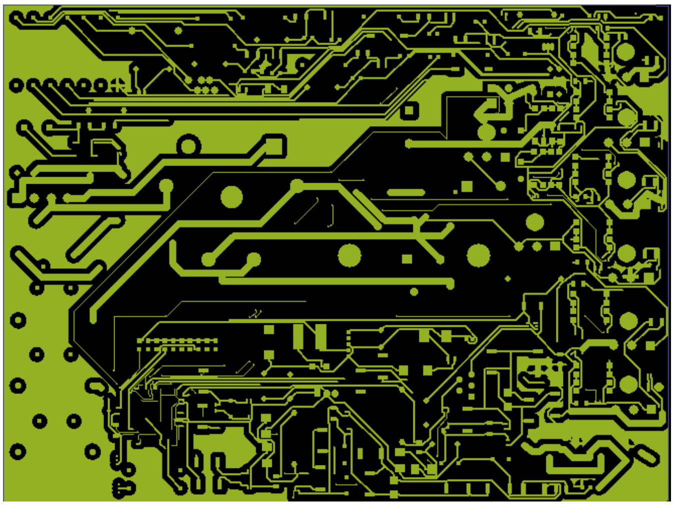

(a) Top Layer (COPPER)

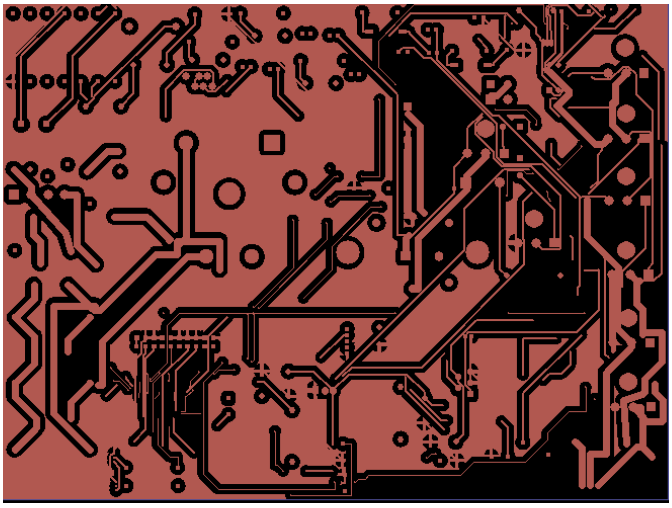

(b) Bottom Layer (COPPER)

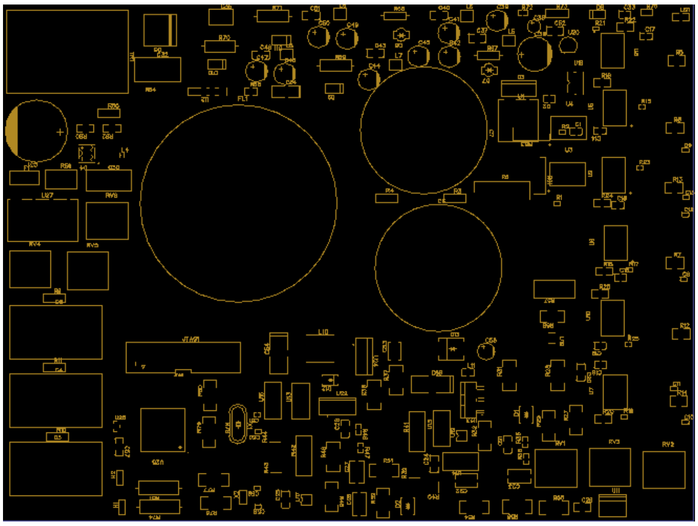

(c) Silkscreen TOP

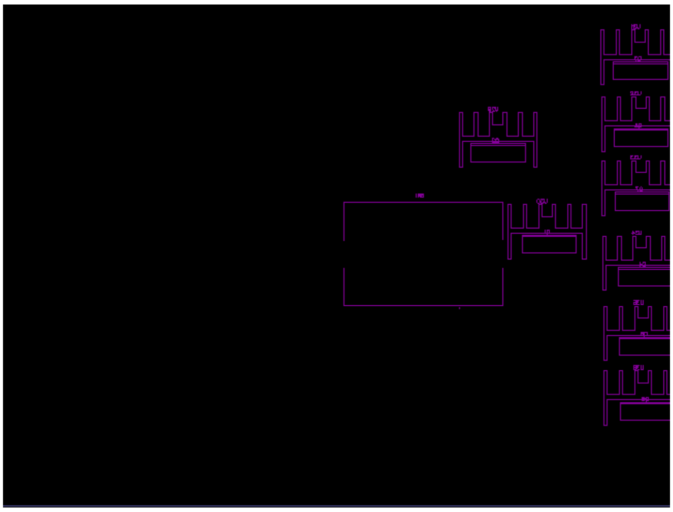

(d) Silkscreen BOTTOM

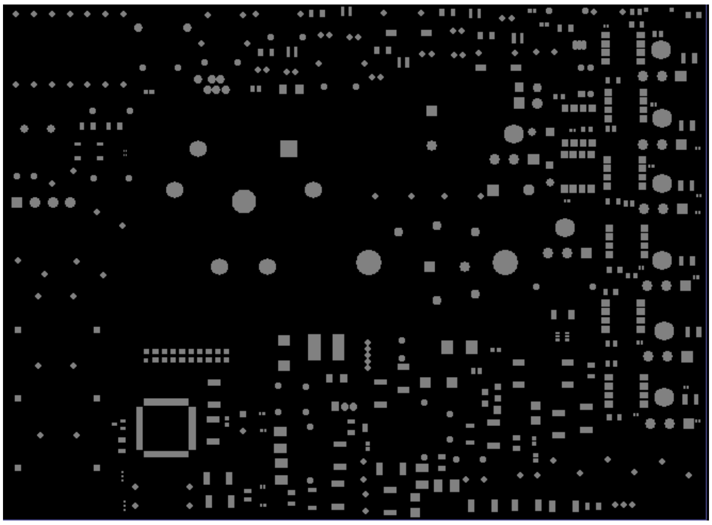

(e) Soldermark TOP

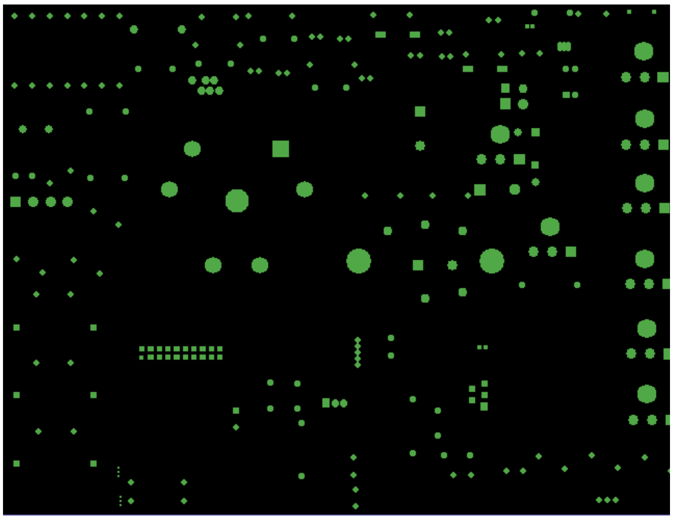

(f) Soldermark BOTTOM

**Figure IV-13 the used layers for the PCB (discrete IGBTs)**

IPM case:

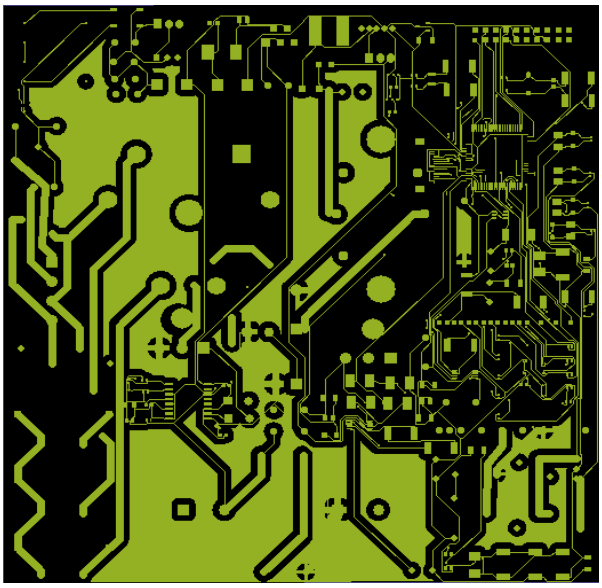

(a) Top Layer (COPPER)

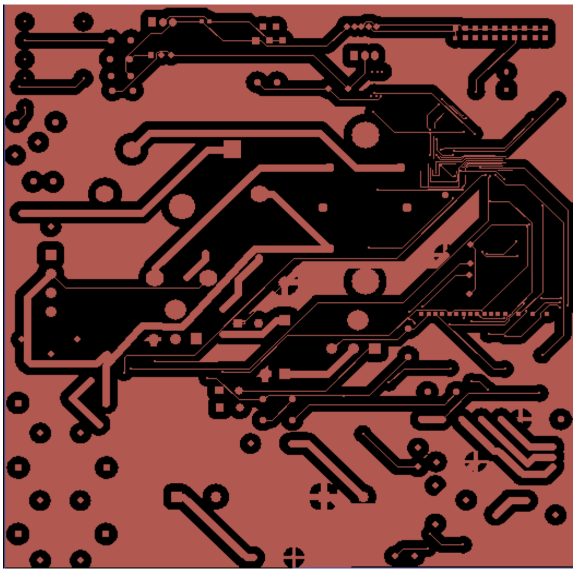

(b) Bottom Layer (COPPER)

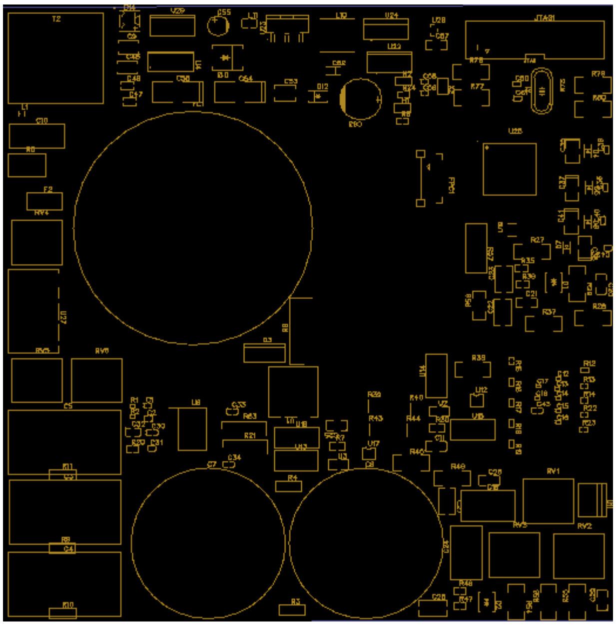

(c) Silkscreen TOP

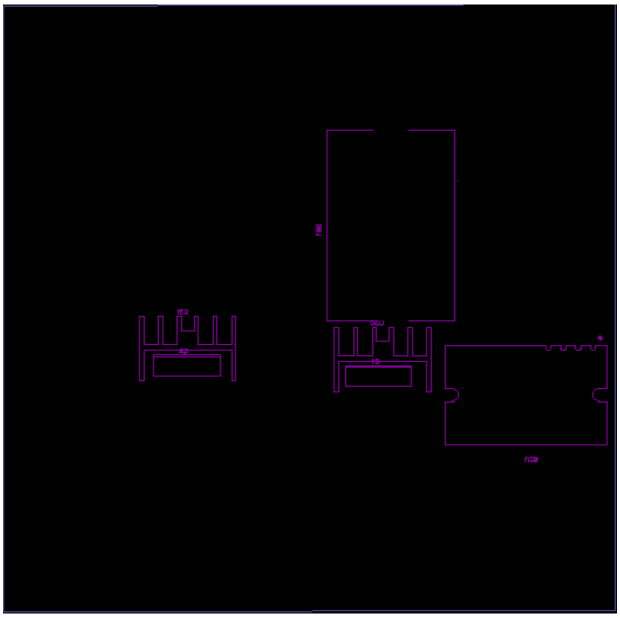

(d) Silkscreen BOTTOM

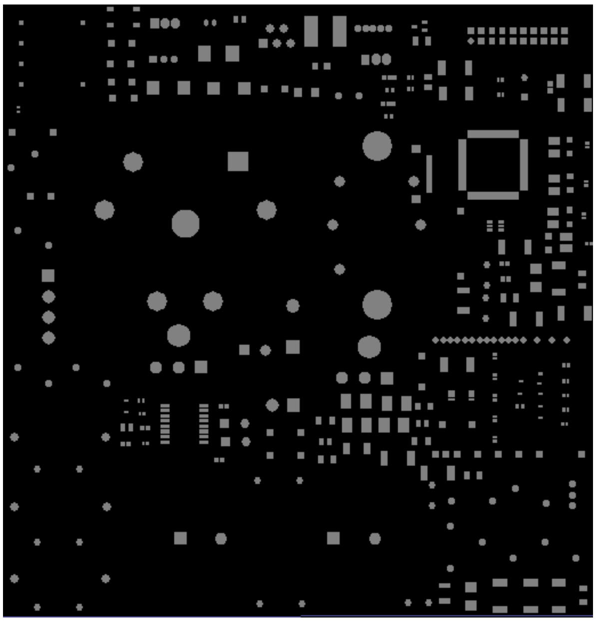

(e) Soldermark TOP

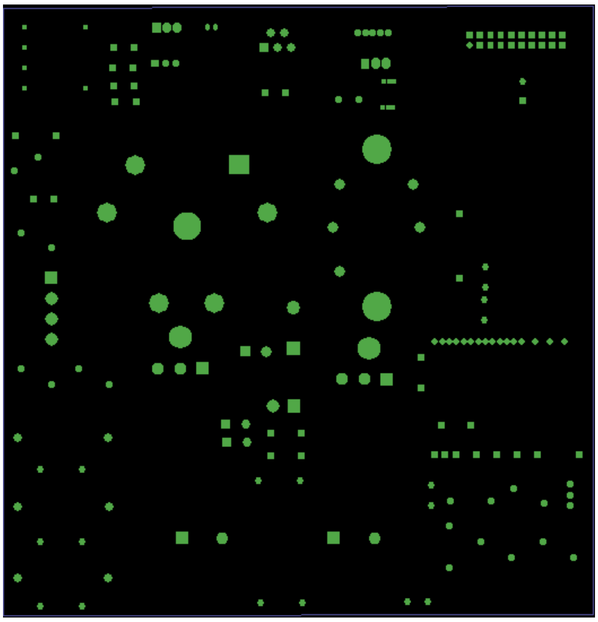

(f) Soldermark BOTTOM

**Figure IV-14 the used layers for the PCB (IPM)**

#### IV.4.2.2 Drill file viewing

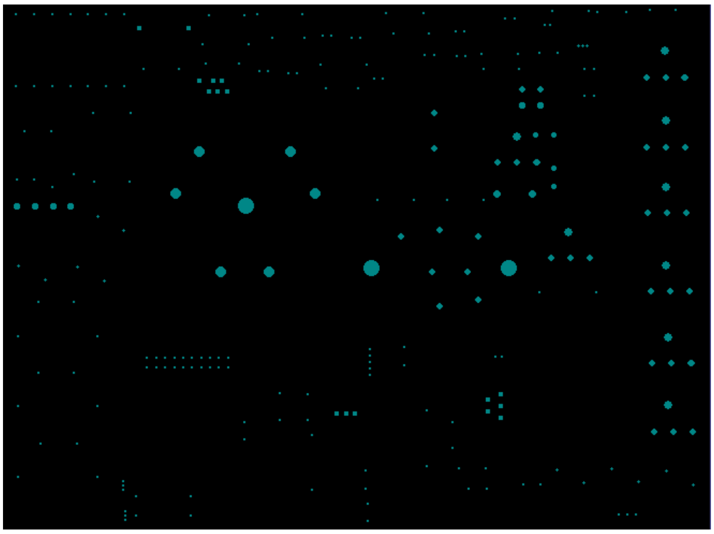

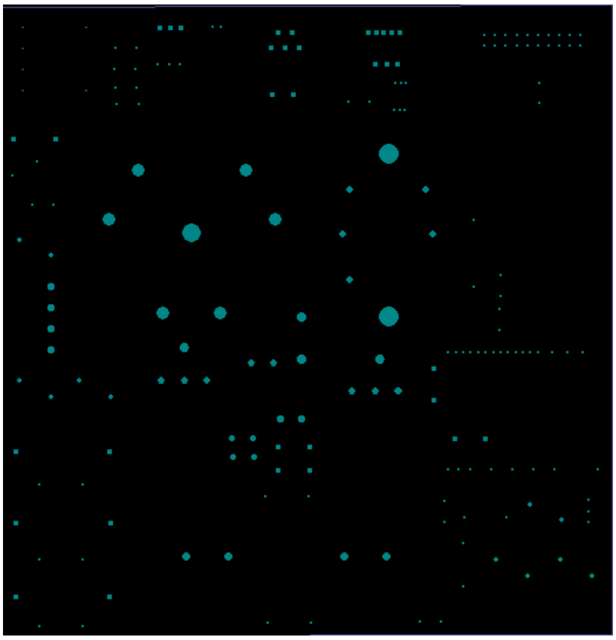

(a) Discrete IGBTs case (b) IPM case

**Figure IV-15 drill files visualisation**

#### IV.4.2.3 The overall circuit

In the end the overall circuit that will be seen to the naked eye will be the following:

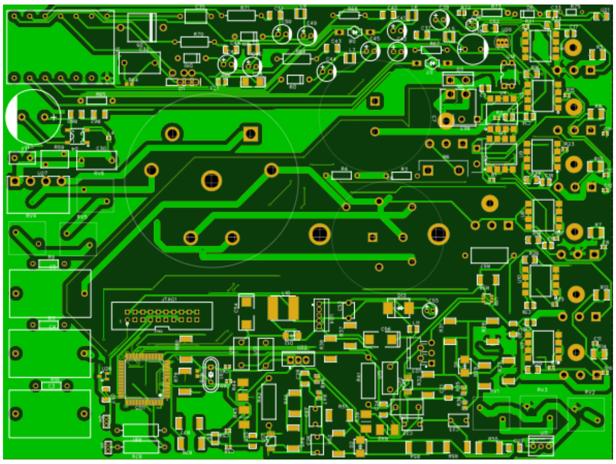

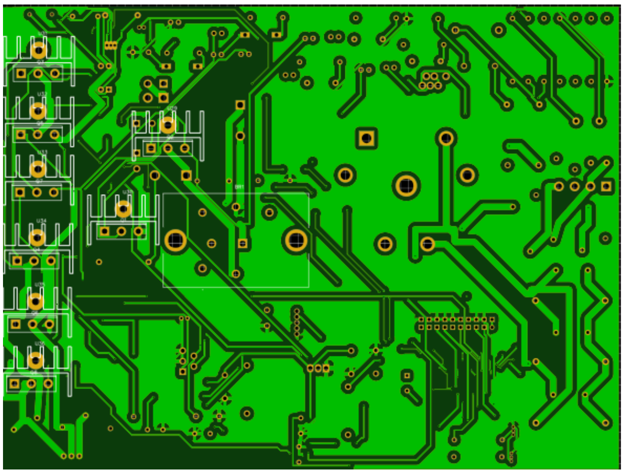

(a) Top view, discrete IGBTS (b) bottom view, discrete IGBTS

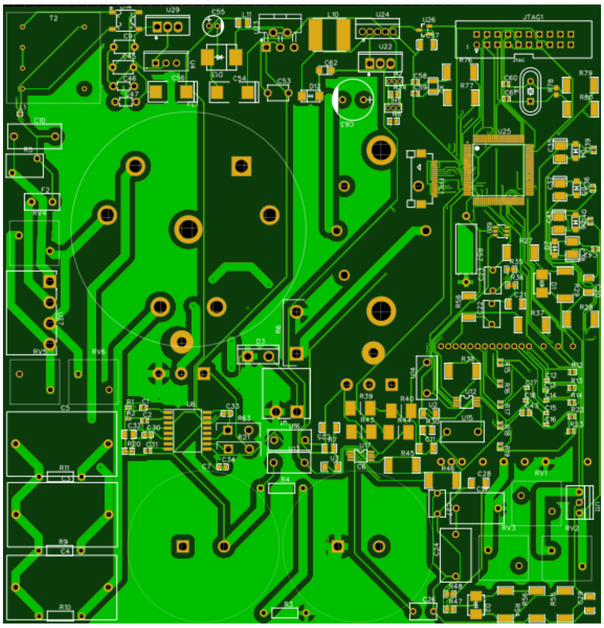

(c) Top view, IPM

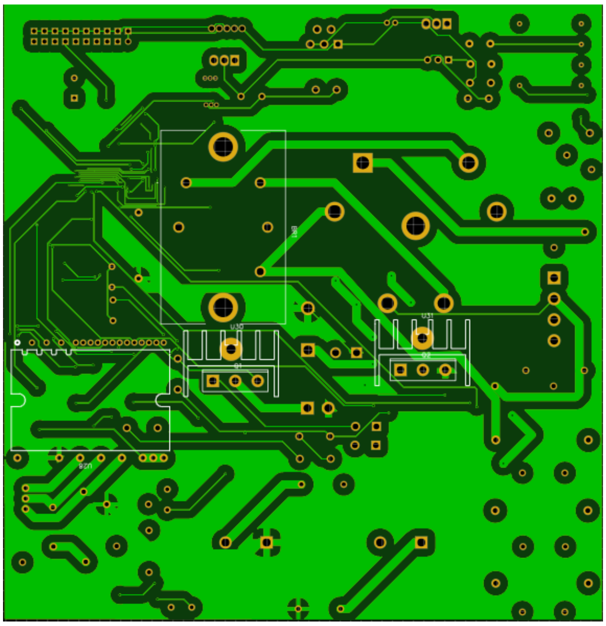

(d) bottom, IPM

**Figure IV-16 The VSD circuit Boards**

The price estimate for the manufacture of this PCB was established on the JLCPCB site at 25.2 €, The total price of the components is 317.857 € in case of IPM and 351.007 € for discrete IGBTs, which leads to a final price of $ 344.057 and 376.207 €. In the case of manufacturing on an industrial scale (mass production) the price will be lower.

## Conclusion:

This PCB is the crossroads where all the components chosen in the previous chapters are putted.

All the rules for the design of printed circuits have been taken into account in order to avoid any possibility of producing crosstalk or any EMI interference that was presented in the end of chapter III.

The layout of the components has been made in a way to minimize the size of the circuit taking into consideration the criteria used and the price of each component as well.

The manufacture of this card and all the tests must be applied through practice.

We presented in this chapter a simulation of the VSD using MATLAB/SIMULINK, where two important cases were presented (the three phases and single-phase simulation). As a result, we conclude that the proposed VSD can work in both cases.

In the end, two PCBs were presented, one using the IPM technology while the other is made by discrete IGBTs. As we saw from the study presented using the IPM is cheaper than using discrete IGBTs plus it makes the whole VSD smaller and it provides some protections as well. Thus, the use of the IPM is ideal in the VSDs in term of quality price and size.

# GENERAL CONCLUSION

Changing the speed of motors was not that easy before the introduction of variable speed drives. These last were a great revolution that changed the industrial word forever. After their introduction in the late 1950's, the market of VSDs has been rising exponentially. The advance in technology created new application where the VSDs were the best choice.

Many companies were and are still competing with each other. They manufacture new VSDs with enhanced parameter, new topologies, new control techniques …etc. This fierce competition, as well as the still rising market, inspired new company and young engineers to enter this battle with their new ideas in order to build their own VDS, which was the purpose of this project.

In this report we started by presenting the VSDs, and in general the AC-AC converters, which is the main topologies of the VSDs. A stat of the art was presented giving various topologies that were discussed and compered with each other in order to choose one topology. Another study regarding the market was presented, where the trends of the VSDs, the prediction of their future market was given. In this study, it is clear that the market is still raising which means there is always need for new VSDs developments and innovations.

The second chapter was about a study of the chosen main topology, its specification and some additional circuits that were presented and sized according to the specification given by the company (GA-Tech). This step is very important because it defines the criteria of and total shape of the built VSD. In this same part, we performed the sizing of the components to match them to the desired operation of the global circuit.

In the third chapter, an extensive research was presented and supported by a comparative study, in order to allow an adequate choice between the different components constituting the global circuit of the VSD. Many manufacturers and choices were presented. So, the choice was made taking into account the rule of price, size and quality optimization.

Two solutions were presented, where one of them is the discrete IGBT solution which is the basic structure of the VSD, the other one is an optimized one using the IPM technology.

Using the IPM technology made the VSD cheaper in price, and more efficient. Since the IPMs contain protections while normal IGBTs don't.

In the end chapter three an estimated price of the whole VSD was calculated, taking into account two cases of solutions (using IPM or discrete IGBTs).

The last chapter was about doing a simulation of the VSD using MATLAB/SIMULINK tool, in order to evaluate its performances. This simulation was done in three cases: a normal three-phases functioning, a faulty three-phases functioning (where one phase is down, the machines works with only two phases, mono phase functioning).

As a result, we saw that the VSD can work in those cases, but the most preferable is the three-phase case, since the other two cases will introduce more harmonic components (the harmonics multiple of three).

Another part of the past chapter was devoted to the design of the circuit board. The procedure was presented in the form of a tutorial where all the steps of the design were worked out in using OrCAD Capture and OrCAD PCB designer software as well as another software called EasyEDA. PCB design ended with the generation of the Gerber file that will be provided to the manufacturer in order to actually make the circuit board. Two PCB designs were presented, one for the IPM solution with a size of 150 x 150mm and another one with discrete IGBTs with 200 x 150mm which means that in addition to the efficiency and the low price of the IPM it also presents a smaller size compared to the Discrete IGBTs solution.

As perspective to this work we propose

The implementation of this project so as to be a prototype for the future version of the VSDs manufactured locally. Tests will be done on the prototype to see its accuracy.

We propose also to change the rectifier bridge with IGBTs instead diodes, in order to insure the regenerative braking system and to limit the power dissipation in the braking stage.

Another proposition is the use of the direct matrix converter (MC), this topology will make the VSD very small due to the reduced number in semiconductor components. The DC link capacitor will be gone as well. Thus, another reduction in size.

The MC provides the possibility to control the Input current. As a result, the ability to correct the power factor as well.

# BIBLIOGRAPHY

[1] D. E. Roethemeyer et D. Yankaskas, « Evolution of motor and variable frequency drive technology », 1995, p. 541-552.
[2] « https://en.wikipedia.org/wiki/Variable-frequency_drive ». .
[3] M. Barnes, Practical Variable Speed Drives and Power Electronics. Elsevier Science, 2003.
[4] S. Bhowmik et R. Spee, « A guide to the application-oriented selection of AC/AC converter topologies », IEEE Trans. Power Electron., vol. 8, no 2, p. 156-163, avr. 1993, doi: 10.1109/63.223967.
[5] J. W. Kolar, T. Friedli, J. Rodriguez, et P. W. Wheeler, « Review of Three-Phase PWM AC–AC Converter Topologies », IEEE Trans. Ind. Electron., vol. 58, no 11, p. 4988-5006, nov. 2011, doi: 10.1109/TIE.2011.2159353.
[6] P. Szczesniak, « Three-Phase AC–AC Power Converters Based on Matrix Converter Topology », Springer, 2013.
[7] M. P. Kazmierkowski, R. Krishnan, et F. Blaabjerg, Control in power electronics. Elsevier, 2002.
[8] J. Arrillaga et N. R. Watson, Power system harmonics. John Wiley & Sons, 2004.
[9] J. W. Wilson, « The forced-commutated inverter as a regenerative rectifier », IEEE Trans. Ind. Appl., no 4, p. 335-340, 1978.
[10] D. G. Holmes et T. A. Lipo, Pulse width modulation for power converters: principles and practice, vol. 18. John Wiley & Sons, 2003.
[11] M. P. Kazmierkowski, R. Krishnan, et F. Blaabjerg, Control in power electronics. Elsevier, 2002.
[12] Fang Zheng Peng et al., « Z-source inverter for motor drives », IEEE Trans. Power Electron., vol. 20, no 4, p. 857-863, juill. 2005, doi: 10.1109/TPEL.2005.850938.
[13] F. Z. Peng, X. Yuan, X. Fang, et Z. Qian, « Z-source inverter for adjustable speed drives », IEEE Power Electron. Lett., vol. 1, no 2, p. 33-35, 2003.
[14] T. Friedli et J. W. Kolar, « Milestones in matrix converter research », IEEJ J. Ind. Appl., vol. 1, no 1, p. 2-14, 2012.
[15] L. Empringham, J. W. Kolar, J. Rodriguez, P. W. Wheeler, et J. C. Clare, « Technological issues and industrial application of matrix converters: A review », IEEE Trans. Ind. Electron., vol. 60, no 10, p. 4260-4271, 2012.
[16] F. Gruson, « Modulation naturelle généralisée des convertisseurs matriciels pour la variation de vitesse », 2010.
[17] A. Alesina et M. G. Venturini, « Analysis and design of optimum-amplitude nine-switch direct AC-AC converters », IEEE Trans. Power Electron., vol. 4, no 1, p. 101-112, 1989.
[18] K. Ghedamsi, « Contribution à la modélisation et la commande d'un convertisseur direct de fréquence », 2008.
[19] P. D. Ziogas, Y. Kang, et V. R. Stefanovic, « Rectifier-Inverter Frequency Changers with Suppressed DC Link Components », IEEE Trans. Ind. Appl., vol. IA-22, no 6, p. 1027-1036, nov. 1986, doi: 10.1109/TIA.1986.4504834.
[20] J. W. Kolar, M. Baumann, F. Schafmeister, et H. Ertl, « Novel three-phase AC-DC-AC sparse matrix converter », 2002, vol. 2, p. 777-791.

[21] A. Benachour, « Commande sans Capteur basée sur DTC d'une Machine Asynchrone alimentée par Convertisseur Matriciel », 2017.
[22] M. Y. Lee, « Three-level neutral-point-clamped matrix converter topology », 2009.
[23] J. W. Kolar, F. Schafmeister, S. D. Round, et H. Ertl, « Novel three-phase AC–AC sparse matrix converters », IEEE Trans. Power Electron., vol. 22, no 5, p. 1649-1661, 2007.
[24] T. Friedli et J. W. Kolar, « A Semiconductor Area Based Assessment of AC Motor Drive Converter Topologies », in 2009 Twenty-Fourth Annual IEEE Applied Power Electronics Conference and Exposition, févr. 2009, p. 336-342, doi: 10.1109/APEC.2009.4802678.
[25] T. Friedli et J. W. Kolar, « Comprehensive comparison of three-phase AC-AC Matrix Converter and Voltage DC-Link Back-to-Back Converter systems », in The 2010 International Power Electronics Conference - ECCE ASIA -, juin 2010, p. 2789-2798, doi: 10.1109/IPEC.2010.5543814.
[26] R. Vargas, U. Ammann, J. Rodriguez, et J. Pontt, « Predictive Strategy to Control Common-Mode Voltage in Loads Fed by Matrix Converters », IEEE Trans. Ind. Electron., vol. 55, no 12, p. 4372-4380, déc. 2008, doi: 10.1109/TIE.2008.2007016.
[27] R. Vargas, U. Ammann, et J. RodrÍguez, « Predictive Approach to Increase Efficiency and Reduce Switching Losses on Matrix Converters », IEEE Trans. Power Electron., vol. 24, no 4, p. 894-902, avr. 2009, doi: 10.1109/TPEL.2008.2011907.
[28] F. Villarroel, J. Espinoza, C. Rojas, C. Molina, et E. Espinosa, « A multiobjective ranking based finite states model predictive control scheme applied to a direct matrix converter », in IECON 2010 - 36th Annual Conference on IEEE Industrial Electronics Society, nov. 2010, p. 2941-2946, doi: 10.1109/IECON.2010.5675066.
[29] S. L. Arevalo, P. Zanchetta, P. W. Wheeler, A. Trentin, et L. Empringham, « Control and Implementation of a Matrix-Converter-Based AC Ground Power-Supply Unit for Aircraft Servicing », IEEE Trans. Ind. Electron., vol. 57, no 6, p. 2076-2084, juin 2010, doi: 10.1109/TIE.2009.2034180.
[30] A. Trentin, P. Zanchetta, P. Wheeler, et J. Clare, « Power flow analysis in electro-mechanical actuators for civil aircraft », IET Electr. Power Appl., vol. 5, no 1, p. 48-58, janv. 2011, doi: 10.1049/iet-epa.2009.0270.
[31] J.-P. Caron et J.-P. Hautier, Modélisation et commande de la machine asynchrone. éditions Technip Paris, 1995.
[32] T. Riad, « Contribution à la commande directe du couple de la machine asynchrone », 2017.
[33] A. Yousef et S. Abdel maksoud, « Review on Field Oriented Control of Induction Motor », Int. J. Res. Emerg. Sci. Technol. IJREST, vol. 2, juill. 2015.
[34] I. Takahashi et T. Noguchi, « A new quick-response and high-efficiency control strategy of an induction motor », IEEE Trans. Ind. Appl., no 5, p. 820-827, 1986.
[35] U. Baader, M. Depenbrock, et G. Gierse, « Direct self control (DSC) of inverter-fed induction machine: A basis for speed control without speed measurement », IEEE Trans. Ind. Appl., vol. 28, no 3, p. 581-588, 1992.
[36] M. Matteini, « Control techniques for matrix converter adjustable speed drives », 2001.
[37] M. H. Rashid, Power electronics handbook. Butterworth-Heinemann, 2017.
[38] J. Zhang, L. Li, et D. G. Dorrell, « Control and applications of direct matrix converters: A review », Chin. J. Electr. Eng., vol. 4, no 2, p. 18-27, 2018.

[39] V. Yaramasu, B. Wu, P. C. Sen, S. Kouro, et M. Narimani, « High-power wind energy conversion systems: State-of-the-art and emerging technologies », Proc. IEEE, vol. 103, no 5, p. 740-788, mai 2015, doi: 10.1109/JPROC.2014.2378692.

[40] « International Journal of Power Electronics and Drive System (IJPEDS) Vol. 3, No. 1, March 2013, pp. 74~82 ». .

[41] « Variable-speed drives for belt-conveyor systems ». [En ligne]. Disponible sur: https://library.e.abb.com/public/b353080c210c00af832573fc005038b6/Project_Report_VSD_on_Conveyors.pdf.

[42] « [https://www.marketsandmarkets.com/Market-Reports/variable-frequency-drive-market-878.html] ». .

[43] « https://www.fortunebusinessinsights.com/industry-reports/variable-frequency-drive-market-100876 ». .

[44] « https://www.totallyintegratedautomation.com/2017/05/trends-variable-frequency-drive-technology/ ». .

[45] Schnetzka et al., « United States Patent, Patent No.: US 7.746,020 B2,Jun. 29, 201 ». .

[46] « Biricha Digital Power Ltd www.biricha.com ». .

[47] Ashok Singroly with the Electrical & Electronics Engineering Department, « Stabilized Power AC-DC-AC Converter using Different Type of Passive Filters », International Journal of Engineering Research & Technology (IJERT) ISSN: 2278-0181, août 01, 2012.

[48] P. T. Kilpailijavertailu, « Elektroniikka ja automaatio », p. 61.

[49] B. Wunsch, U. Drofenik, S. Skibin, et V. Forsstrom, « Impact of diode-rectifier on EMC-noise propagation and filter design in AC-fed motor drives », 2017, p. 237-242.

[50] [En ligne]. Disponible sur: https://www.ecmweb.com/national-electrical-code/code-basics/article/20892807/dont-let-voltage-drop-get-your-system-down.

[51] H. Soltani, P. Davari, D. Kumar, F. Zare, et F. Blaabjerg, Effects of DC-link filter on harmonic and interharmonic generation in three-phase adjustable speed drive systems. 2017, p. 681.

[52] A. Hava, U. Ayhan, et V. Aban, A DC bus capacitor design method for various inverter applications. 2012, p. 4599.

[53] F. Peng et al., « Z-Source Inverter for Motor Drives », Power Electron. IEEE Trans. On, vol. 20, p. 857-863, août 2005, doi: 10.1109/TPEL.2005.850938.

[54] P. C. Loh, F. Gao, P. Tan, et F. Blaabjerg, « Three-Level AC–DC–AC Z-Source Converter Using Reduced Passive Component Count », IEEE Trans. Power Electron., vol. 24, no 7, p. 1671-1681, juill. 2009, doi: 10.1109/TPEL.2008.2011756.

[55] M. Barnes, Practical variable speed drives and power electronics. Newnes, 2003.

[56] F.Rahman, « Lecture 2 - Overview of power switches », sept. 2010.

[57] « (15) (PDF) Advanced Driver Circuits », ResearchGate. https://www.researchgate.net/publication/317007938_Advanced_Driver_Circuits/citations (consulté le avr. 14, 2020).

[58] « https://www.fujielectric.com/products/semiconductor/model/igbt/application/index.html ». .

[59] « https://www.fujielectric.com/products/semiconductor/model/igbt/ipm.html ». .

[60] « dynamic braking resistor selection calculation ». https://fr.slideshare.net/abhisit1983/dynamic-braking-resistor-selection-calculation.

[61] Rudy Severns, « DESIGN OF SNUBBERS FOR POWER CIRCUITS ». .

[62] « Ap-Guide-Snubber-Caps.pdf ». Consulté le: avr. 28, 2020. [En ligne]. Disponible sur: https://www.cde.com/resources/catalogs/Ap-Guide-Snubber-Caps.pdf.

[63] F. Gruson, « Modulation naturelle généralisée des convertisseurs matriciels pour la variation de vitesse », 2010.

[64] « emi_rfi_suppression_capacitors ». [En ligne]. Disponible sur: https://www.illinoiscapacitor.com/pdf/papers/emi_rfi_suppression_capacitors.pdf.

[65] « 6MBP10VAA120-51 A50L-0001-0438 FUJI ELECTRIC IPM MODULE 10A 1200V ID74474 ». https://www.rgbautomatyka.pl/fr/6mbp10vaa120-51-a50l-0001-0438-fuji-electric-ipm-module-10a-1200v-id74474.html.

[66] « FSBB15CH120D - Module de puissance intelligent (IPM), IGBT, 1.2 kV, 15 A, 2500 Vrms, SPMMF-027, SPM3 ». https://fr.farnell.com/on-semiconductor/fsbb15ch120d/module-ipm-igbt-15a-1200v-spmmf/dp/2762554 (consulté le mai 08, 2020).

[67] « IM818MCCXKMA1 ». https://eu.mouser.com/ProductDetail/Infineon-Technologies/IM818MCCXKMA1?qs=%2Fha2pyFadug8yvvNYHSCpufAr856KGKUEuN43leQ6a2YQUmpqrJNhglV8UNQw6wI&utm_source=octopart&utm_medium=aggregator&utm_campaign=726-IM818MCCXKMA1&utm_content=Infineon.

[68] « STGIB30M60TS-L ». https://eu.mouser.com/ProductDetail/STMicroelectronics/STGIB30M60TS-L?qs=lYGu3FyN48coY36yRqa60A%3D%3D.

[69] « FP15R12W1T7_B3 ». https://www.infineon.com/cms/en/product/power/igbt/igbt-modules/fp15r12w1t7_b3/.

[70] « MUBW10-12A7 ». https://eu.mouser.com/ProductDetail/IXYS/MUBW10-12A7?qs=sGAEpiMZZMsSvCxLCzAHjEvuWU1xtfoiXcBz6YBZj%2FQ%3D&fbclid=IwAR0ayYxa1enxqqF1yuhzfKp3nReBhXYAWwo7k_m4xjX7j3yY5nDDTVEqNW8.

[71] « Optocoupler Performance Comparison: NEC PS9552 vs. Avago HCPL-3120 ». [En ligne]. Disponible sur: http://www.cel.com/pdf/appnotes/AN3006old.pdf.

[72] PEEMD, Research Group, IIT-Delhi, « Design and implementation of a 3-phase, 2-Level Voltage Source Converter (Using discrete IGBTs) ». juin 2017.

[73] « heat sink design for thermal analysis ». [En ligne]. Disponible sur: www.digikey.com.

[74] « selecting the appropriate circuit protection component.pdf ». [En ligne]. Disponible sur: https://www.ieee.li/pdf/viewgraphs/selecting_the_appropriate_circuit_protection_component.pdf.

[75] « VDRUS10T460BSE ». https://eu.mouser.com/ProductDetail/Vishay/VDRUS10T460BSE?qs=%2Fha2pyFaduiRNZoBtpwpq8rMMiaQsrlah318Hu77bQ0NUlhHiaG8gQ%3D%3D.

[76] By Ashish Kumar, Product Engineer Sr and Pushek Madaan, Applications Engineer Sr, Cypress Semiconductor Corp., « Top 10 EMC Design Considerations ». [En ligne]. Disponible sur: https://www.cypress.com/file/106951/download.

[77] « « CHAPTER 6 PRINTED CIRCUIT BOARD DESIGN », yumpu.com. [En ligne] Disponible sur : https://www.yumpu.com/en/document/read/28449466/chapter-6-printedcircuit-board-design ». .

[78] Adlane Arezki MEDJEK et Zoubida AZAIZIA, « Conception d'un circuit de puissance intégré pour une application dans un eSiP ». .

# APPENDICES

## a) APPENDICES A : OrCAD présentation :

OrCAD is a suite of proprietary software tools used primarily for electronic design automation. This software was created by the company OrCAD Systems Corporation in Hillsboro, Oregon in 1985 hence its name which reflects the company and the origins of its software: Oregon + CAD. Then it was taken over by Cadence Design Systems in 1999 and integrated with Cadence Allegro since 2005.

OrCAD is primarily used by engineers in order to create electronic boards, perform simulations and printing for the PCBs.

**OrCAR's Tools :**

OrCAD is one of the most powerful computing environments for design and analysis of printed circuits. It includes several sub-software to guarantee users a wide handling of computer tools related to design electronic, among these we cite:

- A schematic diagram editor (Capture).
- A simulator (PSpice).
- A PCB design application (PCB Designer).

### OrCAD Capture:

It is a schematic design solution, used to create electric circuits using library tools. It is associated with OrCAD CIS for the management of component data

The next figure represents an RLC circuit:

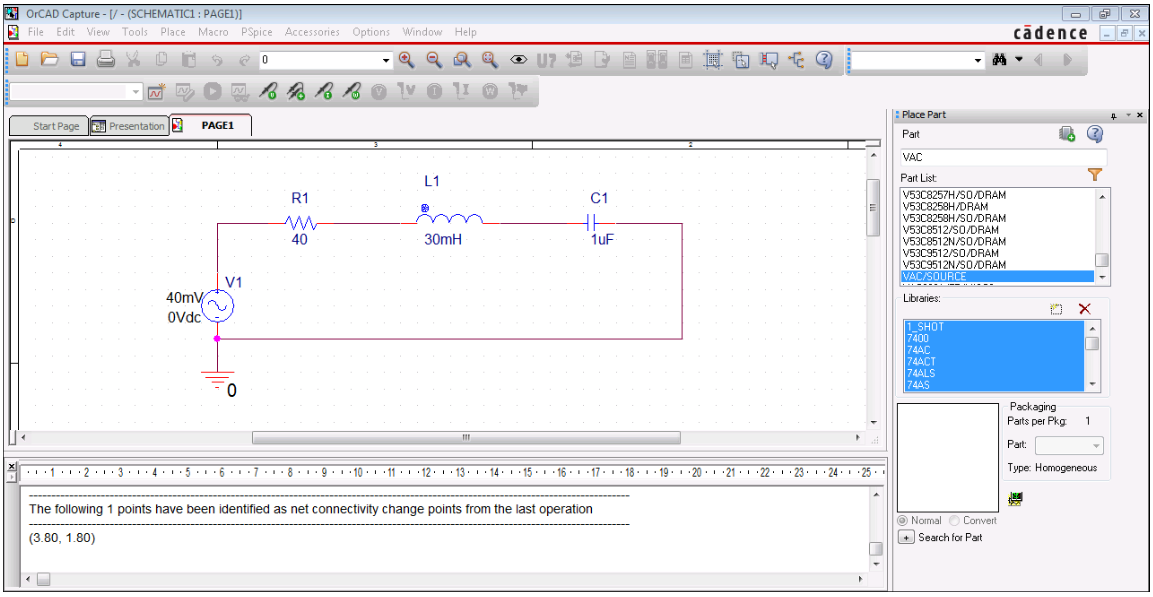


**Figure A. 1 RLC electrical diagram drawn on ORCAD Capture**

On the right of the window you can see the box of available libraries under the name of "Libraries", each library includes a list of component models. In the case where the circuit requires a component which is not found in these libraries, it is possible to download the component model and import it into the software.

## OrCAD PSpice :

OrCAD PSpice is a simulator of digital or analog circuits. It is a modified version of the academically developed SPICE which has been marketed by MicroSim in 1984. MicroSim was bought by OrCAD a decade later in 1998.

This simulator performs several types of analyzes:

- Transient analysis for circuits with sources varying in time: Allows to see the behavior and response of electrical systems as a function of time (variable transient and permanent).
- DC analysis (AC sweep) for circuits with time invariant sources: These are parametric simulations according to a circuit parameter (example: resistance).
- AC analysis (DC sweep) for analyzing small signals from circuits with sources at variable frequencies. This is the frequency analysis of the circuit.

- Bias point analysis: Consists of calculating the voltage and the respective currents at each node of the circuit when the current stabilizes.

The source of the previous circuit is a variable frequency source, hence the AC analysis chosen in Analysis type to visualize the current flowing through the resistor, as shown below:

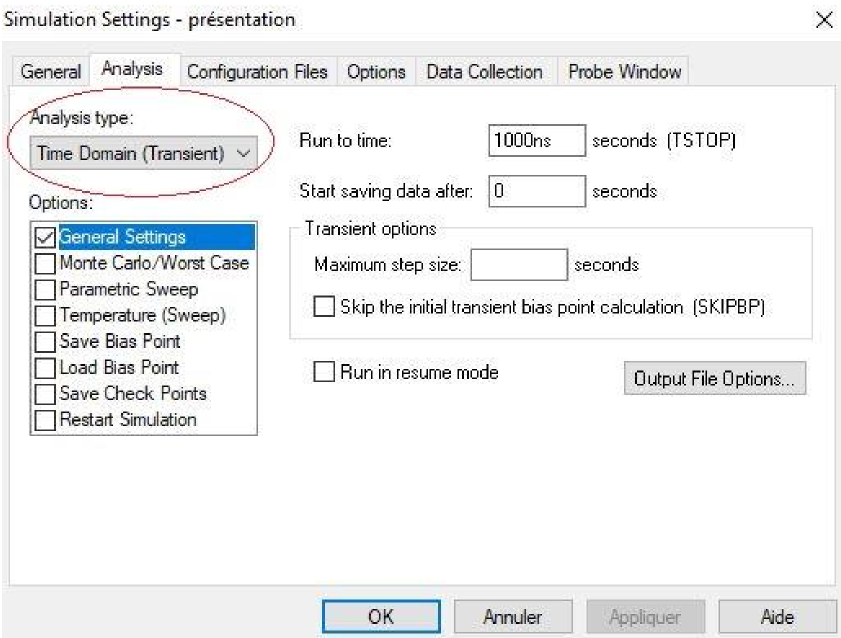


**Figure A. 2 Choice of the type of analysis in the PSpice**

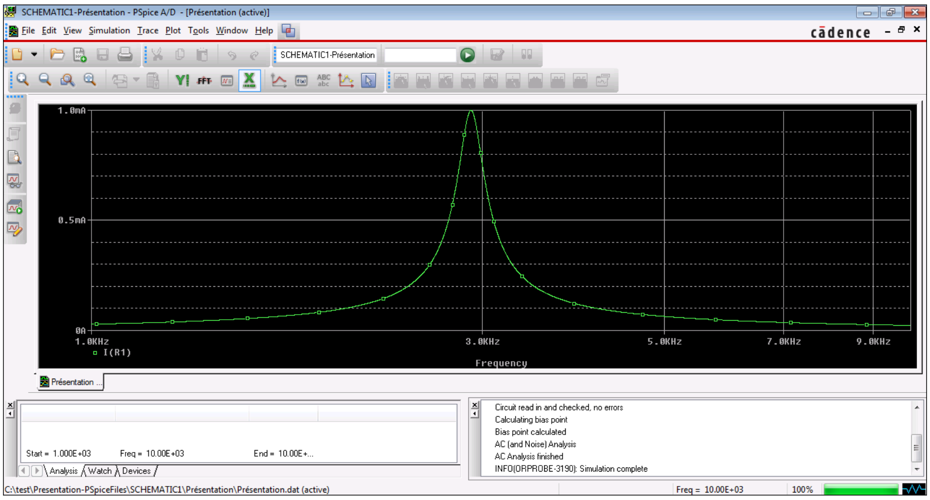


**Figure A. 3 Result of the simulation with the PSpice simulator (AC sweep).**

## OrCAD PCB Designer :

It is a circuit board designing software, includes various automation features for PCB design, board-level analysis and design rule verification (DRC). This design can be achieved by manually tracing PCB tracks or using the supplied automatic router.

The PCB designer can be integrated into Orcad, capture in the case of a construction project of a simulated circuit by generating the "Netlist", which includes all the information on circuit components on Orcad capture and transfer them to the designer PCB. The following figure illustrates the example of this presentation:

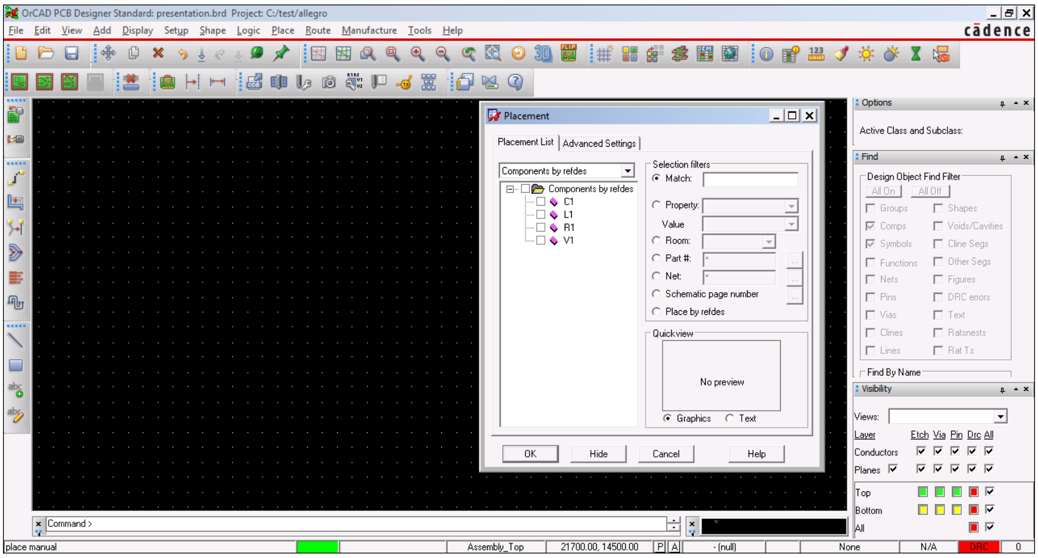


**Figure A. 4 Transfer of components from Orcad capture to the PCB environment designer.**

The components are connected with tracks, which choice of shape and thickness is made by the user:

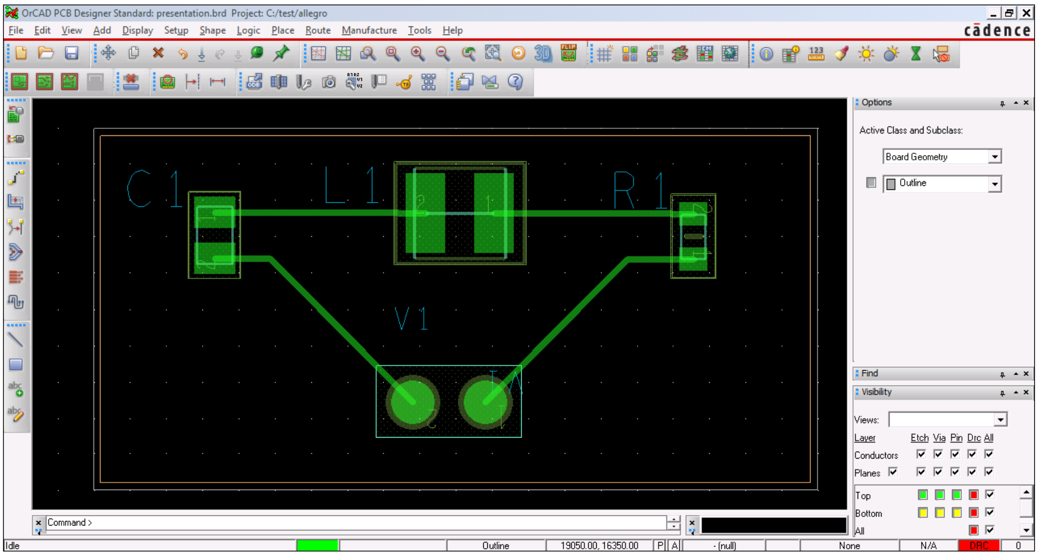


**A. 5 Tracing of PCB tracks between the different components**

## b) APPENDICES B: EasyEDA:

It is a web-based EDA (**Electronic design automation**) tool it was stably released on july 2017, similar to OrCAD, it allows to design, simulate, share - publicly and privately - and discuss schematics, simulations and printed circuit boards.

EasyEDA can generate the bill of materials, Garber files as well (same like OrCAD)

To not do the same thing again, EasyEDA works the same way as OrCAD with the possibility of sharing discussion online that’s why woring with EasyEDA requires internet.

## c) APPENDICES C:

For the heatsink sizing the values that were used are taken from the datasheet

$u_{CEO}$ ,$r_C$ are the output characteristics of the IGBT :

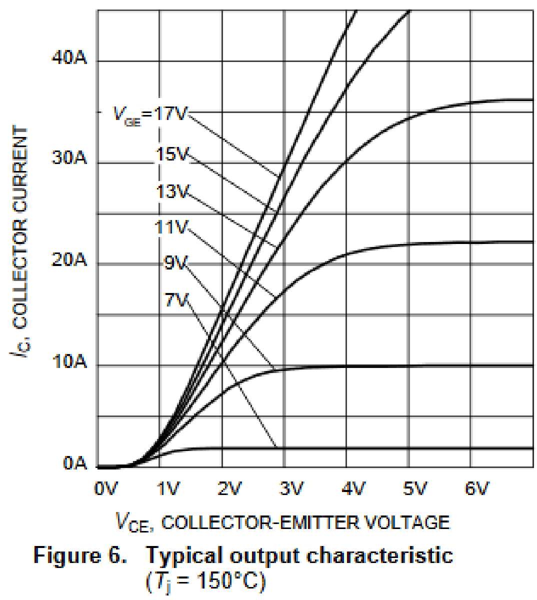


(a)

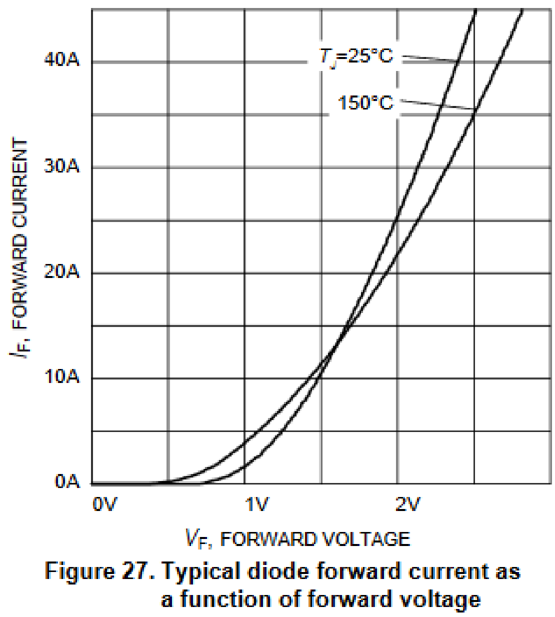


(b)

**Figure C. 1 (a) Output characteristics of IGBT switch, (b) Forward current & voltage characteristics of power diode**

Similarly, $u_{CEO}$ , $r_C$ can be obtained from the forward current and forward voltage.

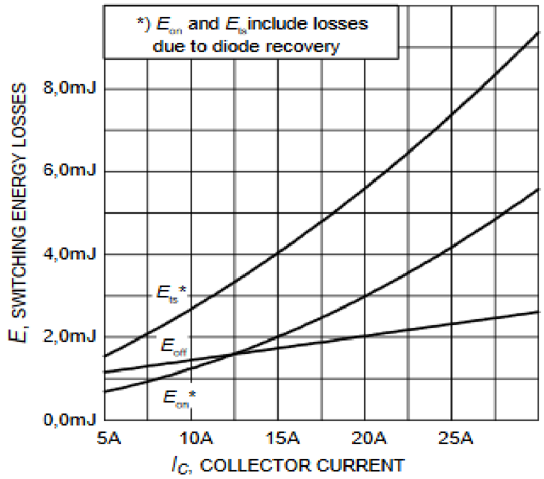


**Figure 13. Typical switching energy losses as a function of collector current**
(inductive load, $T_J$=150°C, $V_{CE}$=600V, $V_{GE}$=0/15V, $R_G$=56Ω, Dynamic test circuit in Figure E)

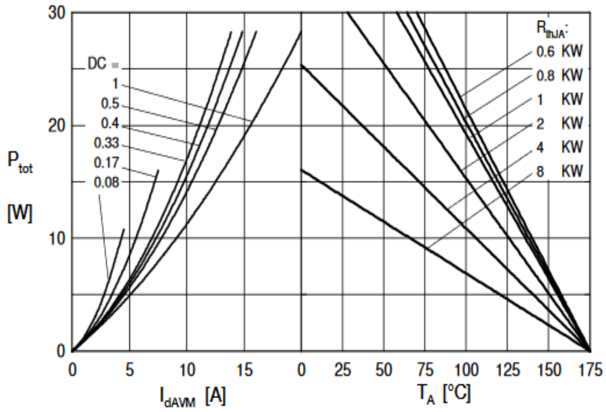


Fig. 4 Power dissipation vs. forward current and ambient temperature per diode

(a) (b)

**Figure C. 2 (a) the switching energy loss in an IGBT switch and diode, (b) Average power dissipation of three-phase diode bridge rectifier**